ACI 445R-99
(Reapproved 2009)

Recent Approaches to Shear Design of Structural Concrete

Reported by Joint ACI-ASCE Committee 445

J. A. Ramirez*
Chair

C. W. French
Secretary

P. E. Adebar*
J. F. Bonacci
M. P. Collins
D. Darwin
W. H. Dilger
A. B. Gogate
N. M. Hawkins
T. T. C. Hsu
G. J. Klein
T. Krauthammer
J. G. MacGregor
D. Mitchell*
R. G. Oesterle
M. A. Polak
K. S. Rajagopalan
K. H. Reineck*
D. M. Rogowsky*
G. M. Sabnis
D. H. Sanders
J. K. Wight
P. Zia

*Members of Subcommittee 445-1 who prepared this report.

Truss model approaches and related theories for the design of reinforced concrete members to resist shear are presented. Realistic models for the design of deep beams, corbels, and other nonstandard structural members are illustrated. The background theories and the complementary nature of a number of different approaches for the shear design of structural concrete are discussed. These relatively new procedures provide a unified, intelligible, and safe design framework for proportioning structural concrete under combined load effects.

Keywords: beams (supports); concrete; design; detailing; failure; models; shear strength; structural concrete; strut and tie.

CONTENTS

ACI 445R-99 became effective November 22, 1999.

CHAPTER 1—INTRODUCTION

1.1—Scope and objectives

Design procedures proposed for regulatory standards should be safe, correct in concept, simple to understand, and should not necessarily add to either design or construction costs. These procedures are most effective if they are based on relatively simple conceptual models rather than on complex empirical equations. This report introduces design engineers to some approaches for the shear design of one-way structural concrete members. Although the approaches explained in the subsequent chapters of this report are relatively new, some of them have reached a sufficiently mature state that they have been implemented in codes of practice. This report builds upon the landmark state-of-the-art report by the ASCE-ACI Committee 426 (1973), *The Shear Strength of Reinforced Concrete Members*, which reviewed the large body of experimental work on shear and gave the background to many of the current American Concrete Institute (ACI) shear design provisions. After reviewing the many different empirical equations for shear design, Committee 426 expressed in 1973 the hope that "the design regulations for shear strength can be integrated, simplified, and given a physical significance so that designers can approach unusual design problems in a rational manner."

The purpose of this report is to answer that challenge and review some of the new design approaches that have evolved since 1973 (CEB 1978, 1982; Walraven 1987; IABSE 1991a,b; Regan 1993). Truss model approaches and related theories are discussed and the common basis for these new approaches are highlighted. These new procedures provide a unified, rational, and safe design framework for structural concrete under combined actions, including the effects of axial load, bending, torsion, and prestressing.

Chapter 1 presents a brief historical background of the development of the shear design provisions and a summary of the current ACI design equations for beams. Chapter 2 discusses a sectional design procedure for structural-concrete one-way members using a compression field approach. Chapter 3 addresses several approaches incorporating the "concrete contribution." It includes brief reviews of European Code EC2, Part 1 and the Comité Euro-International du Béton–Fédération International de la Précontrainte (CEB-FIP) Model Code, both based on strut-and-tie models. The behavior of members without or with low amounts of shear reinforcement is discussed in Chapter 4. An explanation of the concept of shear friction is presented in Chapter 5. Chapter 6 presents a design procedure using strut-and-tie models (STM), which can be used to design regions having a complex flow of stresses and may also be used to design entire members. Chapter 7 contains a summary of the report and suggestions for future work.

1.2—Historical development of shear design provisions

Most codes of practice use sectional methods for design of conventional beams under bending and shear. ACI Building Code 318M-95 assumes that flexure and shear can be handled separately for the worst combination of flexure and shear at a given section. The interaction between flexure and shear is addressed indirectly by detailing rules for flexural reinforcement cutoff points. In addition, specific checks on the level of concrete stresses in the member are introduced to ensure sufficiently ductile behavior and control of diagonal crack widths at service load levels.

In the early 1900s, truss models were used as conceptual tools in the analysis and design of reinforced concrete beams. Ritter (1899) postulated that after a reinforced concrete beam cracks due to diagonal tension stresses, it can be idealized as a parallel chord truss with compression diagonals inclined at 457 with respect to the longitudinal axis of the beam. Mörsch (1920, 1922) later introduced the use of truss models for torsion. These truss models neglected the contribution of the concrete in tension. Withey (1907, 1908) introduced Ritter's truss model into the American literature and pointed out that this approach gave conservative results when compared with test evidence. Talbot (1909) confirmed this finding.

Historically, shear design in the United States has included a concrete contribution V_c to supplement the 45 degree sectional truss model to reflect test results in beams and slabs with little or no shear reinforcement and ensure economy in the practical design of such members. ACI Standard Specification No. 23 (1920) permitted an allowable shear stress of $0.025f'_c$, but not more than 0.41 MPa, for beams without web reinforcement, and with longitudinal reinforcement that did not have mechanical anchorage. If the longitudinal reinforcement was anchored with 180 degree hooks or with plates rigidly connected to the bars, the allowable shear stress was increased to $0.03f'_c$ or a maximum of 0.62 MPa (Fig. 1.1). Web reinforcement was designed by the equation

$$A_v F_v = V's \sin \alpha / jd \qquad (1\text{-}1)$$

where

A_v = area of shear reinforcement within distance s;
f_v = allowable tensile stress in the shear reinforcement;
jd = flexural lever arm;

V' = total shear minus $0.02f_c'bjd$ (or $0.03f_c'bjd$ with special anchorage);
b = width of the web;
s = spacing of shear steel measured perpendicular to its direction; and
α = angle of inclination of the web reinforcement with respect to the horizontal axis of the beam.

The limiting value for the allowable shear stresses at service loads was $0.06f_c'$ or a maximum of 1.24 MPa, or with anchorage of longitudinal steel $0.12f_c'$ or a maximum of 2.48 MPa. This shear stress was intended to prevent diagonal crushing failures of the web concrete before yielding of the stirrups. These specifications of the code calculated the nominal shear stress as $v = V/bjd$.

This procedure, which formed the basis for future ACI codes, lasted from 1921 to 1951 with each edition providing somewhat less-conservative design procedures. In 1951 the distinction between members with and without mechanical anchorage was omitted and replaced by the requirement that all plain bars must be hooked, and deformed bars must meet ASTM A 305. Therefore, the maximum allowable shear stress on the concrete for beams without web reinforcement (ACI 318-51) was $0.03f_c'$ and the maximum allowable shear stress for beams with web reinforcement was $0.12f_c'$.

ACI 318-51, based on allowable stresses, specified that web reinforcement must be provided for the excess shear if the shear stress at service loads exceeded $0.03f_c'$. Calculation of the area of shear reinforcement continued to be based on a 45 degree truss analogy in which the web reinforcement must be designed to carry the difference between the total shear and the shear assumed to be carried by the concrete.

The August 1955 shear failure of beams in the warehouse at Wilkins Air Force Depot in Shelby, Ohio, brought into question the traditional ACI shear design procedures. These shear failures, in conjunction with intensified research, clearly indicated that shear and diagonal tension was a complex problem involving many variables and resulted in a return to forgotten fundamentals.

Talbot (1909) pointed out the fallacies of such procedures as early as 1909 in talking about the failure of beams without web reinforcement. Based on 106 beam tests, he concluded that

> It will be found that the value of v [shear stress at failure] will vary with the amount of reinforcement, with the relative length of the beam, and with other factors which affect the stiffness of the beam.… In beams without web reinforcement, web resistance depends upon the quality and strength of the concrete.… The stiffer the beam the larger the vertical stresses which may be developed. Short, deep beams give higher results than long slender ones, and beams with high percentage of reinforcement [give higher results] than beams with a small amount of metal.

Unfortunately, Talbot's findings about the influence of the percentage of longitudinal reinforcement and the length-to-depth ratio were not reflected in the design equations until much later. The research triggered by the 1956 Wilkins warehouse failures brought these important concepts back to the forefront.

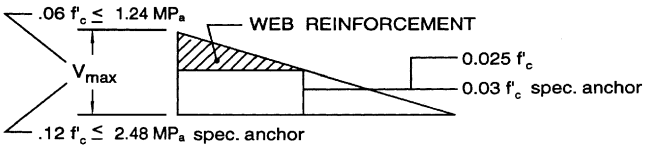

Fig. 1.1—American Specification for shear design (1920-1951) based on ACI Standard No. 23, 1920.

More recently, several design procedures were developed to economize on the design of the stirrup reinforcement. One approach has been to add a concrete contribution term to the shear reinforcement capacity obtained, assuming a 45 degree truss (for example, ACI 318-95). Another procedure has been the use of a truss with a variable angle of inclination of the diagonals. The inclination of the truss diagonals is allowed to differ from 45 degree within certain limits suggested on the basis of the theory of plasticity. This approach is often referred to as the "standard truss model with no concrete contribution" and is explained by the existence of aggregate interlock and dowel forces in the cracks, which allow a lower inclination of the compression diagonals and the further mobilization of the stirrup reinforcement. A combination of the variable-angle truss and a concrete contribution has also been proposed. This procedure has been referred to as the modified truss model approach (CEB 1978; Ramirez and Breen 1991). In this approach, in addition to a variable angle of inclination of the diagonals, the concrete contribution for nonprestressed concrete members diminishes with the level of shear stress. For prestressed concrete members, the concrete contribution is not considered to vary with the level of shear stress and is taken as a function of the level of prestress and the stress in the extreme tension fiber.

As mentioned previously, the truss model does not directly account for the components of the shear failure mechanism, such as aggregate interlock and friction, dowel action of the longitudinal steel, and shear carried across uncracked concrete. For prestressed beams, the larger the amount of prestressing, the lower the angle of inclination at first diagonal cracking. Therefore, depending on the level of compressive stress due to prestress, prestressed concrete beams typically have much lower angles of inclined cracks at failure than nonprestressed beams and require smaller amounts of stirrups.

Traditionally in North American practice, the additional area of longitudinal tension steel for shear has been provided by extending the bars a distance equal to d beyond the flexural cutoff point. Although adequate for a truss model with 45 degree diagonals, this detailing rule is not adequate for trusses with diagonals inclined at lower angles. The additional longitudinal tension force due to shear can be determined from equilibrium conditions of the truss model as $V\cot\theta$, with θ as the angle of inclination of the truss diagonals. Because the shear stresses are assumed uniformly distributed over the depth of the web, the tension acts at the section middepth.

The upper limit of shear strength is established by limiting the stress in the compression diagonals f_d to a fraction of the concrete cylinder strength. The concrete in the cracked web

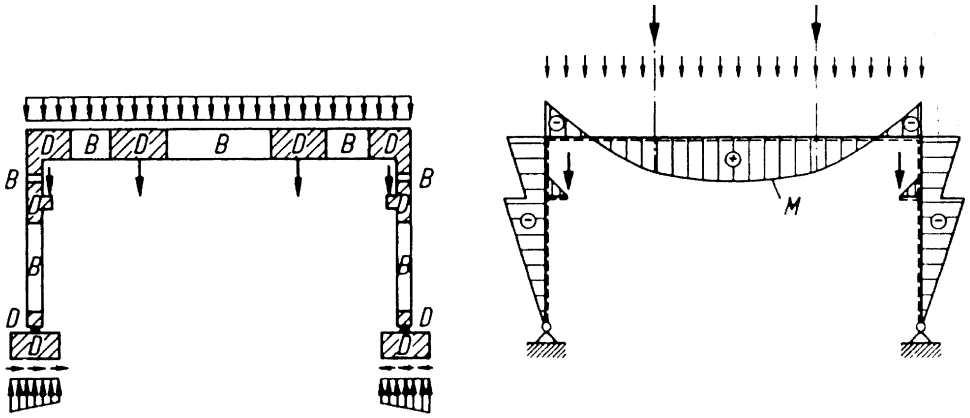

Fig. 1.2—Frame structure containing substantial part of B regions, its statical system, and bending moments (Schlaich et al. 1987).

of a beam is subjected to diagonal compressive stresses that are parallel or nearly parallel to the inclined cracks. The compressive strength of this concrete should be established to prevent web-crushing failures. The strength of this concrete is a function of 1) the presence or absence of cracks and the orientation of these cracks; 2) the tensile strain in the trans-verse direction; and 3) the longitudinal strain in the web. These limits are discussed in Chapters 2, 3, and 6.

The pioneering work from Ritter and Mörsch received new impetus in the period from the 1960s to the 1980s, and there-fore, in more recent design codes, modified truss models are used. Attention was focused on the truss model with diagonals having a variable angle of inclination as a viable model for shear and torsion in reinforced and prestressed concrete beams (Kupfer 1964; Caflisch et al. 1971; Lampert and Thurlimann 1971; Thurlimann et al. 1983). Further development of plasticity theories extended the applicability of the model to nonyielding domains (Nielsen and Braestrup 1975; Muller 1978; Marti 1980). Schlaich et al. (1987) extended the truss model for beams with uniformly inclined diagonals, all parts of the structure in the form of STM. This approach is particularly relevant in regions where the distribution of strains is significantly nonlinear along the depth. Schlaich et al. (1987) introduced the concept of D and B regions, where D stands for discontinuity or disturbed, and B stands for beam or Bernoulli. In D regions the distribution of strains is nonlinear, whereas the distribution is linear in B regions. A structural-concrete member can consist entirely of a D region; however, more often D and B regions will exist within the same member or structure [see Fig. 1.2, from Schlaich et al. (1987)]. In this case, D regions extend a distance equal to the member depth away from any discontinuity, such as a change in cross section or the presence of concentrated loads. For typical slender members, the portions of the structure or member between D regions are B regions. The strut-and-tie approach is discussed in detail in Chapter 6.

By analyzing a truss model consisting of linearly elastic members and neglecting the concrete tensile strength, Kupfer (1964) provided a solution for the inclination of the diagonal cracks. Collins and Mitchell (1980) abandoned the assumption of linear elasticity and developed the compression field theory (CFT) for members subjected to torsion and shear. Based on extensive experimental investigation, Vecchio and Collins (1982, 1986) presented the modified compression field theory (MCFT), which included a rationale for determining the tensile stresses in the diagonally cracked concrete. Although the CFT works well with medium to high percentages of transverse reinforcement, the MCFT provides a more realistic assessment for members having a wide range of amounts of transverse reinforcement, including the case of no web reinforcement. This approach is presented in Chapter 2. Parallel to these developments of the truss model with variable strut inclinations and the CFT, the 1980s also saw the further development of shear friction theory (Chapter 5). In addition, a general theory was developed for beams in shear using constitutive laws for friction and by determining the strains and deformations in the web. Because this approach considers the discrete formation of cracks, the crack spacing and crack width should be determined and equilibrium checked along the crack to evaluate the crack-slip mechanism of failure. This method is presented in Chapter 3. The topic of members without transverse reinforcement is dealt with in Chapter 4.

1.3—Overview of current ACI design procedures

The ACI 318M-95 sectional design approach for shear in one-way flexural members is based on a parallel truss model with 45-degree constant inclination diagonals supplemented by an experimentally obtained concrete contribution. The contribution from the shear reinforcement V_s for the case of vertical stirrups (as is most often used in North American practice), can be derived from basic equilibrium considerations on a 45-degree truss model with constant stirrup spacing s, and effective depth d. The truss resistance is supplemented with a concrete contribution V_c for both reinforced and prestressed concrete beams. Appendix A presents the more commonly used shear design equations for the concrete contribution in normalweight concrete beams, including effects of axial loading and the contribution from vertical stirrups V_s.

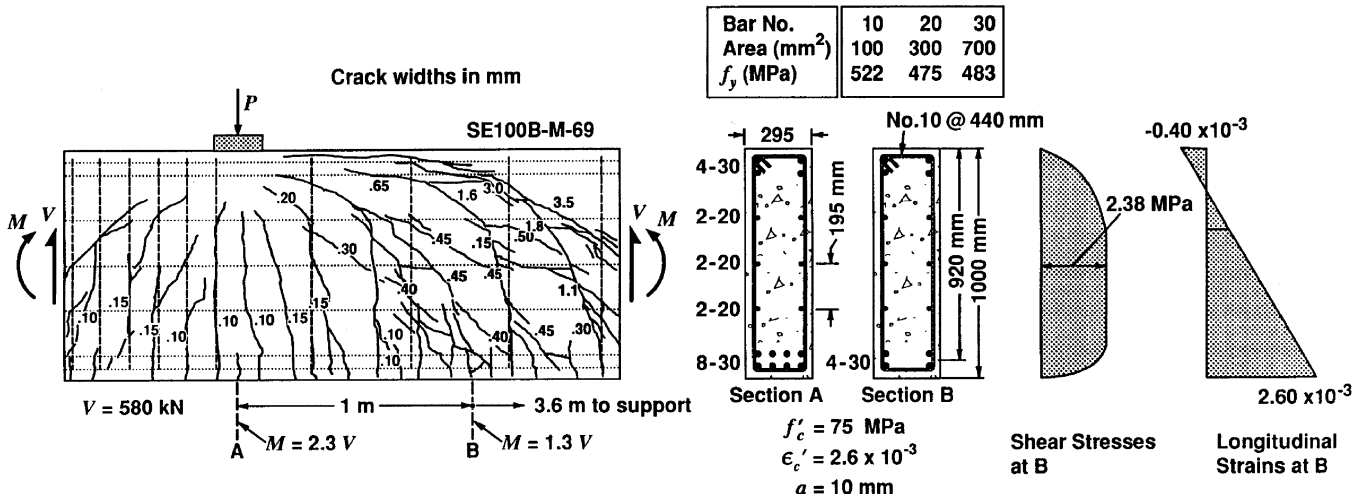

Fig. 2.1—Example of cracked web of beam failing in shear.

1.4—Summary

ACI 318 procedures have evolved into restricted, semiempirical approaches. The primary shortcomings of ACI 318M-95 are the many empirical equations and rules for special cases, and particularly the lack of a clear model that can be extrapolated to cases not directly covered. This situation would be improved if code approaches were based on clear and transparent physical models. Several of such models are discussed in subsequent chapters.

In Chapter 2, a sectional design approach using the MCFT is described. Chapter 3 discusses other truss models incorporating a concrete contribution and provides a brief review of some European code approaches.

The special case of members with no transverse shear reinforcement is addressed in Chapter 4. This chapter also presents an overview of the way the concrete contribution V_c is determined for beams. Chapter 5 presents a method of limit analysis in the form of a shear-friction mechanism. In Chapter 6, the generalized full member truss approach in the form of strut-and-tie systems for one-way flexural members is illustrated. Particular attention is given to the design approach in B and D regions, including the detailing of reinforcement ties, individual struts, and nodal zones.

The aim of this report is to describe these recent approaches to shear design and point out their common roots and complementary natures. This report does not endorse any given approach but provides a synthesis of these truss model-based approaches and related theories. The final goal of this report is to answer the challenge posed by Committee 426 over 20 years ago.

CHAPTER 2—COMPRESSION FIELD APPROACHES

2.1—Introduction

The cracked web of a reinforced concrete beam transmits shear in a relatively complex manner. As the load is increased, new cracks form while preexisting cracks spread and change inclination. Because the section resists moment as well as shear, the longitudinal strains and the crack inclinations vary over the depth of the beam (Fig. 2.1).

The early truss models of Ritter (1899) and Mörsch (1920, 1922) approximated this behavior by neglecting tensile stresses in the diagonally cracked concrete and assuming that the shear would be carried by diagonal compressive stresses in the concrete inclined at 45 degree to the longitudinal axis. The diagonal compressive concrete stresses push apart the top and bottom faces of the beam, while the tensile stresses in the stirrups pull them together. Equilibrium requires that these two effects be equal. According to the 45 degree truss model, the shear capacity is reached when the stirrups yield and will correspond to a shear stress of

$$v = \frac{A_v f_y}{b_w s} = \rho_v f_y \qquad (2\text{-}1)$$

For the beam shown in Fig. 2.1, this equation would predict a maximum shear stress of only 0.80 MPa. As the beam actually resisted a shear stress of about 2.38 MPa, it can be seen that the 45 degree truss equation can be very conservative.

One reason why the 45 degree truss equation is often very conservative is that the angle of inclination of the diagonal compressive stresses measured from the longitudinal axis θ is typically less than 45 degrees. The general form of Eq. (2-1) is

$$v = \rho_v f_y \cot\theta \qquad (2\text{-}2)$$

With this equation, the strength of the beam shown in Fig. 2.1 could be explained if θ was taken equal to 18.6 degrees. Most of the inclined cracks shown in Fig. 2.1 are not this flat.

Before the general truss equation can be used to determine the shear capacity of a given beam or to design the stirrups to resist a given shear, it is necessary to know the angle θ. Discussing this problem, Mörsch (1922) stated, "it is absolutely impossible to mathematically determine the slope of the secondary inclined cracks according to which one can design the stirrups." Just seven years after Mörsch made this statement, another German engineer, H. A. Wagner (1929), solved an analogous problem while dealing with the shear

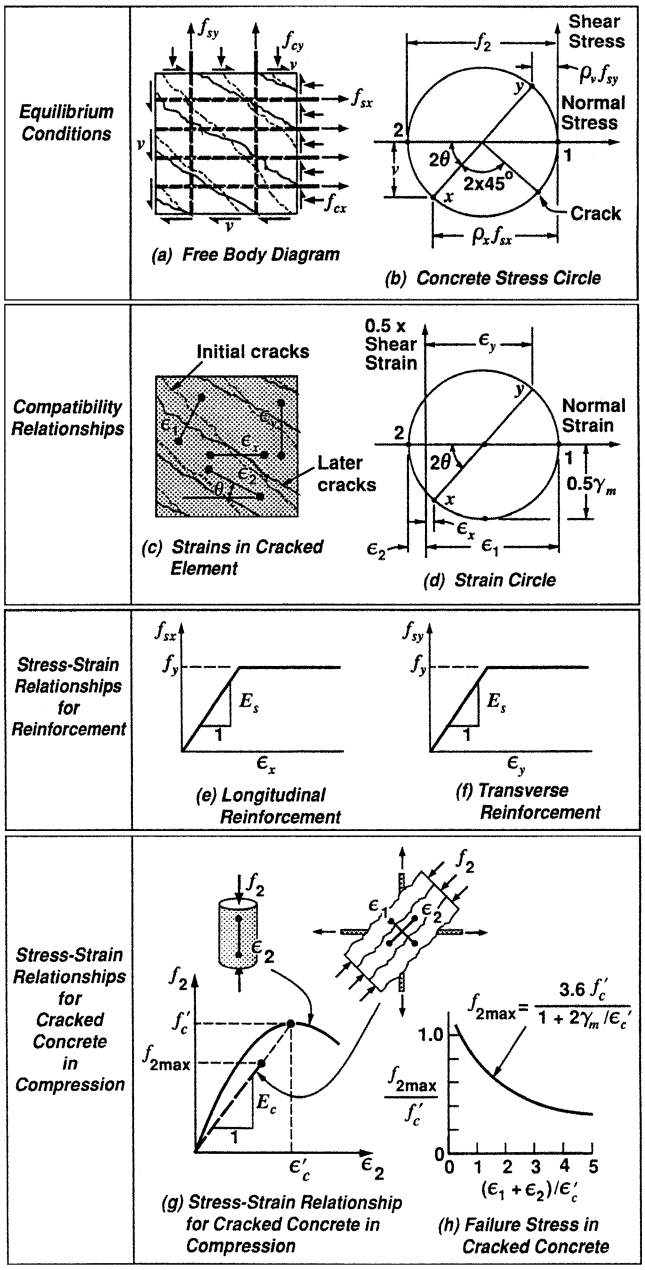

Fig. 2.2—Compression field theory (Mitchell and Collins 1974).

design of "stressed-skin" aircraft. Wagner assumed that after the thin metal skin buckled, it could continue to carry shear by a field of diagonal tension, provided that it was stiffened by transverse frames and longitudinal stringers. To determine the angle of inclination of the diagonal tension, Wagner considered the deformations of the system. He assumed that the angle of inclination of the diagonal tensile stresses in the buckled thin metal skin would coincide with the angle of inclination of the principal tensile strain as determined from the deformations of the skin, the transverse frames, and the longitudinal stringers. This approach became known as the tension field theory.

Shear design procedures for reinforced concrete that, like the tension field theory, determine the angle θ by considering the deformations of the transverse reinforcement, the longitudinal reinforcement, and the diagonally stressed concrete have become known as compression field approaches. With these methods, equilibrium conditions, compatibility conditions, and stress-strain relationships for both the reinforcement and the diagonally cracked concrete are used to predict the load-deformation response of a section subjected to shear.

Kupfer (1964) and Baumann (1972) presented approaches for determining the angle θ assuming that the cracked concrete and the reinforcement were linearly elastic. Methods for determining θ applicable over the full loading range and based on Wagner's procedure were developed by Collins and Mitchell (1974) for members in torsion and were applied to shear design by Collins (1978). This procedure was known as CFT.

2.2—Compression field theory

Figure 2.2 summarizes the basic relationships of the CFT. The shear stress v applied to the cracked reinforced concrete causes tensile stresses in the longitudinal reinforcement f_{sx} and the transverse reinforcement f_{sy} and a compressive stress in the cracked concrete f_2 inclined at angle θ to the longitudinal axis. The equilibrium relationships between these stresses can be derived from Fig. 2.2 (a) and (b) as

$$\rho_v f_{sy} = f_{cy} = v \tan\theta \tag{2-3}$$

$$\rho_x f_{sx} = f_{cx} = v \cot\theta \tag{2-4}$$

$$f_2 = v(\tan\theta + \cot\theta) \tag{2-5}$$

where ρ_x and ρ_v are the reinforcement ratios in the longitudinal and transverse directions.

If the longitudinal reinforcement elongates by a strain of ε_x, the transverse reinforcement elongates by ε_y, and the diagonally compressed concrete shortens by ε_2, then the direction of principal compressive strain can be found from Wagner's (1929) equation, which can be derived from Mohr's circle of strain (Fig. 2.2(d)) as

$$\tan^2\theta = \frac{\varepsilon_x + \varepsilon_2}{\varepsilon_y + \varepsilon_2} \tag{2-6}$$

Before this equation can be used to determine θ, however, stress-strain relationships for the reinforcement and the concrete are required. It is assumed that the reinforcement strains are related to the reinforcement stresses by the usual simple bilinear approximations shown in Fig. 2.2(e) and (f). Thus, after the transverse strain ε_y exceeds the yield strain of the stirrups, the stress in the stirrups is assumed to equal the yield stress f_y, and Eq. (2-3) becomes identical to Eq. (2-2).

Based on the results from a series of intensively instrumented beams, Collins (1978) suggested that the relationship between the principal compressive stress f_2 and the principal compressive strain ε_2 for diagonally cracked concrete would differ from the usual compressive stress-strain curve derived from a cylinder test (Fig 2.2(g)). He postulated that as the strain circle becomes larger, the compressive stress required

to fail the concrete f_{2max} becomes smaller (Fig. 2.2(h)). The relationships proposed were

$$f_{2max} = \frac{3.6f_c'}{1 + 2\gamma_m/\varepsilon_c'} \quad (2\text{-}7)$$

where

γ_m = diameter of the strain circle (that is, $\varepsilon_1 + \varepsilon_2$); and
ε_c' = strain at which the concrete in a cylinder test reaches the peak stress f_c'.

For values of f_2 less than f_{2max}

$$\varepsilon_2 = \frac{f_2}{f_c'\varepsilon_c'} \quad (2\text{-}8)$$

It was suggested that the diagonally cracked concrete fails at a low compressive stress because this stress must be transmitted across relatively wide cracks. If the initial cracks shown in Fig. 2.2(a) formed at 45 degrees to the longitudinal reinforcement, and if θ is less than 45 degrees, which will be the case if ρ_y is less than ρ_x, then significant shear stresses should be transmitted across these initial cracks (Fig. 2.2(b)). The ability of the concrete to transmit shear across cracks depends on the width of the cracks, which, in turn, is related to the tensile straining of the concrete. The principal tensile strain ε_1 can be derived from Fig. 2.2(d) as

$$\varepsilon_1 = \varepsilon_x + (\varepsilon_x + \varepsilon_2)\cot^2\theta \quad (2\text{-}9)$$

For shear stresses less than that causing first yield of the reinforcement, a simple expression for the angle θ can be derived by rearranging the previous equations to give

$$\tan^4\theta = \left(1 + \frac{1}{n\rho_x}\right)/\left(1 + \frac{1}{n\rho_y}\right) \quad (2\text{-}10)$$

where

n = modular ratio E_s/E_c; and
E_c is taken as f_c'/ε_c'.

For the member shown in Fig. 2.1, ρ_x is 0.0303, ρ_y is 0.00154, and $n = 6.93$; therefore, Eq. (2-10) would give a θ value of 26.4 degrees. This would imply that the stirrups would yield at a shear stress of 1.62 MPa.

After the stirrups have yielded, the shear stress can still be increased if θ can be reduced. Reducing θ will increase the tensile stress in the longitudinal reinforcement and the compressive stress in the concrete. Failure will be predicted to occur either when the longitudinal steel yields or when the concrete fails. For the member shown in Fig. 2.1, failure of the concrete is predicted to occur when θ is lowered to 15.5 degrees, at which stage the shear stress is 2.89 MPa and ε_x is 1.73×10^{-3}. Note that these predicted values are for a section where the moment is zero. Moment will increase the longitudinal tensile strain ε_x, which will reduce the shear capacity. For example, if ε_x was increased to 2.5×10^{-3}, concrete failure would be predicted to occur when θ is 16.7 degrees and the shear stress is 2.68 MPa.

2.3—Stress-strain relationships for diagonally cracked concrete

Since the CFT was published, a large amount of experimental research aimed at determining the stress-strain characteristics of diagonally cracked concrete has been conducted. This work has typically involved subjecting reinforced concrete elements to uniform membrane stresses in special-purpose testing machines. Significant experimental studies have been conducted by Aoyagi and Yamada (1983), Vecchio and Collins (1986), Kollegger and Mehlhorn (1988), Schlaich et al. (1987), Kirschner and Collins (1986), Bhide and Collins (1989), Shirai and Noguchi (1989), Collins and Porasz (1989), Stevens et al. (1991), Belarbi and Hsu (1991), Marti and Meyboom (1992), Vecchio et al. (1994), Pang and Hsu (1995), and Zhang (1995). A summary of the results of many of these studies is given by Vecchio and Collins (1993).

These experimental studies provide strong evidence that the ability of diagonally cracked concrete to resist compression decreases as the amount of tensile straining increases (Fig. 2.3). Vecchio and Collins (1986) suggested that the maximum compressive stress f_{2max} that the concrete can resist reduces as the average principal tensile strain ε_1 increases in the following manner

$$f_{2max} = \frac{f_c'}{0.8 + 170\varepsilon_1} \le f_c' \quad (2\text{-}11)$$

The Norwegian concrete code (1989) recommended a similar relationship except the coefficient of 170 was reduced to 100. Belarbi and Hsu (1995) suggested

$$f_{2max} = \frac{0.9f_c'}{\sqrt{1 + 400\varepsilon_1}} \quad (2\text{-}12)$$

The various relationships for the reduction in compressive strength are compared with the experimental results from 73 element tests in Fig. 2.3. It can be seen that Eq. (2-11) lies near the middle of the data scatter band. For larger strains, Eq. (2-12) gives higher values to better fit some data at strains of up to 4%.

The compression field approach requires the calculation of the compressive strain in the concrete ε_2 associated with the compressive stress f_2 [Eq. (2-6)]. For this purpose, Vecchio and Collins (1986) suggested the following simple stress-strain relationship

$$f_2 = f_{2max}\left[2\left(\frac{\varepsilon_2}{\varepsilon_c'}\right) - \left(\frac{\varepsilon_2}{\varepsilon_c'}\right)^2\right] \quad (2\text{-}13)$$

where f_{2max} is given by Eq. (2-11).

Somewhat more complex expressions relating f_2 and ε_2 were suggested by Belarbi and Hsu (1995). They are

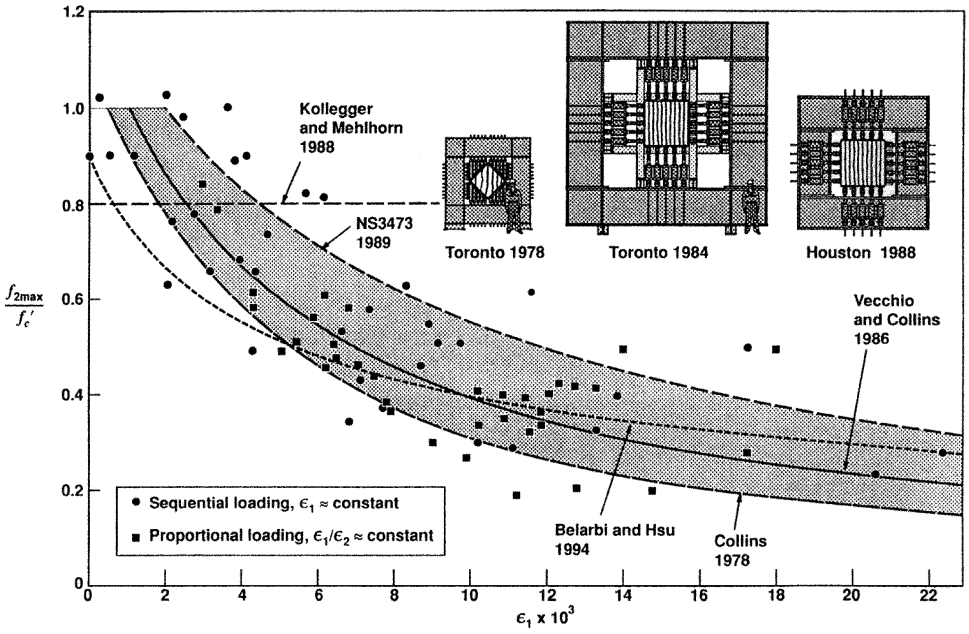

Fig. 2.3—Maximum concrete compressive stress as function of principal tensile strain.

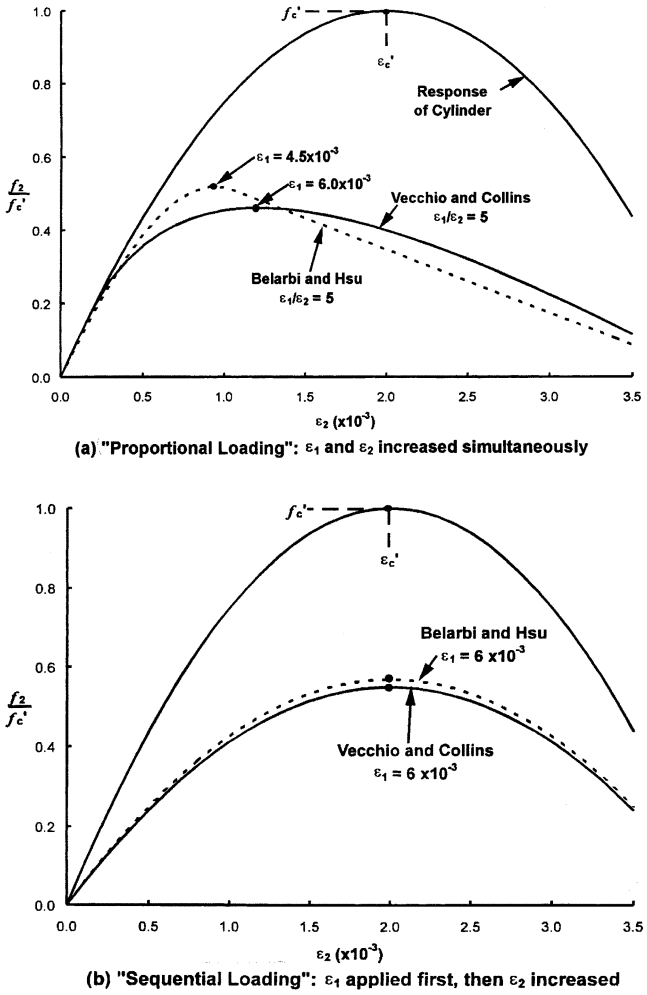

Fig. 2.4—Compressive stress-compressive strain relationships for diagonally cracked concrete: (a) proportion loading, ε_1 and ε_2 increased simultaneously; and (b) sequential loading ε_1 applied first then ε_2 increased.

$$f_2 = \zeta_{\sigma 0} f_c' \left[2\left(\frac{\varepsilon_2}{\zeta_{\varepsilon 0}\varepsilon_c'}\right) - \left(\frac{\varepsilon_2}{\zeta_{\varepsilon 0}\varepsilon_c'}\right)^2 \right] \text{ if } \frac{\varepsilon_2}{\zeta_{\varepsilon 0}\varepsilon_c'} \le 1 \quad (2\text{-}14a)$$

$$f_2 = \zeta_{\sigma 0} f_c' \left[1 - \left(\frac{\varepsilon_2/\zeta_{\varepsilon 0}\varepsilon_c' - 1}{2/\zeta_{\varepsilon 0} - 1}\right)^2 \right] \text{ if } \frac{\varepsilon_2}{\zeta_{\varepsilon 0}\varepsilon_c'} > 1 \quad (2\text{-}14b)$$

where, for "proportional loading"

$$\zeta_{\alpha 0} = \frac{0.9}{\sqrt{1 + 400\varepsilon_1}} \quad \text{and} \quad \zeta_{\varepsilon 0} = \frac{1}{\sqrt{1 + 500\varepsilon_1}} \quad (2\text{-}14c)$$

and for "sequential loading"

$$\zeta_{\alpha 0} = \frac{0.9}{\sqrt{1 + 250\varepsilon_1}} \quad \text{and} \quad \zeta_{\varepsilon 0} = 1 \quad (2\text{-}14d)$$

As the cracked web of a reinforced concrete beam is subjected to increasing shear forces, both the principal compressive strain ε_2 and the principal tensile strain ε_1 are increased. Before yield of the reinforcement, the ratio $\varepsilon_1/\varepsilon_2$ remains reasonably constant. Figure 2.4(a) shows that the compressive stress–compressive strain relationships predicted by Eq. (2-13) and (2-14) for the case where the ratio $\varepsilon_1/\varepsilon_2$ is held constant at a value of 5 are similar. Figure 2.4(b) compares the relationship for the less realistic situation of holding ε_1 constant while increasing ε_2. The predicted stress-strain relationships depend on the sequence of loading. Once again, the predictions of Eq. (2-13) and (2-14) are very similar.

For typical reinforced concrete beams, the percentage of longitudinal reinforcement ρ_x will greatly exceed the percentage of stirrup reinforcement ρ_v. In this situation there

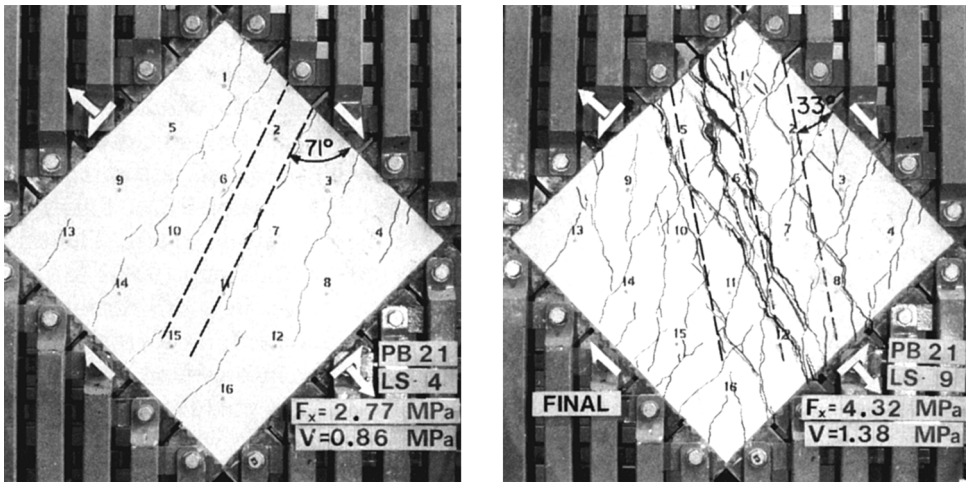

Fig. 2.5—Change of inclination of crack direction with increase in load.

will be a substantial reduction in the inclination θ of the principal compressive stresses after cracking. Figure 2.5 shows the observed crack patterns for a reinforced concrete element that contained reinforcement only in the direction of tension (x-direction) and was loaded in combined tension and shear. The first cracks formed at about 71 degrees to the x-axis. These initial cracks were quite narrow and remained reasonably constant in width throughout the test. As the load was increased, new cracks formed in directions closer to the reinforcement direction, and the width of these new cracks increased gradually. Failure was characterized by the rapid widening of the cracks that formed at about 33 degrees to the x-axis. For this extreme case, the direction of principal stress in the concrete differed by up to 20 degrees from the direction of principal strain (Bhide and Collins 1989). The predicted angle, based on Wagner's assumption that the principal stress direction coincides with the principal strain direction, lay about halfway between the observed strain direction and the observed stress direction. For elements with both longitudinal and transverse reinforcement, the directions of principal stress in the concrete typically deviated by less than 10 degrees from the directions of the principal strain (Vecchio and Collins 1986). Based on these results, it was concluded that determining the inclination of the principal stresses in the cracked concrete by Wagner's equation was a reasonable simplification.

The CFT assumes that after cracking there will be no tensile stresses in the concrete. Tests on reinforced concrete elements, such as that shown in Fig. 2.5, demonstrated that even after extensive cracking, tensile stresses still existed in the cracked concrete and that these stresses significantly increased the ability of the cracked concrete to resist shear stresses. It was found (Vecchio and Collins 1986, Belarbi and Hsu 1994) that after cracking the average principal tensile stress in the concrete decreases as the principal tensile strain increases. Collins and Mitchell (1991) suggest that a suitable relationship is

$$f_1 = \frac{0.33\sqrt{f_c'}}{1 + \sqrt{500\varepsilon_1}} \quad \text{(MPa) units} \qquad (2\text{-}15)$$

while Belarbi and Hsu (1994) suggest

$$f_1 = \frac{0.31\sqrt{f_c'}}{(12{,}500\varepsilon_1)^{0.4}} \quad \text{(MPa) units} \qquad (2\text{-}16)$$

Equation (2-16) predicts a faster decay for f_1 with increasing ε_1 than does Eq. (2-15). For example, for a 35 MPa concrete and an ε_1 value of 5×10^{-3}, Eq. (2-15) would predict an average tensile stress of 0.76 MPa, whereas Eq. (2-16) would predict 0.35 MPa.

2.4—Modified compression field theory

The MCFT (Vecchio and Collins 1986) is a further development of the CFT that accounts for the influence of the tensile stresses in the cracked concrete. It is recognized that the local stresses in both the concrete and the reinforcement vary from point to point in the cracked concrete, with high reinforcement stresses but low concrete tensile stresses occurring at crack locations. In establishing the angle θ from Wagner's equation, Eq. (2-6), the compatibility conditions relating the strains in the cracked concrete to the strains in the reinforcement are expressed in terms of average strains, where the strains are measured over base lengths that are greater than the crack spacing (Fig. 2.2(c) and (d)). In a similar manner, the equilibrium conditions, which relate the concrete stresses and the reinforcement stresses to the applied loads, are expressed in terms of average stresses; that is, stresses averaged over a length greater than the crack spacing. These relationships can be derived from Fig. 2.6(a) and (b) as

$$\rho_v f_{sy} = f_{cy} = v\tan\theta - f_1 \qquad (2\text{-}17)$$

$$\rho_x f_{sx} = f_{cx} = v\cot\theta - f_1 \qquad (2\text{-}18)$$

$$f_2 = v(\tan\theta + \cot\theta) - f_1 \qquad (2\text{-}19)$$

These equilibrium equations, the compatibility relationships from Fig. 2.2(d), the reinforcement stress-strain relationships

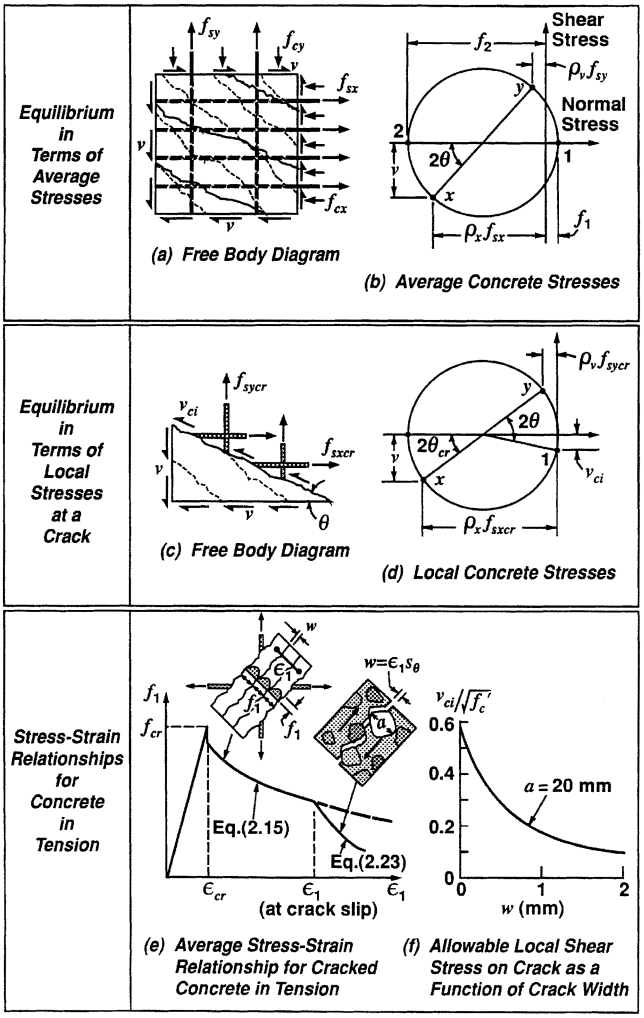

Fig. 2.6—Aspects of modified compression field theory.

from Fig. 2.2(e) and (f), and the stress-strain relationships for the cracked concrete in compression (Eq. (2-13)) and tension (Fig. 2.6(e)) enable the average stresses, the average strains, and the angle θ to be determined for any load level up to the failure.

Failure of the reinforced concrete element may be governed not by average stresses, but rather by local stresses that occur at a crack. In checking the conditions at a crack, the actual complex crack pattern is idealized as a series of parallel cracks, all occurring at angle θ to the longitudinal reinforcement and space a distance s_θ apart. From Fig. 2.6(c) and (d), the reinforcement stresses at a crack can be determined as

$$\rho_v f_{syer} = v\tan\theta - v_{ci}\tan\theta \qquad (2\text{-}20)$$

$$\rho_x f_{sxer} = v\cot\theta - v_{ci}\cot\theta \qquad (2\text{-}21)$$

It can be seen that the shear stress v_{ci} on the crack face reduces the stress in the transverse reinforcement but increases the stress in the longitudinal reinforcement. The maximum possible value of v_{ci} is taken (Bhide and Collins 1989) to be related to the crack width w and the maximum

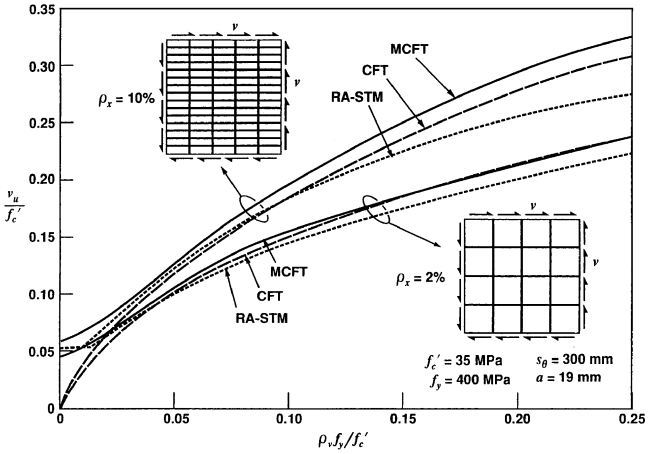

Fig. 2.7—Comparison of predicted shear strengths of two series of reinforced concrete elements.

aggregate size a by the relationship illustrated in Fig. 2.6(f) and given by

$$v_{ci} \le 0.18\sqrt{f_c'}\Big/\left(0.3 + \frac{24w}{a+16}\right) \quad \text{(MPa, mm)} \qquad (2\text{-}22)$$

The crack width w is taken as the crack spacing times the principal tensile strain ε_1. At high loads, the average strain in the stirrups ε_y will typically exceed the yield strain of the reinforcement. In this situation, both f_{sy} in Eq. (2-17) and f_{sycr} in Eq. (2-20) will equal the yield stress in the stirrups. Equating the right-hand sides of these two equations and substituting for v_{ci} from Eq. (2-22) gives

$$f_1 \le 0.18\sqrt{f_c'}\tan\theta\Big/\left(0.3 + \frac{24w}{a+16}\right) \qquad (2\text{-}23)$$

Limiting the average principal tensile stress in the concrete in this manner accounts for the possibility of failure of the aggregate interlock mechanisms, which are responsible for transmitting the interface shear stress v_{ci} across the crack surfaces.

Figure 2.7 illustrates the influence of the tensile stresses in the cracked concrete on the predicted shear capacity of two series of reinforced concrete elements. In this figure, RA-STM stands for rotating-angle softened-truss model. If tensile stresses in the cracked concrete are ignored, as is done in the CFT, elements with no stirrups ($\rho_v = 0$) are predicted to have no shear strength. When these tensile stresses are accounted for, as is done in the MCFT, even members with no stirrups are predicted to have significant postcracking shear strengths. Figure 2.7 shows that predicted shear strengths are a function not only of the amount of stirrup reinforcement, but also of the amount of longitudinal reinforcement. Increasing the amount of longitudinal reinforcement increases the shear capacity. Increasing the amount of longitudinal reinforcement also increases the difference between the CFT prediction and the MCFT prediction. For the elements with 2% of longitudinal reinforcement and with

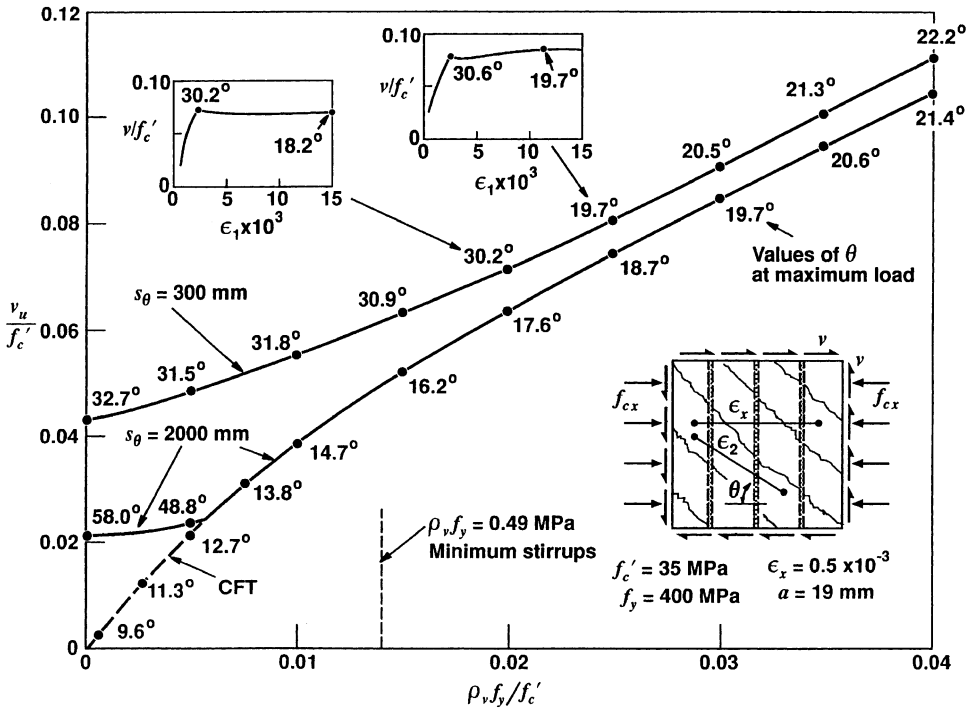

Fig. 2.8—Influence of crack spacing on predicted shear capacity.

$\rho_v f_y/f_c'$ greater than about 0.10, yielding of the longitudinal reinforcement at a crack (Eq. (2-21)) limits the maximum shear capacity. In this situation, the influence of the tensile stresses in the cracked concrete on the predicted shear strength is negligibly small. On the other hand, when the total longitudinal reinforcement is 10% of the web area, this longitudinal reinforcement remains well below yield stress, and the failure, for larger amounts of stirrups, is then governed by crushing of the concrete. The tensile stresses in the cracked concrete stiffen the element, reduce the concrete strains, and make it possible to resist larger shear stresses before failure. The predicted shear strength of elements that contain relatively small amounts of stirrups are influenced by the spacing of the diagonal cracks s_θ. If this spacing is increased, the crack width, w, associated with a given value of ε_1 increases, and the tension transmitted through the cracked concrete decreases (Eq. (2-23)). This aspect of behavior is illustrated in Fig. 2.8, which compares the shear capacities predicted by the MCFT for two series of elements. In one series, the crack spacing is taken as 300 mm, whereas in the other, it is taken as 2000 mm. It is assumed that the amount of longitudinal reinforcement and the axial loading of the elements is such that the longitudinal strain, εx, is held constant at 0.5×10^{-3}. It can be seen that the predicted shear capacity becomes more sensitive to crack spacing as the amount of stirrup reinforcement, ρ_v, is reduced. When ρ_v is zero, the element with a 2000 mm crack spacing is predicted to have only about half the shear capacity of the element with a 300 mm crack spacing.

2.5—Rotating-angle softened-truss model

A somewhat different procedure to account for tensile stresses in diagonally cracked concrete has been developed by Hsu and his coworkers at the University of Houston (Belarbi and Hsu 1991, 1994, 1995; Pang and Hsu 1995; Hsu 1993). This procedure is called the rotating-angle softened-truss model (RA-STM). Like the MCFT, this method assumes that the inclination of the principal stress direction θ in the cracked concrete coincides with the principal strain direction. For typical elements, this angle will decrease as the shear is increased, hence the name rotating angle. Pang and Hsu (1995) limit the applicability of the rotating-angle model to cases where the rotating angle does not deviate from the fixed angle by more than 12 degrees. Outside this range, they recommend the use of a fixed-angle model, which is discussed in Section 3.5.

The method formulates equilibrium equations in terms of average stresses (Fig. 2.6(b)) and compatibility equations in terms of average strains (Fig. 2.2(d)). The softened stress-strain relationship of Eq. (2-14) is used to relate the principal compressive stress in the concrete f_2 to the principal compressive strain ε_2, whereas Eq. (2-16) is used to relate the average tensile stress in the concrete f_1 to the principal tensile strain ε_1.

Instead of checking the stress conditions at a crack, as is done by the MCFT, the RA-STM adjusts the average stress-average strain relationships of the reinforcement to account for the possibility of local yielding at the crack. The relationships suggested are

$$f_s = E_s \varepsilon_s \quad \text{if} \quad \varepsilon_s \le \varepsilon_n \tag{2-24a}$$

$$f_s = f_y \left[(0.91 - 2B) + (0.02 + 0.25B) \frac{E_s}{f_y} \varepsilon_s \right] \tag{2-24b}$$

$$\left[1 - \frac{2 - \alpha_2/45}{1000\rho} \right] \quad \text{if} \quad \varepsilon_s > \varepsilon_n$$

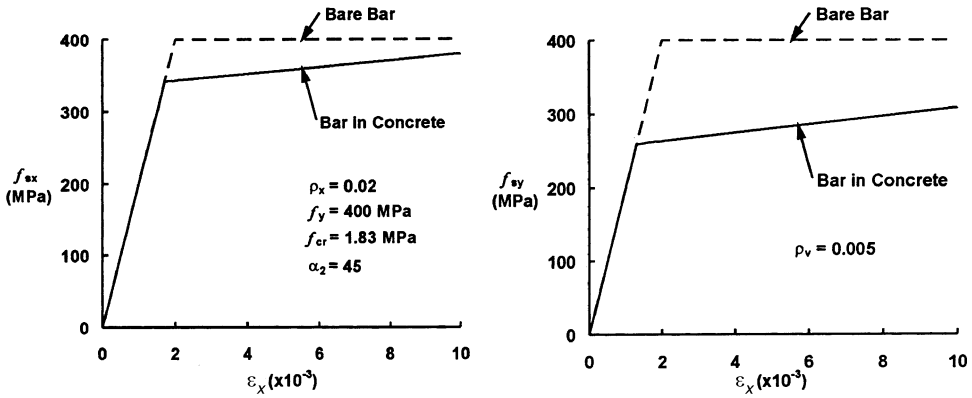

Fig. 2.9—Average-reinforcement-stress/average-reinforcement-strain relationships used in rotating-angle softened-truss model.

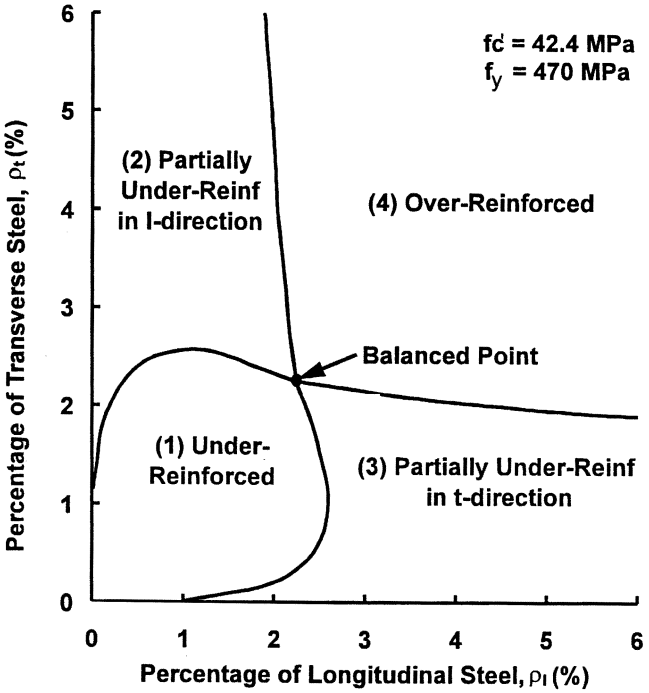

Fig. 2.10—Four failure modes predicted by rotating-angle softened-truss model for element loaded in pure shear (adapted from Pang and Hsu [1995]).

$$\varepsilon_n = \frac{f_y}{E_s}(0.93 - 2B)\left[1 - \frac{2 - \alpha_2/45}{1000\rho}\right] \quad (2\text{-}24c)$$

$$B = \left(\frac{f_{cr}}{fy}\right)^{1.5}/\rho \quad (2\text{-}24d)$$

where

ρ = reinforcement ratio; and

α_2 = angle between the initial crack direction and the longitudinal reinforcement.

The resulting relationships for a case where the longitudinal reinforcement ratio is 0.02 and the transverse reinforcement ratio is 0.005 are illustrated in Fig. 2.9.

Figure 2.7 shows the shear strength-predictions for the RA-STM for the two series of reinforced concrete elements. Although the MCFT and the RA-STM give similar predictions for low amounts of reinforcement, the predicted strengths using the RA-STM are somewhat lower than those given by the MCFT for elements with higher amounts of reinforcement.

Both the MCFT and the RA-STM are capable of predicting not only the failure load but also the mode of failure. Thus, as shown in Fig. 2.10, a reinforced concrete element loaded in pure shear can fail in four possible modes. Both the longitudinal and transverse reinforcement can yield at failure (Mode 1), only the longitudinal reinforcement yields at failure (Mode 2), only the transverse reinforcement yields at failure (Mode 3), or neither reinforcement yields at failure (Mode 4).

2.6—Design procedure based on modified compression field theory

The relationships of the MCFT can be used to predict the shear strength of a beam such as that shown in Fig. 2.11. Assuming that the shear stress in the web is equal to the shear force divided by the effective shear area $b_w d_v$, and that, at failure, the stirrups will yield, equilibrium equations (2-17) can be rearranged to give the following expression for the shear strength V_n of the section

$$V_n = V_c + V_s + V_p \quad (2\text{-}25a)$$

$$V_n = f_1 b_w d_v \cot\theta + \frac{A_v f_y}{s} d_v \cot\theta + V_p \quad (2\text{-}25b)$$

$$V_n = \beta\sqrt{f_c'}\, b_w d_v + \frac{A_v f_y}{s} d_v \cot\theta + V_p \quad (2\text{-}25c)$$

where

V_c = shear strength provided by tensile stresses in the cracked concrete;

V_s = shear strength provided by tensile stresses in the stirrups;

V_p = vertical component of the tension in inclined prestressing tendon;

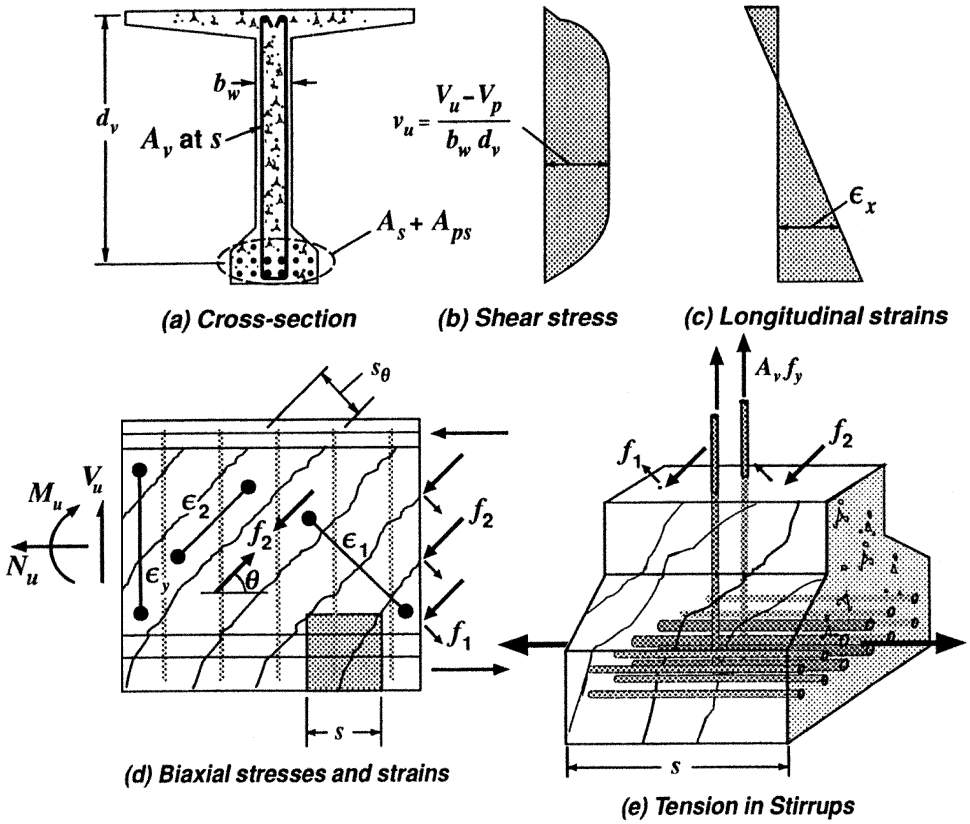

Fig. 2.11—Beam subjected to shear, moment, and axial load.

b_w = effective web width, taken as the minimum web width within the shear depth;
d_v; d_v = effective shear depth, taken as the flexural lever arm, but which need not be taken less than $0.9d$; and
β = concrete tensile stress factor indicating the ability of diagonally cracked concrete to resist shear.

The shear stress that the web of a beam can resist is a function of the longitudinal straining in the web. The larger this longitudinal straining becomes, the smaller the shear stress required to fail the web. In determining the shear capacity of the beam, it is conservative to use the highest longitudinal strain ε_x occurring within the web. For design calculations, ε_x can be approximated as the strain in the tension chord of the equivalent truss. Therefore

$$\varepsilon_x = \frac{(M_u/d_v) + 0.5N_u + 0.5V_u\cot\theta - A_{ps}f_{po}}{E_sA_s + E_pA_{ps}} \quad (2\text{-}26)$$

but need not be taken greater than 0.002, where

f_{po} = stress in the tendon when the surrounding concrete is at zero stress, which may be taken as 1.1 times the effective stress in the prestressing f_{se} after all losses;
A_s = area of nonprestressed longitudinal reinforcement on the flexural tension side of the member;
A_{ps} = area of prestressed longitudinal reinforcement on the flexural tension side of the member;
M_u = moment at the section, taken as positive; and
N_u = axial load at the section, taken as positive if tensile and negative if compressive.

The determination of ε_x for a nonprestressed beam is illustrated in Fig. 2.12.

The longitudinal strain parameter, ε_x, accounts for the influence of moment, axial load, prestressing, and amount of longitudinal reinforcement on the shear strength of a section. If ε_x and the crack spacing s_θ are known, the shear capacity corresponding to a given quantity of stirrups can be calculated (Fig. 2.8). This is equivalent to finding the values of β and θ in Eq. (2-25).

Values of β and θ determined from the modified compression field theory (Vecchio and Collins 1986) and suitable for members with at least minimum web reinforcement are given in Fig. 2.13. In determining these values, it was assumed that the amount and spacing of the stirrups would limit the crack spacing to about 300 mm. The θ values given in Fig. 2.13 ensure that the tensile strain in the stirrups, ε_v, is at least equal to 0.002 and that the compressive stress, f_2, in the concrete does not exceed the crushing strength f_{2max}. Within the range of values of θ that satisfy these requirements, the values given in Fig. 2.13 result in close to the smallest amount of total shear reinforcement being required to resist a given shear.

2.6.1 *Minimum shear reinforcement*—A minimum amount of shear reinforcement is required to control diagonal cracking and provide some ductility. In ACI 318M-95, this amount is specified as

$$\frac{A_v f_y}{b_w s} > 0.33 \text{ MPa} \quad (2\text{-}27)$$

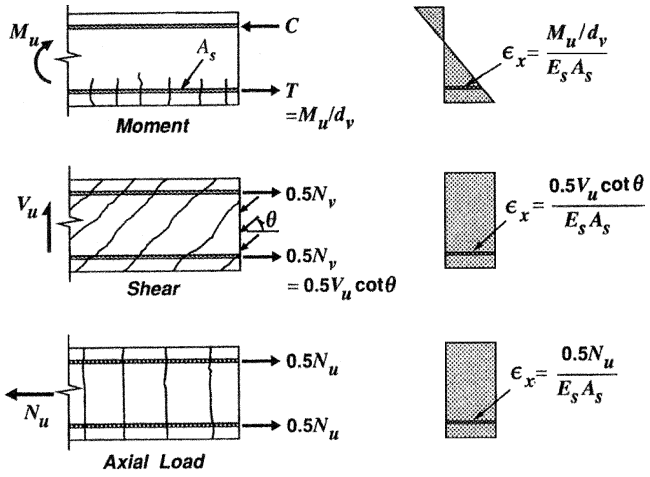

Fig. 2.12—Determination of strains, ε_x, for nonprestressed beam.

The AASHTO specifications (1994) relate the minimum reinforcement required to the concrete strength and require a larger quantity of stirrups for high-strength concrete. The AASHTO specifications require that

$$\frac{A_v f_y}{b_w s} > 0.083\sqrt{f'_c} \quad \text{MPa} \qquad (2\text{-}28)$$

This type of relationship was found to give reasonable estimates compared with experiments conducted by Yoon et al. (1996). There is some concern, however, that the equation may not be conservative enough for large reinforced concrete members that contain low percentages of longitudinal reinforcement (ASCE-ACI 426 1973).

2.6.2 *Example: Determine stirrup spacing in reinforced concrete beam*—To illustrate the method, it will be used to determine the stirrup spacing at Section B for the member tested as shown in Fig. 2.1, which will result in a predicted shear strength of 580 kN with a capacity-reduction factor of 1.0

$$\frac{v_u}{f'_c} = \frac{V_u}{b_w d_v f'_c} = \frac{580{,}000}{295 \times 0.9 \times 920 \times 75} = 0.032$$

From Eq. (2-26)

$$\varepsilon_x = \frac{(M_u/d_v) + 0.5V_u \cot\theta}{E_s A_s}$$

$$\varepsilon_x = \frac{(580{,}000 \times 1300/828) + 0.5 \times 580{,}000 \cot\theta}{200{,}000\,(4 \times 700 + 3 \times 300)}$$

$$\varepsilon_x = 1.23 \times 10^{-3} + 0.329 \times 10^{-3} \cot\theta$$

Figure 2.13 shows that if v_u/f'_c is less than 0.05 and ε_x is between 1.5×10^{-3} and 2×10^{-3}, θ is about 42 degrees. With this value of θ, the calculated value of ε_x is 1.67×10^{-3} and β is approximately 0.155, according to Fig. 2.13. Equation (2-25) then becomes

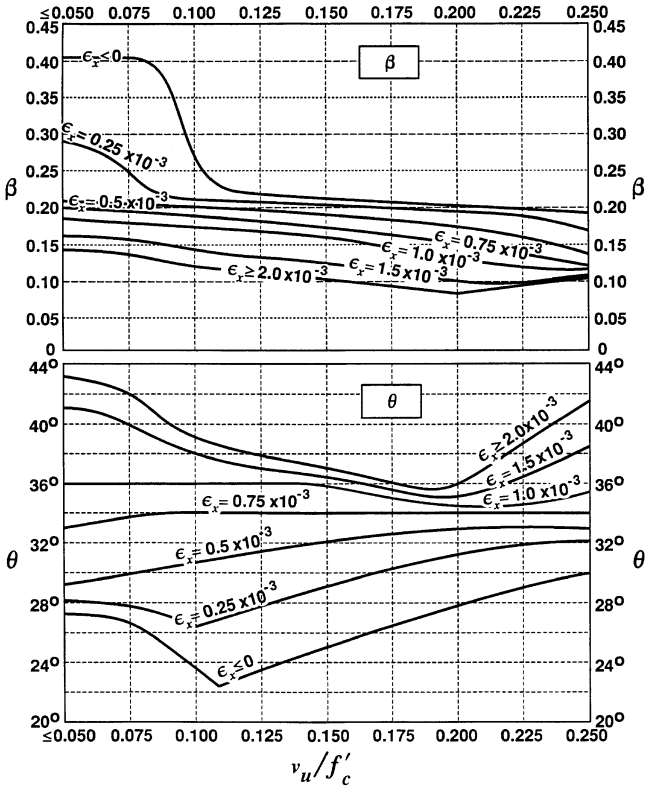

Fig. 2.13—Values of β and θ for members containing at least the minimum amount of stirrups.

$$580{,}000 = 0.155\sqrt{75} \times 295 \times 828 + \frac{200 \times 522}{s}$$

$$\times\, 828\cot 42 \text{ degrees}$$

which gives a required stirrup spacing of 381 mm. Note that because the tested beam contained stirrups at a spacing of 440 mm, the design method is a little conservative.

2.6.3 *Example: Determine stirrup spacing in a prestressed concrete beam*—If the member had also contained a straight post-tensioned tendon near the bottom face consisting of six 13 mm strands with an effective stress of 1080 MPa, the calculations for the required stirrup spacing would change in the following manner. Equation (2-26) becomes

$$\varepsilon_x \times \{[(580{,}000 \times 1300/828) + 0.5 \times 580{,}000\cot\theta$$

$$- 6 \times 99 \times 1.1 \times 1080]/[200{,}000(4 \times 700 + 3 \times 300 + 6 \times 99)]\}$$

Figure 2.13 shows that if v_u/f'_c is less than 0.05 and ε_x is approximately 0.75×10^{-3}, θ is about 33 degrees. With this value of θ, the calculated value of ε_x is 0.76×10^{-3}. For this value of ε_x, the value of β is approximately 0.155, according to Fig. 2.13. Equation (2-25) then becomes

$$580{,}000 = 0.20\sqrt{75} \times 295 \times 828 + \frac{200 \times 522}{s}$$

$$\times\, 828 \cot 33 \text{ degrees}$$

which gives a required stirrup spacing of 848 mm.

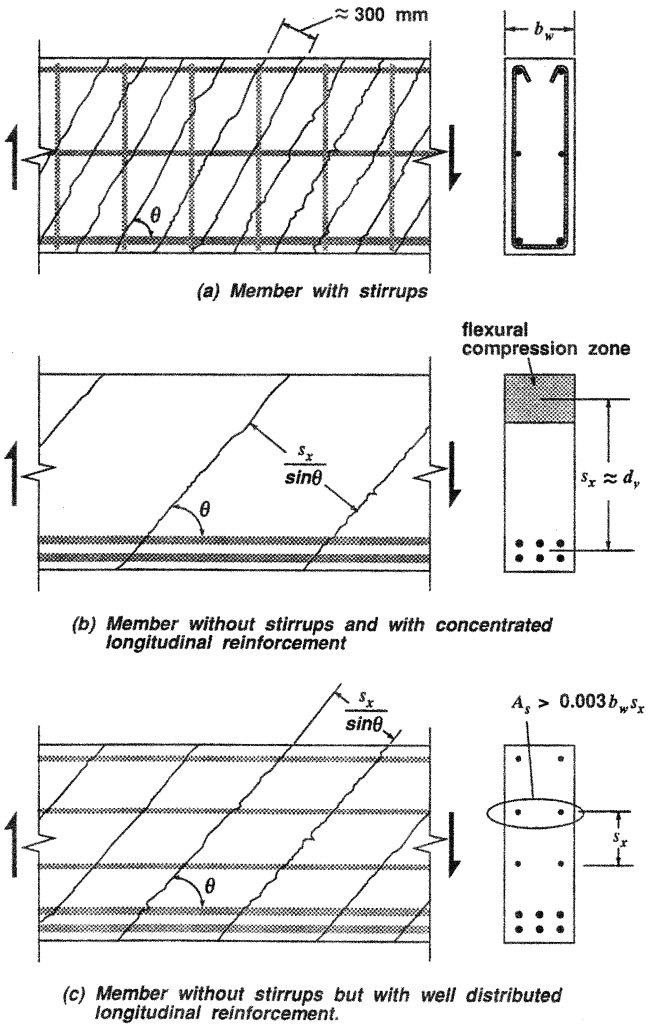

Fig. 2.14—Influence of reinforcement on spacing of diagonal cracks.

Stirrups spaced at 848 mm in the member shown in Fig. 2.1 would not provide adequate crack control, and the assumption that the crack spacing was about 300 mm would no longer be valid. The AASHTO specifications (1994) require that the stirrup spacing not exceed $0.8d_v$ or 600 mm.

To satisfy the minimum stirrup amount requirement of Eq. (2-28), the stirrup spacing for the beam shown in Fig. 2.1 should be

$$s < \frac{200 \times 522}{295 \times 0.083\sqrt{75}} = 492 \text{ mm}$$

2.6.4 *Design of member without stirrups*—For members without stirrups or with less than the minimum amount of stirrups, the diagonal cracks will typically be more widely spaced than 300 mm. For these members, the diagonal cracks will become more widely spaced as the inclination of the cracks θ is reduced (Fig. 2.5 and 2.14). The crack spacing when θ equals 90 degrees is called s_x, and this spacing is primarily a function of the maximum distance between the longitudinal reinforcing bars (Fig. 2.14). As shown in Fig. 2.5 the values of β and θ for members with less than the minimum amount of stirrups depend on the longitudinal strain parameter, ε_x, and the crack spacing parameter, s_x, where s_x need not be taken as greater than 2000 mm. As s_x increases, β decreases, and the predicted shear strength decreases.

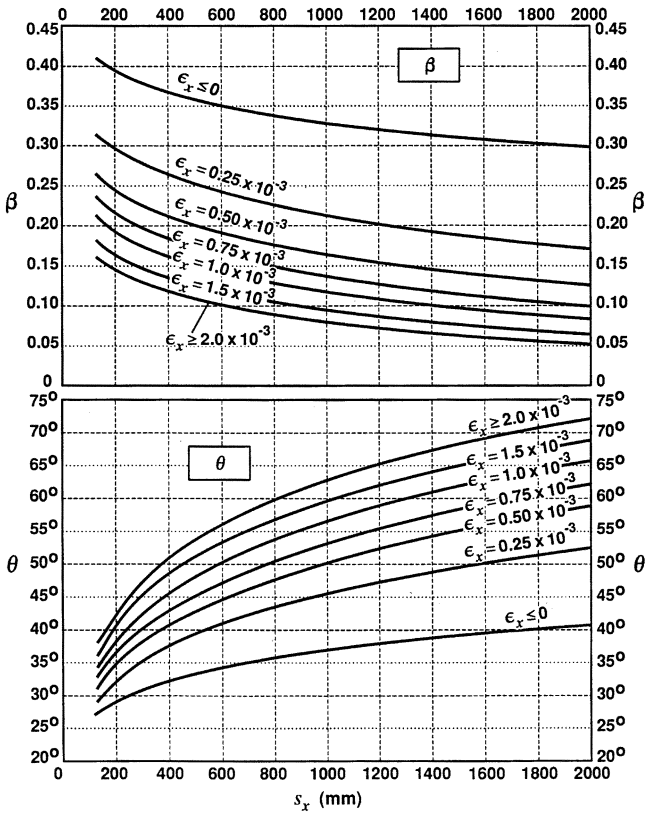

Fig. 2.15—Values of β and θ for members containing less than the minimum amount of stirrups.

The β and θ values given in Fig. 2.15 were calculated assuming that the maximum aggregate size a is 19 mm. The values can be used for other aggregate sizes by using an equivalent crack spacing parameter

$$s_{xe} = s_x \frac{35}{a + 16} \tag{2-29}$$

If the member shown in Fig. 2.1 did not contain any stirrups, the shear strength at Section B could be predicted from Fig. 2.15 in the following manner. As the longitudinal bars are spaced 195 mm apart and the maximum aggregate size is 10 mm, the crack spacing parameter is

$$s_{xe} = 195 \frac{35}{10 + 16} = 263 \text{ mm}$$

If ε_x is estimated to be 1.0×10^{-3}, then from Fig. 2.15, θ is about 41 degrees and β is about 0.18. Equation (2-25) then gives

$$V_n = 0.18\sqrt{75} \times 295 \times 828 = 381 \text{ kN}$$

whereas Eq. (2-26) gives

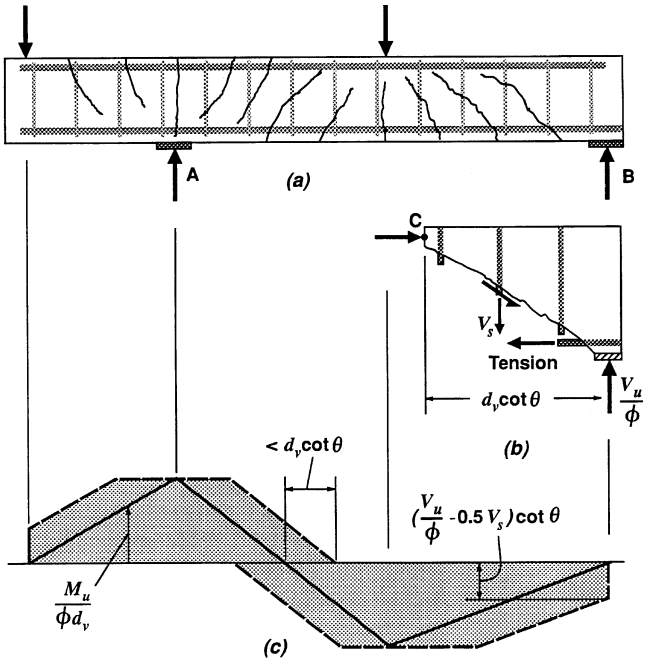

Fig. 2.16—Influence of shear on tension in longitudinal reinforcement.

$$\varepsilon_x = \frac{(381{,}000 \times 1300/828) + 0.5 \times 381{,}000 \cot 41 \text{ degree}}{200{,}000(4 \times 700 + 3 \times 300)}$$

$$= 1.10 \times 10^{-3}$$

Using the calculated value of ε_x of 1.10×10^{-3}, β would be about 0.17, and a more accurate estimate of the failure shear would be 360 kN.

If the member did not contain the six 20 mm diameter skin-reinforcement bars, the crack spacing parameter would increase to

$$s_{xe} = 828\frac{35}{10+16} = 1115 \text{ mm}$$

If ε_x is estimated to be 0.75×10^{-3}, then from Fig. 2.15, θ is about 55.5 degrees and β is about 0.13. With these values, V_n would be reduced to 275 kN and ε_x would be calculated as 0.71×10^{-3}. A second iteration would give the predicted shear strength as 283 kN.

2.6.5 *Additional design considerations*—In the design approach based on the MCFT, the stirrups required at a particular section can be determined from Eq. (2-25) as

$$V_s \geq \frac{V_u}{\phi} - V_c - V_p \tag{2-30}$$

given the shear, moment, and axial load acting at the section. Although this calculation is performed for a particular section, shear failure caused by yielding of the stirrups involves yielding this reinforcement over a length of beam of about $d_v \cot\theta$. Therefore, a calculation for one section can be taken as representing a length of beam $d_v \cot\theta$ long with the calculated section being in the middle of this length. Near a support, the first section checked is the section $0.5d_v \cot\theta$ from the face of the support. In addition, near concentrated loads, sections closer than $0.5d_v \cot\theta$ to the load need not be checked. As a simplification, the term $0.5d_v \cot\theta$ may be approximated as d_v. The required amount of stirrups at other locations along the length of the beam can be determined by calculating sections at about every tenth point along the span, until it is evident that shear is no longer critical.

Shear causes tensile stresses in the longitudinal reinforcement as well as in the stirrups (Eq. (2-21)). If a member contains an insufficient amount of longitudinal reinforcement, its shear strength may be limited by yielding of this reinforcement. To avoid this type of failure, the longitudinal reinforcement on the flexural tension side of the member should satisfy the following requirement

$$A_s f_y + A_{ps} f_{ps} \geq \frac{M}{\phi d_v} + \frac{0.5N_u}{\phi} + \left(\frac{V_u}{\phi} - 0.5V_s - V_p\right)\cot\theta \tag{2-31}$$

Figure 2.16 illustrates the influence of shear on the tensile force required in the longitudinal reinforcement. Whereas the moment is zero at the simple support, there still needs to be considerable tension in the longitudinal reinforcement near this support. The required tension T at a simple support can be determined from the free-body diagram in Fig. 2.16 as

$$T = \left(\frac{V_u}{\phi} - 0.5V_s - V_p\right)\cot\theta \tag{2-32}$$

but

$$T \geq 0.5\left(\frac{V_u}{\phi} - V_p\right)\cot\theta \tag{2-33}$$

The reinforcement provided at the support should be detailed in such a manner that this tension force can be safely resisted and that premature anchorage failures do not occur.

At the maximum moment locations shown in Fig. 2.16, the shear force changes sign, causing fanning of the diagonal compressive stresses as θ passes through 90 degrees. See also Fig. 2.1. Because of this, the maximum tension in these regions need not be taken as larger than that required for the maximum moment. The traditional North American procedure for accounting for the influence of shear on the longitudinal reinforcement involves extending the longitudinal reinforcement a distance d beyond the point at which it is no longer required to resist flexure, in addition to other detailing requirements. As can be seen from Fig. 2.16, the requirements of Eq. (2-31) can be satisfied in a conservative manner by simply extending the longitudinal reinforcement a

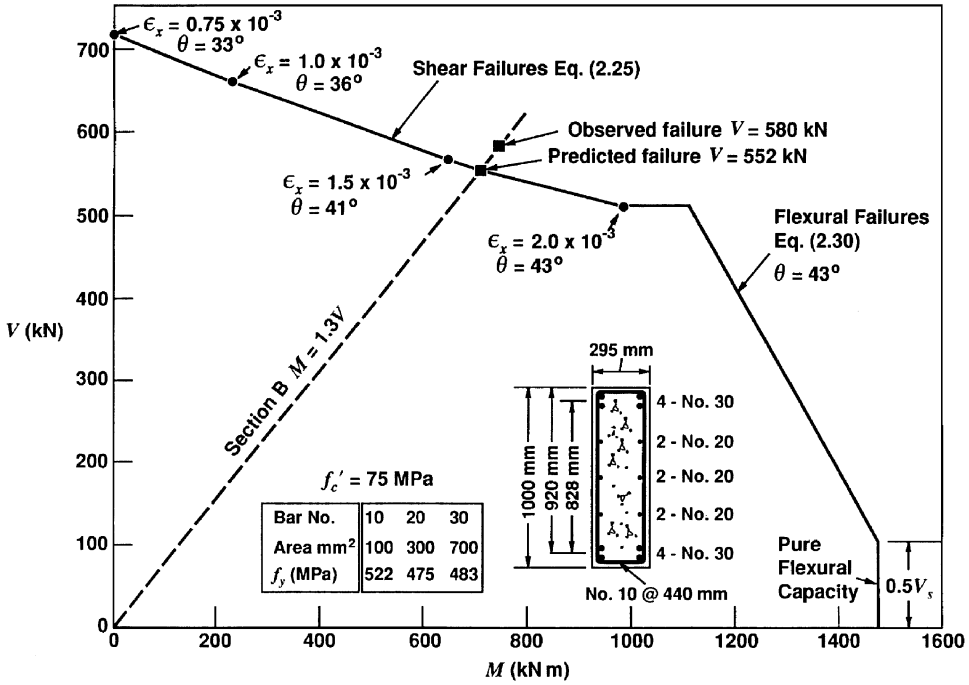

Fig. 2.17—Shear-moment interaction diagram for rectangular section.

distance d_v cot θ past the point at which it is no longer required for flexure alone.

For sections at least a distance d_v away from the maximum moment locations, the MCFT predicts that increasing the moment decreases the shear strength, while increasing the shear decreases the flexural strength. This point is illustrated in Fig. 2.17, which gives the shear-moment interaction diagram for Section B of the beam described in Fig. 2.1. The shear-failure line shown in this figure was determined by calculating V from Eq. (2-25) with the β and θ values corresponding to chosen values of ε_x and then using Eq. (2-26) to determine the corresponding values of M. The flexural-failure line, which corresponds to yielding of the longitudinal steel, was determined from Eq. (2-31) with ϕ taken as unity. A shear-moment interaction diagram, such as that shown in Fig. 2.17, can be used to determine the predicted failure load of a section when it is subjected to a particular loading ratio. Section B of the beam shown in Fig. 2.1 is loaded such that the moment-to-shear ratio equals 1.3 m (that is, $M/Vd = 1.41$). At this loading ratio, the section is predicted to fail in shear with yielding of the stirrups and slipping of the cracks when the shear reaches a value of 552 kN. For this beam, the experimentally determined failure shear was about 5% higher than this value.

CHAPTER 3—TRUSS APPROACHES WITH CONCRETE CONTRIBUTION

3.1—Introduction

The traditional truss model assumes that the compression struts are parallel to the direction of cracking and that no stresses are transferred across the cracks. This approach has been shown to yield conservative results when compared with test evidence. More recent theories consider one or both of the following two resisting mechanisms: 1) tensile stresses in concrete that exist transverse to the struts; or 2) shear stresses that are transferred across the inclined cracks by aggregate interlock or friction. Both mechanisms are interrelated and result in: 1) the angle of the principal compression stress in the web being less than the crack angle; and 2) a vertical component of the force along the crack that contributes to the shear strength of the member. The resisting mechanisms give rise to V_c, the concrete contribution. These theories typically assume that there is no transfer of tension across cracks.

In this chapter, several approaches incorporating the so-called concrete contribution are discussed, which begin with the assumptions for the angle and the spacing of the inclined cracks. Then, the principal tensile strain, ε_1, in the web and the widths of the inclined cracks are calculated, as in the MCFT, discussed in Chapter 2. The stress transfer across the cracks can then be determined, giving V_c. The state of stress in the web results in tensile stress in the web perpendicular to the principal compressive stresses.

This chapter also contains a brief review of the recent European codes EC2, Part 1 (1991) and CEB-FIP Model Code 1990 (1993), which are based on related approaches.

3.2—Overview of recent European codes

The strut-and-tie model approaches have influenced recent European codes including, to a lesser extent, EC2, Part 1 (1991) and, to a larger extent, CEB-FIP Model Code 1990 (1993). EC2, Part 1 is primarily based on the previous CEB-FIP Model Code 1978, although the design clauses contain several changes. The static or lower-bound approach of the theory of plasticity may be used in the design. Appropriate measures should be taken to ensure ductile behavior (EC2, Part 1, Section 2.5.3.6.3). Corbels, deep beams, and anchorage zones for post-tensioning forces (EC2, Part 1,

Section 2.5.3.7) may be analyzed, designed, and detailed in accordance with lower-bound plastic solutions. In this approach, the average design compressive stress may be taken as νf_{cd} with $\nu = 0.60$ and $f_{cd} = f_{ck}/1.5$ the factored design strength (with $f_{ck} = 0.9f_c'$ for a concrete of about 28 MPa, the value of $0.60f_{cd}$ corresponds to about $0.54f_c'/1.5 = 0.36f_c'$). Them aximum strength to be used in axial compression is $0.85f_{cd}$, including an allowance for sustained load.

The shear design expressions use three different values for shear resistance: V_{Rd1}, V_{Rd2}, and V_{Rd3}. The shear resistance V_{Rd1} is for members without shear reinforcement and is based on an empirical formula. This formula incorporates the influence of concrete strength, reinforcing ratio, member depth, and axial forces.

The resistance V_{Rd2} is the upper limit of the shear strength intended to prevent web-crushing failures. The limiting value is a function of: 1) the inclination and spacing of the cracks; 2) the tensile strain in the transverse reinforcement; and 3) the longitudinal strain in the web. The limiting value of the shear strength is calculated using an effective diagonal stress in the struts $f_{dmax} = (\nu f_{cd})$. As a simplification, the effectiveness factor ν in EC2, Part 1 is given by the expression

$$\nu = 0.70 - f_{ck}/200 \tag{3-1}$$

with f_{ck} (MPa) as the characteristic cylinder strength (approximately $0.9f_c'$). The stress in the inclined struts is calculated from equilibrium as

$$f_d = V_u/b_v d_v \cos\theta \sin\theta \tag{3-2}$$

The resistance V_{Rd3}, provided by the shear reinforcement, may be determined from two alternative design methods—the standard method or the variable-angle truss method. The standard method is similar to the current U.S. design practice where a concrete contribution is added to that of the shear reinforcement

$$V_{Rd3} = V_{cd} + V_{wd} \tag{3-3}$$

The concrete contribution V_{cd} is assumed equal to V_{Rd1}, the shear resistance of members without shear reinforcement. The resistance of the vertical shear reinforcement is given by

$$V_{wd} = A_v f_y 0.9d/s \tag{3-4}$$

based on a flexural lever arm of $0.9d$ between the truss chords (d = effective depth).

The variable-angle truss method uses a truss with struts inclined at an angle θ. The strength provided by the shear reinforcement for beams with transverse stirrups follows from the vertical equilibrium

$$V_{Rd3} = V_s = (A_v/s) f_{yv} 0.9d \cot\theta \tag{3-5}$$

where

A_v = area of the transverse stirrups at spacing s;

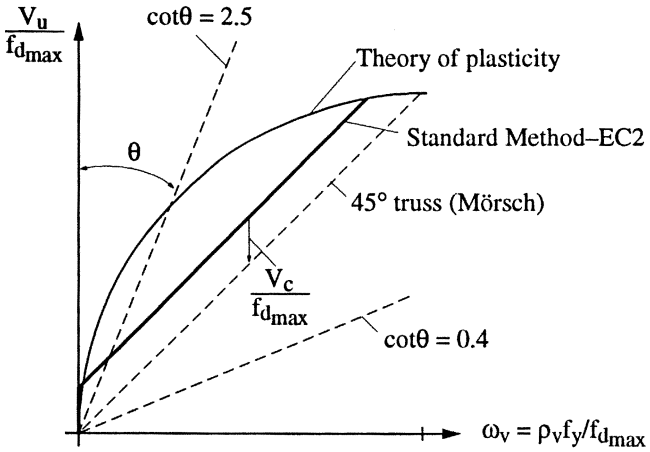

Fig. 3.1—Calculated shear strength as function of θ and shear reinforcement index ($\rho_v = A_v/b_w s$).

f_{yv} = yield strength of the shear reinforcement;
$0.9d$ = flexural lever arm or effective truss depth; and
θ = angle of inclined struts.

The theory of plasticity assumes that the capacity of the web is achieved by reaching simultaneously the yielding of the shear reinforcement and the limiting stress, f_d, in the inclined struts (web crushing), Eq. (3-2). This assumption yields a condition for the angle θ of the inclined struts and a function for the capacity depending on the amount of shear reinforcement. This function may be plotted in a dimensionless format, and it appears as a quarter circle (Fig. 3.1). This figure shows that, for given amounts of transverse reinforcement, much larger capacities are predicted than those based on the traditional Mörsch model, which assumes a strut inclination $\theta = 45$ degrees. For very low amounts of transverse reinforcement, very flat angles θ are predicted so that mostly lower limits are given to avoid under-reinforced members. For comparison, Fig. 3.1 also shows the predictions using Eq. (3-3) according to the standard method of EC2. According to EC2, Section 4.3.2.4.4, the angle θ in Eq. (3-5) may be varied between:

- $-0.4 < \cot\theta < 2.5$ for beams with constant longitudinal reinforcement; and
- $-0.5 < \cot\theta < 2.0$ for beams with curtailed longitudinal reinforcement

There are different interpretations of these limits. For example, in Germany, the minimum inclination was increased to $\cot\theta = 1.75$ for reinforced concrete members. For members subjected also to axial forces, the following value is suggested

$$\cot\theta = (1.25 - 3\sigma_{cp}/f_{cd}) \tag{3-6}$$

with σ_{cp} = axial stress in middle of web. In the presence of axial tension, larger strut angles are required, and the limits of EC2 are considered unsafe.

The provisions for member design have been based on strut-and-tie models instead of a separate sectional design for the different effects of bending, axial load, shear, and torsion. The shear design is based on the theory of plasticity using the

variable-angle truss method. The strut angle may be assumed as low as about 18 degrees, corresponding to cot θ = 3. CEB-FIP Model Code 1990 (1993) limits the compressive stress in the struts in a form similar to that given by Eq. (3-1).

In EC2, Part 1 (1991), minimum reinforcement amounts are required in beams for the longitudinal reinforcement as well as for the shear reinforcement. The latter is made dependent on the concrete class and the steel class, and, for example, amounts to a minimum required percentage of shear reinforcement, min $\rho_v = 0.0011$ for steel with f_y = 500 MPa and medium concrete strengths between $f'_c = 23$ and 33 MPa. For higher concrete strengths, the value is increased to min $\rho_v = 0.0013$. For slabs, no minimum transverse reinforcement is required.

CEB-FIP Model Code 1990 requires a minimum longitudinal reinforcement in the tension zone of 0.15%. The required minimum amount for the shear reinforcement in webs of beams is expressed in terms of a mechanical reinforcing ratio rather than a geometrical value min ρ_v. The requirement is min $\omega v = \rho_v f_y / f_{ctm} = 0.20$. This correctly expresses that, for higher concrete strengths (that is, higher values of average tensile strengths f_{ctm}), more minimum transverse reinforcement is required. In terms of min ρ_v, this means about 0.090% for concrete having a compressive strength of about 22 MPa, 0.14% for concrete with 41 MPa compressive strength, and 0.20% for 67 MPa concrete.

3.3—Modified sectional-truss model approach

In the so-called "modified sectional-truss model" approach (CEB-FIP 1978; EC2 1991; Ramirez and Breen 1991) the nominal shear strength of nonprestressed or prestressed concrete beams with shear reinforcement is $V_n = V_c + V_s$, where V_c represents an additional concrete contribution as a function of the shear stress level, and V_s = strength provided by the shear reinforcement.

For nonprestressed concrete beams, the additional concrete contribution V_c has been suggested (Ramirez and Breen 1991) as

$$V_c = \frac{1}{2}(3v_{cr} - v)b_w d \tag{3-7}$$

where

v_{cr} = shear stress resulting in the first diagonal tension cracking in the concrete; and

v = shear stress level due to factored loads.

For prestressed concrete beams (Ramirez and Breen 1991), the additional concrete contribution takes the form of

$$V_c = K\left(\frac{\sqrt{f'_c}}{6}\right)b_w 0.9d \tag{3-8}$$

with f'_c in MPa, where K is the factor representing the beneficial effect of the prestress force on the concrete diagonal tensile strength and further capacity after cracking. The expression for the K factor can be derived from a Mohr circle analysis of an element at the neutral axis of a prestressed concrete beam before cracking and is

$$K = \left[1 + \frac{f_{pc}}{f_t}\right]^{0.5} \tag{3-9}$$

where

f_t = principal diagonal tension stress; and

f_{pc} = normal stress at the neutral axis.

This expression is the same one used in ACI 318M-95 as the basis for the web cracking criteria V_{cw}. The factor K is usually limited to 2.0, and is set equal to 1.0 in those sections of the member where the ultimate flexural stress in the extreme tension fiber exceeds the concrete flexural tensile strength. This limitation is similar to the provision in 318M-95 that limits the concrete contribution to the smaller of the two values, V_{cw} and V_{ci}.

The strength provided by the shear reinforcement, V_s, for beams with vertical stirrups represents the truss capacity in shear derived from the equilibrium condition by summing the vertical forces on an inclined crack free-body diagram. The resulting expression is given in Eq. (3-5). According to Ramirez and Breen (1991), the lower limit of angle of inclination θ for the truss diagonals is 30 degrees for nonprestressed concrete and 25 degrees for prestressed beams. The additional longitudinal tension force due to shear can be determined from equilibrium conditions of the truss model as V_u cot θ, where V_u = factored shear force at the section. Because the shear stresses are assumed uniformly distributed over the depth of the web, this force acts as the section middepth; thus, it may be resisted by equal additional tension forces acting at the top and bottom longitudinal truss chords, with each force being equal to $0.5V$ cot θ. In this approach, a limit of $2.5\sqrt{f'_c}$ (MPa) has also been proposed (Ramirez and Breen 1991) that represents the diagonal compressive strength as a function of the shear that can be carried along the diagonal crack surface. The diagonal compression stress can be calculated from equilibrium and geometry considerations in the diagonally cracked web, resulting in an expression similar to Eq. (3-2).

The term V_c is reflected in the design of the stirrup reinforcement, but it does not affect dimensioning of the longitudinal reinforcement or the check of diagonal compressive stresses. This is justified by the fact that experimental observations have shown that dimensioning of the shear reinforcement (stirrups) based entirely on the equilibrium conditions of the parallel chord truss model described in this section unduly penalizes the majority of members that are subjected to low levels of shear stress or that have no or low amounts of shear reinforcement. A similar effect on the longitudinal reinforcement, however, has not been fully verified. The fact that there are relatively few large-scale specimens, that most tests consist of beams with continuous longitudinal reinforcement, and that almost all of the test beams are simply supported under a point load would seem to justify a simple expression for the required amount of longitudinal reinforcement at this time. The check of diagonal compressive stresses is a

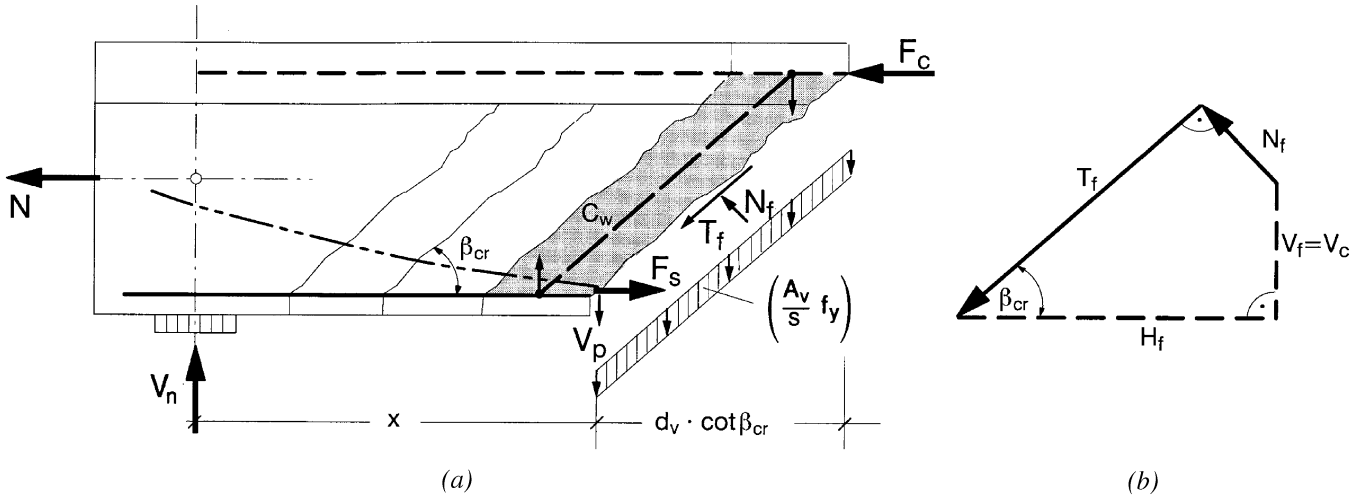

Fig. 3.2—Free-body diagram of B region at end support and forces at crack due to friction: (a) free-body diagram of end support region; and (b) forces due to friction (Reineck 1991a).

conservative check on the maximum shear force that can be carried by the reinforced concrete member without a web-crushing failure.

3.4—Truss models with crack friction

3.4.1 *Equilibrium of truss models with crack friction*—The truss model with crack friction starts with basic assumptions for the spacing and shape of cracks in a B region of a structural-concrete member subjected to shear. It is assumed that forces are transferred across the cracks by friction, which depends on the crack displacements (slips and crack widths); therefore, the strains in the member have to be calculated. This approach was developed for the shear design of webs by several researchers, including Gambarova (1979), Dei Poli et al. (1987, 1990), Kupfer et al. (1979, 1983), Kirmair (1987), Kupfer and Bulicek (1991), and Reineck (1990, 1991a).

The approach uses the free-body diagram in Fig. 3.2, which is obtained by separating the member along an inclined crack in the B region of a structural-concrete member with transverse reinforcement. Vertical equilibrium of this body gives the basic equation

$$V_n = V_s + V_c + V_p \tag{3-10}$$

where

V_n = total shear resisted (nominal shear strength);
V_s = shear force carried by the stirrups;
V_c = sum of the vertical components of the tangential friction forces at the crack T_f, and the normal force at the crack N_f (see Fig. 3.2(b)); and
V_p = vertical component of force in prestressing tendon.

The dowel force of the longitudinal reinforcement, which has a role in members without transverse reinforcement, is neglected (see Fig. 3.2). Furthermore, the chords are assumed to be parallel to the axis of the member so that there is no vertical component of an inclined compression chord of the truss. Leonhardt (1965, 1977), Mallee (1981), and Park and Paulay (1975) have proposed truss models with inclined chords, but these models are more complicated. For a nonprestressed concrete member of constant depth, Eq. (3-10) simplifies to

$$V_n = V_s + V_c \tag{3-11}$$

The shear force component carried by all the stirrups crossing the crack is

$$V_s = A_v f_y d_v \frac{\cot\beta_{cr}}{s} \tag{3-12}$$

where

β_{cr} = crack inclination;
d_v = inner level arm; and
s = stirrup spacing.

The force, V_f, is the vertical component of the combined friction forces, T_f and N_f, across the inclined crack in the web, as shown in Fig. 3.2(b). The tangential force T_f has two components: T_{fo}, the tangential force that may be resisted with N_f equal to zero; and $T_{f\sigma}$, the additional tangential force due to N_f. Equation (3-11) shows that the shear force component, V_f, due to friction is additive with the shear force carried by the stirrups. This is also the case for all design methods with a concrete contribution such as ACI 318M-95 or EC2 with either the standard method (Section 3.2) or the modified truss model approach (Section 3.3). So far, the concrete contribution has mainly been justified empirically, but Eq. (3-11) offers a clear physical explanation for the V_c term; that is, that it is the shear force component, V_f, transferred by friction across the cracks.

3.4.2 *Inclination and spacing of inclined cracks*—In the use of the truss model with crack friction, a necessary condition is that the crack inclination and the crack spacing should be assumed or determined by nonlinear analysis. The angle of the inclined cracks is normally assumed at 45 degrees for nonprestressed concrete members. Kupfer et al. (1983) has pointed out that this angle could be up to 5 degrees flatter, because of a reduction of Young's modulus caused by micro-

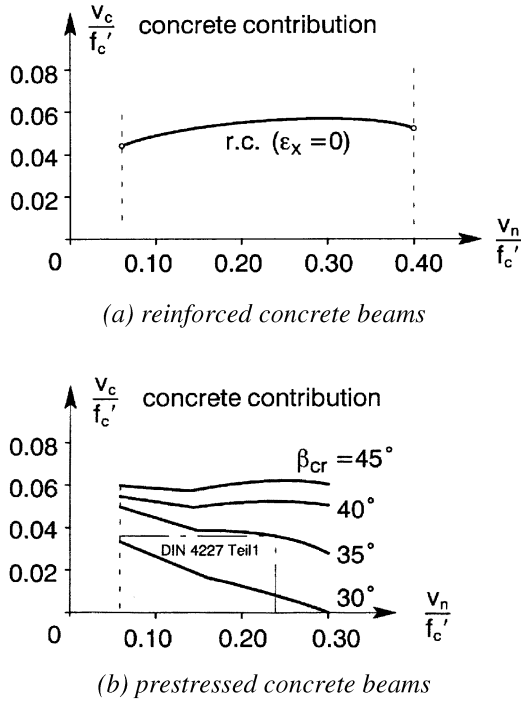

(a) reinforced concrete beams

(b) prestressed concrete beams

Fig. 3.3—Shear force carried by crack friction versus ultimate shear force plotted in a dimensionless diagram.

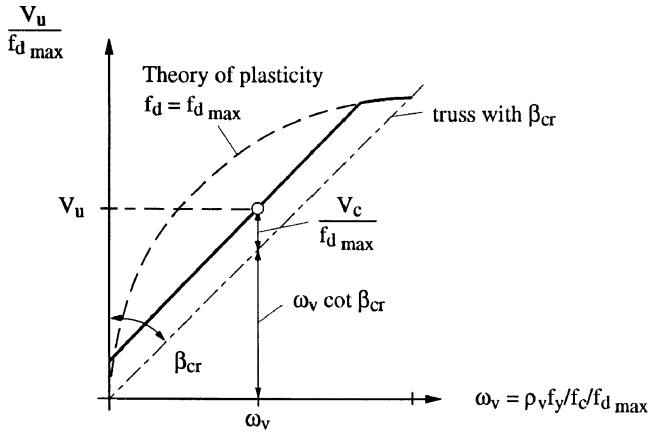

Fig. 3.4—Design diagram with simplified shear force component V_f *due to friction, proposed by Reineck (1990, 1991a).*

cracking. Flatter angles will appear for prestressed concrete members or for members with axial compression, and steeper angles will occur for members with axial tension. For such members, the angle of the principal compressive stress at the neutral axis of the uncracked state is commonly assumed as the crack angle (Loov and Patniak 1994).

The spacing of the inclined cracks is primarily determined by the amount and spacing of reinforcement, and relevant formulas have been proposed by Gambarova (1979), Kupfer and Moosecker (1979), Kirmair (1987), and Dei Poli et al. (1990).

3.4.3 *Constitutive laws for crack friction*—The truss model with crack friction requires constitutive laws for the transfer of forces across cracks by friction or interface shear. Before 1973, this shear transfer mechanism was known and clearly defined by the works of Paulay and Fenwick, Taylor, and others (see Section 4.3.3), but only a few tests and no theories were available for formulating reliable constitutive laws. This has changed considerably in the last 20 years due to the work of Hamadi (1976), Walraven (1980), Walraven and Reinhardt (1981), Gambarova (1981), Daschner and Kupfer (1982), Hsu et al. (1987), Nissen (1987), and Tassios and Vintzeleou (1987). An extensive state-of-the-art report on interface shear was recently presented by Gambarova and Prisco (1991).

The constitutive law proposed by Walraven (1980) has often been used by others because it describes not only the shear stress-slip relation for different crack widths but also the associated normal stresses. It was based on a physical model for the contact areas between crack surfaces, and the proposed laws were corroborated with tests on concrete with normal as well as lightweight aggregates (see Section 4.3.3).

3.4.4 *Determining shear resistance* $V_f = V_c$ *due to crack friction*—The shear force component $V_f = V_c$ in Eq. (3-10) and (3-11) transferred by friction across the cracks depends on the available slip and on the crack width, requiring that the strains in the chords and in the web be determined. In addition, the displacements and the strains should be compatible with the forces in the model according to the constitutive laws for the shear force components. Often the capacity of the crack friction mechanism is reached before crushing of the concrete struts between the cracks. Figure 3.3 gives the results of different calculations of the shear force component $V_f = V_c$ in terms of stress from Dei Poli et al. (1987) and Kupfer and Bulicek (1991), but similar results have been obtained by Leonhardt (1965) and Reineck (1990, 1991a). The shear stress, v_c, in Fig. 3.3 depends on the magnitude of the shear, the strains of the struts and stirrups on the longitudinal strain ε_x in the middle of the web, and on the crack spacing. The results in Fig. 3.3 support the notion that, for a wide range of applications and for code purposes, a constant value of the concrete contribution may be assumed. The practical result for the shear design is the dimension-free design diagram shown in Fig. 3.4, which is well known and used in many codes (see also Fig. 3.1). Crack friction governs the design for low and medium shear. For very high shear, the strength of the compression struts governs, which is characterized by the quarter circle in Fig. 3.4, as explained in Fig. 3.1. The crack friction approach considers the influence of axial forces (tension and compression) as well as prestress, as shown in Fig. 3.5. For a member with axial tension (Fig. 3.5(a)), steeper inclined cracks occur in the web and the term V_c is reduced so that more transverse reinforcement is required in comparison with a member without axial forces (Fig. 3.4). The opposite is the case for prestressed members or members with axial compression (Fig. 3.5(b)); the cracks are flatter, so that less transverse reinforcement is required than for a member without axial force (Fig. 3.4), although the term V_c is reduced and may even disappear.

3.4.5 *Stresses and strength of concrete between cracks*—The main function of the concrete between the cracks is to act as the struts of a truss formed together with the stirrups as described by Mörsch (1920, 1922) (see Fig. 3.6(a)). The additional friction forces acting on the crack surfaces result

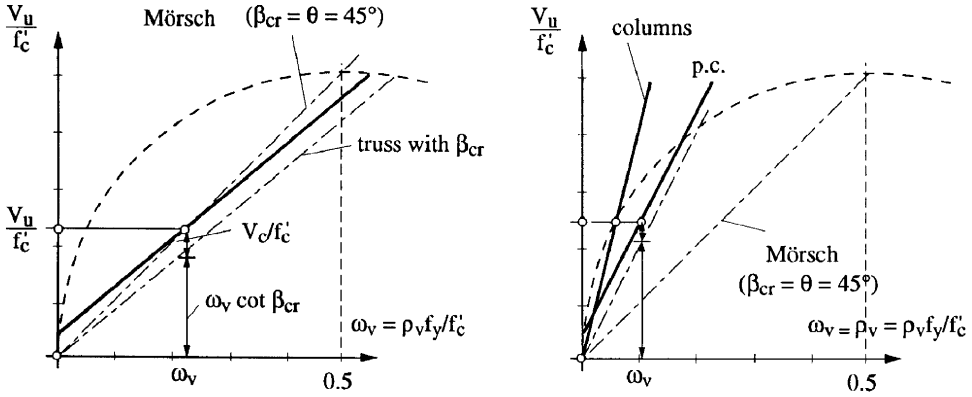

(a) reinforced concrete beams *(b) prestressed concrete beams*

Fig. 3.5—Simplified design diagram for members subjected to shear and axial forces as proposed by Reineck (1991).

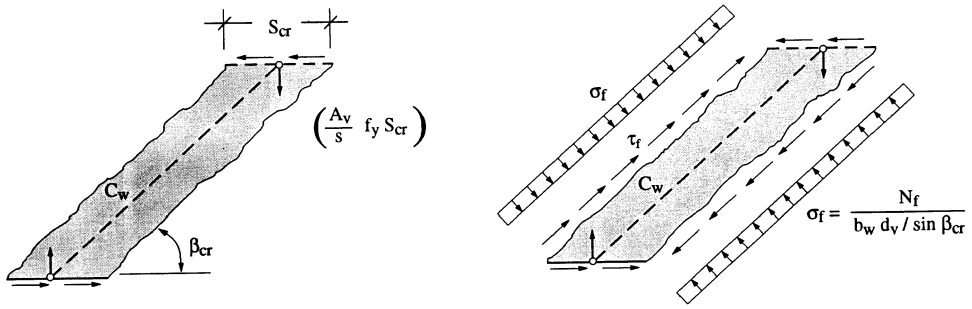

(a) stirrup forces acting on strut *(b) friction forces acting on strut*

Fig. 3.6—Forces and stress fields in discrete concrete struts between cracks (Kupfer et al. 1983; Reineck 1991a).

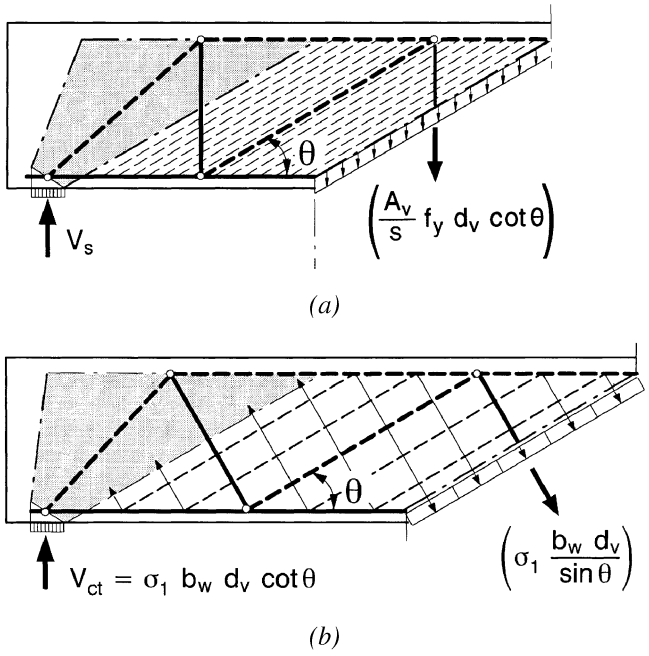

Fig. 3.7—Smeared truss-models corresponding to principal struts between cracks as proposed by Reineck (1991a): (a) truss with uniaxial compression field; and (b) truss with biaxial tension-compression field.

in a biaxial state of stress with a principal compression field at a flatter inclination than the crack angle β_{cr}.

The minor principal stress is tensile for small shear forces so the state of stress may be visualized by the two trusses shown in Fig. 3.7. The usual truss model with uniaxial compression inclined at the angle θ in Fig. 3.7(a) is superimposed on a truss with concrete tension ties perpendicular to the struts (Fig. 3.7(b)). Thus, there are two load paths for the shear transfer, as defined by Schlaich et al. (1987) and as earlier shown by Reineck (1982), and with different explanations by Lipski (1971, 1972) and Vecchio and Collins (1986) in their MCFT. The model in Fig. 3.7(b) is the same as that proposed by Reineck (1989; 1991a,b) for members without transverse reinforcement, so that the transition from members with to members without transverse reinforcement is consistently covered.

For high shear forces, the minor principal stress is compressive. These compressive stresses are so small, however, that they are usually neglected, and only the truss of Fig. 3.7(a) remains with a uniaxial compression field. This is the model used in the theory of plasticity.

The concrete between the cracks is uncracked and forms the strut. Apart from the compressive stresses due to the truss action, however, there is also transverse tension in the struts due to the friction stresses and forces induced by the bonded stirrups. This reduces the strength below that allowed in

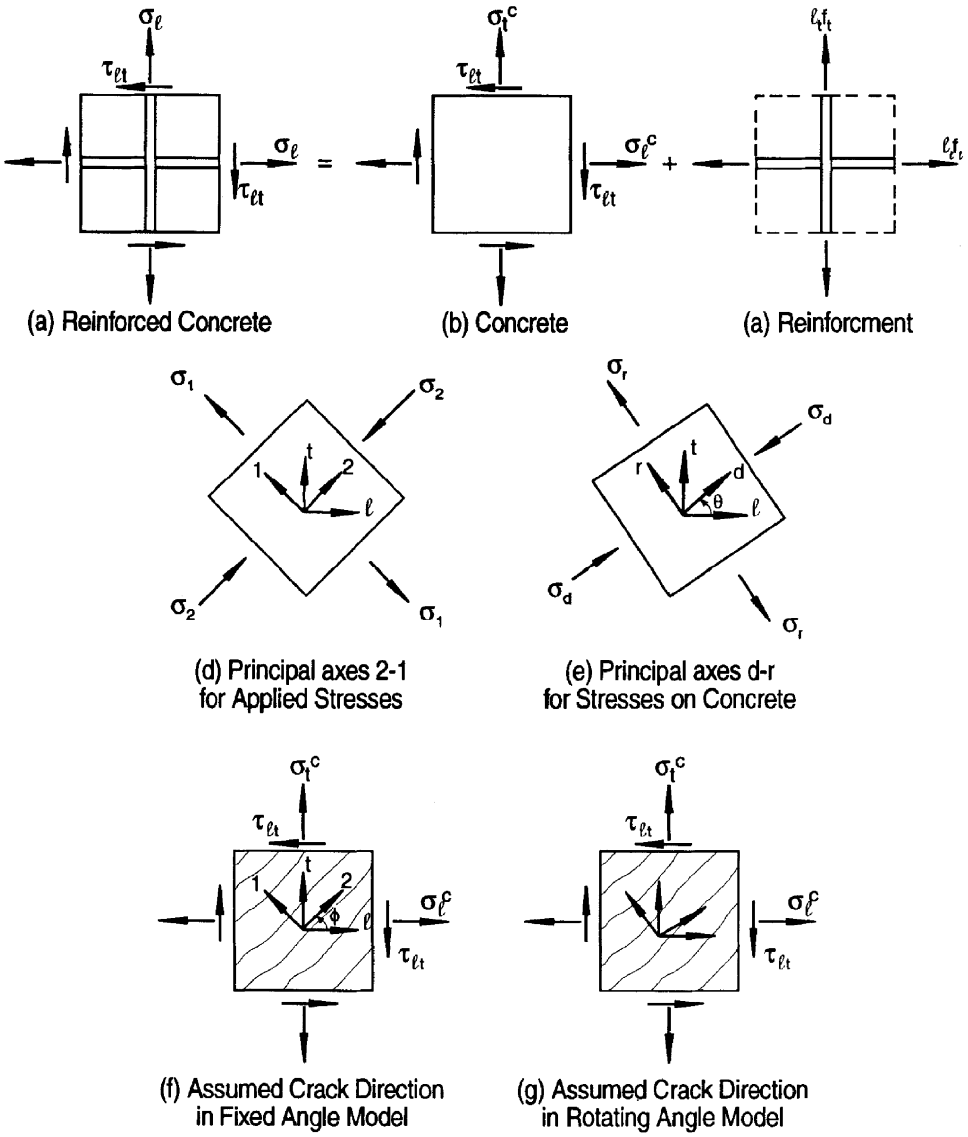

Fig. 3.8—Reinforced concrete membrane elements subjected to in-plane stresses.

compression chords. Further reasons for such a reduction are also the smaller effective width of the strut (rough crack surfaces) and the disturbances by the crossing stirrups. Schlaich and Schafer (1983), Eibl and Neuroth (1988), Kollegger/Mehlhorn (1990), and Schafer et al. (1990) reached the conclusions that the effective concrete strength of the struts could be assumed as

$$f_{dmax} = 0.80 f_{ck} = 0.72 f_c' \qquad (3\text{-}13)$$

This is a relatively high value compared to those discussed in Chapters 2 and 6 and the so-called "effective strengths" of, for example, $0.60 f_{ck} = 0.54 f_c'$ or $0.50 f_{ck} = 0.45 f_c'$ used in the theory of plasticity. The results of the higher value for compressive strength is that, for high ratios of transverse reinforcement, excessively high shear capacities may be predicted.

3.5—Fixed-angle softened-truss models

Hsu and his colleagues have proposed two different softened-truss models to predict the response of membrane elements subjected to shear and normal stress (Pang and Hsu 1992, 1996; Zhang 1995). The rotating angle softened-truss model considers the reorientation of the crack direction that occurs as the loads are increased from initial cracking up to failure (see Fig. 3.8(g)). This first model has been discussed in Chapter 2. The second model, known as the fixed-angle softened-truss model, assumes that the concrete struts remain parallel to the initial cracks. This initial crack direction depends on the principal concrete stress directions just before cracking (see Fig. 3.8(f)). With the terms defined as in Fig. 3.8, the equilibrium and compatibility equations for this fixed-angle softened-truss model are as follows

- Equilibrium equations

$$\sigma_l = \sigma_2^c \cos^2\phi + \sigma_1^c \sin^2\phi + \tau_{21}^c 2\sin\phi\cos\phi + \rho_l f_l \qquad (3\text{-}14)$$

$$\sigma_t = \sigma_2^c \sin^2\phi + \sigma_1^c \cos^2\phi - \tau_{21}^c 2\sin\phi\cos\phi + \rho_t f_t \qquad (3\text{-}15)$$

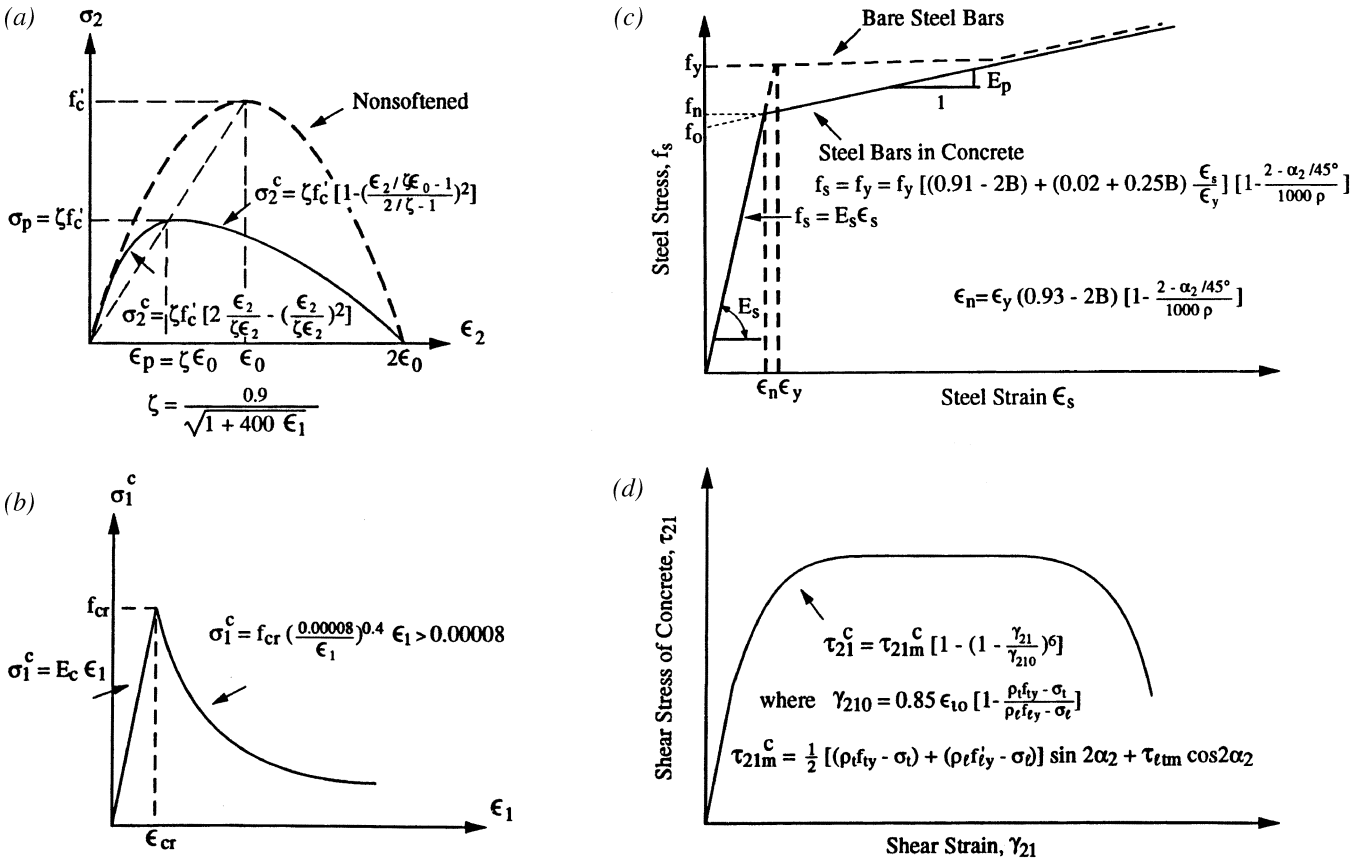

Fig. 3.9—Constitutive laws of concrete and steel: (a) softened stress-strain curve of concrete in compression; (b) average stress-strain curve of concrete in tension; (c) average stress-strain curve of steel bars in concrete; (d) average stress-strain curve of concrete in shear.

$$\tau_{lt} = (-\sigma_2^c + \sigma_1^c)\sin\phi\cos\phi + \tau_{21}^c(\cos^2\phi - \sin^2\phi) \quad (3\text{-}16)$$

where

σ_2^c, σ_1^c = average normal stresses of concrete in Directions 2 and 1, respectively;

τ_{21}^c = average shear stress of concrete in 2-1 coordinate; and

ϕ = angle of inclined cracks.

[In the following equations, the symbol ϕ is kept, following previous works by Pang and Hsu (1992, 1996) and Zhang (1995); ϕ actually is the same as β_{cr} in this chapter.]

- Compatibility equations

$$\varepsilon_l = \varepsilon_2\cos^2\phi + \varepsilon_1\sin^2\phi + \gamma_{21}\sin\phi\cos\phi \quad (3\text{-}17a)$$

$$\varepsilon_t = \varepsilon_2\sin^2\phi + \varepsilon_1\cos^2\phi - \gamma_{21}\sin\phi\cos\phi \quad (3\text{-}17b)$$

$$\gamma_{lt} = 2(-\varepsilon_2 + \varepsilon_1)\sin\phi\cos\phi + \gamma_{21}(\cos^2\phi - \sin^2\phi) \quad (3\text{-}18)$$

where

$\varepsilon_1, \varepsilon_2$ = average normal strain of element in Directions 2 and 1, respectively; and

γ_{21} = average shear strain of element in 2-1 coordinate.

Because Eq. (3-14) to (3-18) are based on the 2-1 coordinate, they include the terms for shear stress, τ_{21}^c, and shear strain, γ_{21}, of cracked concrete. After cracking, the principal compressive stress direction in the concrete struts will typically not coincide with the crack direction; that is, $\theta \neq \phi$. This corresponds to the concept of friction across the cracks as discussed in Section 3.4. In applying these equations, the stresses are determined from the strains using the constitutive laws shown in Fig. 3.9. An efficient algorithm for the solution of the equations in the fixed-angle softened-truss model has been developed (Zhang 1995).

The shear yield strength of a membrane element has been derived from the fixed-angle softened truss model (Pang and Hsu 1996) to be

$$\tau_{lt} = \frac{(\tau_{21}^c)^2}{2\sqrt{\rho_l f_{ly}\rho_t f_{ty}}} + \sqrt{\rho_l f_{ly}\rho_t f_{ty}} \quad (3\text{-}19)$$

The right-hand side of Eq. (3-19) consists of two terms: the first term is the contribution of concrete, V_c, attributable to τ_{21}^c the shear stress of cracked concrete in the 2-1 coordinate; and the second term is the contribution of steel V_s.

3.6—Summary

Shear design codes require a simple means of computing a realistic V_c term. This so-called concrete contribution is

important in the design of beams where the factored shear force is near the value of the shear force required to produce diagonal tension cracking. This term is necessary for the economic design of beams and slabs with little or no shear reinforcement.

In this chapter, several truss model approaches incorporating a concrete contribution term have been discussed. The implementation of this philosophy in recent European codes has also been illustrated. In this chapter, a physical explanation is given of the concrete contribution term, V_c, in the form of the vertical component of the forces transferred across the inclined cracks. This crack leads to a sliding failure through the compression strut. In other approaches, this phenomenon is accounted for by permissible stresses for the struts, that is, reduction factors v as explained, for example, in Section 3.2.

The approaches discussed in this chapter as well as the MCFT in Chapter 2 describe the structural behavior of beams under increasing load. This behavior cannot be covered by the truss model alone. Furthermore, the truss model with crack friction discussed in Section 3.4 can be extended to regions of geometrical discontinuities (D regions). In those regions, the formation of a single crack indicating a failure surface is very likely. Common examples are beams with openings, dapped end-supports, frame corners, and corbels (Marti 1991). In all of these cases, a crack will start from the corner, and a premature failure may occur before the steel yields.

The fixed-angle softened-truss model proposed by Hsu and his colleagues assumes that the initial crack direction remains unchanged. The orientation of these initial cracks is dictated by the orientation of principal stresses just prior to cracking. After cracking, shear stresses due to friction develop in these cracks so that the principal compressive stress direction is not the same as the crack direction. Such was the case also in the truss model with crack friction approach. The fixed-angle method also results in a concrete contribution term.

CHAPTER 4—MEMBERS WITHOUT TRANSVERSE REINFORCEMENT

4.1—Introduction

Structural-concrete members with sufficient reinforcement in both directions (longitudinal and transverse) can be designed using the simple strut-and-tie models described in Chapter 6 or the theories described in Chapters 2 and 3. Many structural-concrete members are constructed without transverse reinforcement (that is, no stirrups or bent-up bars), such as slabs, footings, joists, and lightly stressed members. The application of a simple strut-and-tie model, as shown in Fig. 4.1, may result in an unsafe solution. Assuming that the shear in this slender member without transverse reinforcement is carried by a flat compression strut predicts that failure will be due to yielding of the longitudinal reinforcement, whereas in reality, a brittle shear failure occurred due a diagonal crack.

The 1973 ASCE-ACI Committee 426 report gave a detailed explanation of the behavior of beams without transverse reinforcement, including the different shear-

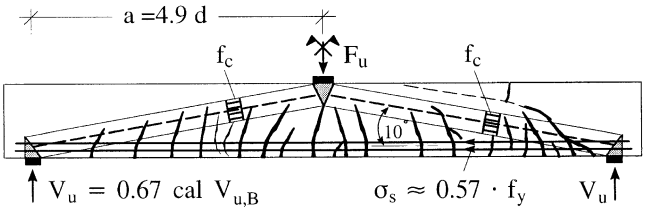

Fig. 4.1—Crack pattern at shear failure of beam with unsafe strut-and-tie model (Kupfer and Gerstle 1973).

transfer mechanisms and failure modes. The main parameters influencing shear failure were discussed, and numerous empirical formulas were given. These equations continue to be the basis of shear design rules in many building codes around the world.

The main goal of this chapter is to review design models and analytical methods for structural-concrete members without transverse reinforcement in light of new developments that have occurred since the early 1970s. Only the two-dimensional problem of shear in one-way members is considered. Punching shear, which is a complex three-dimensional problem, is not discussed here; however, it should be noted that an important reason for the continued research on structural-concrete beams without transverse reinforcement is the development of more rational methods for punching shear. Information on punching shear can be found in the CEB state-of-the-art report prepared by Regan and Braestrup (1985).

4.2—Empirical methods

The simplest approach, and the first to be proposed (Mörsch 1909), is to relate the average shear stress at failure to the concrete tensile strength. This empirical approach is presented first because it forms the basis of ACI 318M-95 and several other codes of practice. Experimental results have shown that the average principal tensile stress to cause secondary diagonal cracking (that is, flexure-shear cracking) is usually much less than concrete tensile strength. One reason is the stress concentration that occurs at the tip of initial cracks. Another factor is the reduction in cracking stress due to coexisting transverse compression (Kupfer and Gerstle 1973). Woo and White (1991) have suggested recently that the reason for the low average stress at flexure-shear cracking is a nonuniform shear stress distribution at the outermost flexural crack as a result of a concentration of bond stresses and a reduction of the internal lever arm due to arch action in the flexurally cracked zone.

A simple lower-bound average shear stress at diagonal cracking is given by the following equation (in MPa units)

$$\frac{V_c}{bd} = v_c = \frac{\sqrt{f'_c}}{6} \tag{4-1}$$

This well-known equation is a reasonable lower bound for smaller slender beams that are not subjected to axial load and have at least 1% longitudinal reinforcement (Fig. 4.2).

The 1962 ASCE-ACI Committee 326 report presented a more complex empirical equation for calculating the shear

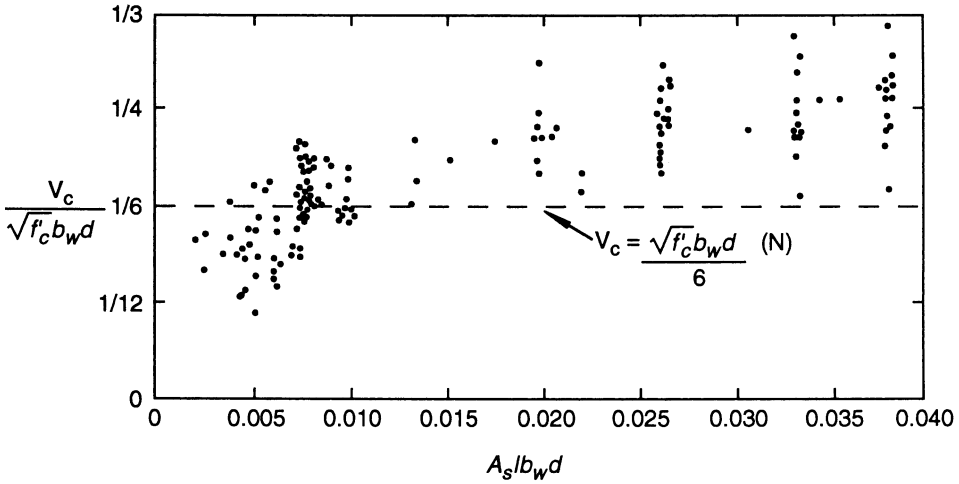

Fig. 4.2—Influence of longitudinal reinforcement amount on shear strength of members without transverse reinforcement (MacGregor 1992).

capacity of beams without web reinforcement (Eq. (11-5) of ACI 318M-95). For a number of reasons, this equation is now considered inappropriate (MacGregor 1992), and in 1977, ASCE-ACI Committee 426 suggested this equation no longer be used. Zsutty (1971) presented the following empirical equation

$$v_c = 59\left(f'_c\,\rho\frac{d}{a}\right)^{1/3} \tag{4-2}$$

where

f'_c = psi (1 MPa = 145.03 psi).

This equation is a significant improvement over Eq. (11-5) in ACI 318M-95.

Many other empirical equations have since been proposed. These equations typically contain the following parameters: the concrete tensile strength, usually expressed as a function of f'_c; the longitudinal reinforcement ratio $\rho = A_s/b_w d$; the shear span-to-depth ratio a/d or M/Vd; the axial force or amount of prestress; and the depth of the member, to account for size effect. Bažant and Kim (1984) also included the maximum size of the aggregates in his formula that is based on fracture mechanics. The empirical formula by Okamura and Higai (1980) and Niwa et al. (1986) considers all the main parameters

$$v_c = 0.20\frac{\rho^{1/3}}{d^{1/4}}(f'_c)\left(0.75 + \frac{1.40}{a/d}\right) \tag{4-3}$$

where ρ = a percentage; d in meters; and f'_c in MPa. This equation may be considered one of the more reliable empirical formulas as recent test results on large beams were considered for the size effect.

With respect to the various empirical formulas, considerable differences exist as a result of the following factors: the uncertainty in assessing the influence of complex parameters in a simple formula; the scatter of the selected test results due to inappropriate tests being considered (for example, bending failures or anchorage failures); the poor representation of some parameters in tests (for example, very few specimens with a low reinforcement amount or high concrete strength); and finally, the concrete tensile strength often not being evaluated from control specimens. These issues limit the validity of empirical formulas and increase the necessity for rational models and theoretically justified relationships.

4.3—Mechanisms of shear transfer

4.3.1 *Overview*—Before shear failure, the state of stress in the web of a cracked reinforced concrete member (that is, the zone between the flexural tension and flexural compression zones) differs considerably from what is predicted by the theory of linear elasticity. Therefore, the question of how a cracked concrete member transmits shear (combined with axial load and bending moment) should be considered. The 1973 ASCE-ACI Committee 426 report identified the following four mechanisms of shear transfer: 1) shear stresses in uncracked concrete, that is, the flexural compression zone; 2) interface shear transfer, often called aggregate interlock or crack friction; 3) dowel action of the longitudinal reinforcing bars; and 4) arch action. Since that report was issued, a new mechanism has been identified, namely 5) residual tensile stresses transmitted directly across cracks.

The question of what mechanisms of shear transfer will contribute most to the resistance of a particular beam is difficult to answer. A cracked concrete beam is a highly indeterminate system influenced by many parameters. Different researchers assign a different relative importance to the basic mechanisms of shear transfer, resulting in different models for members without transverse reinforcement. In the following, the different mechanisms of shear transfer are briefly reviewed, before discussion of the different models in Section 4.4.

4.3.2 *Uncracked concrete and flexural compression zone*—In uncracked B regions of a member, the shear force is transferred by inclined principal tensile and compressive stresses, as visualized by the principal stress-trajectories. In cracked B regions, this state of stress is still valid in the

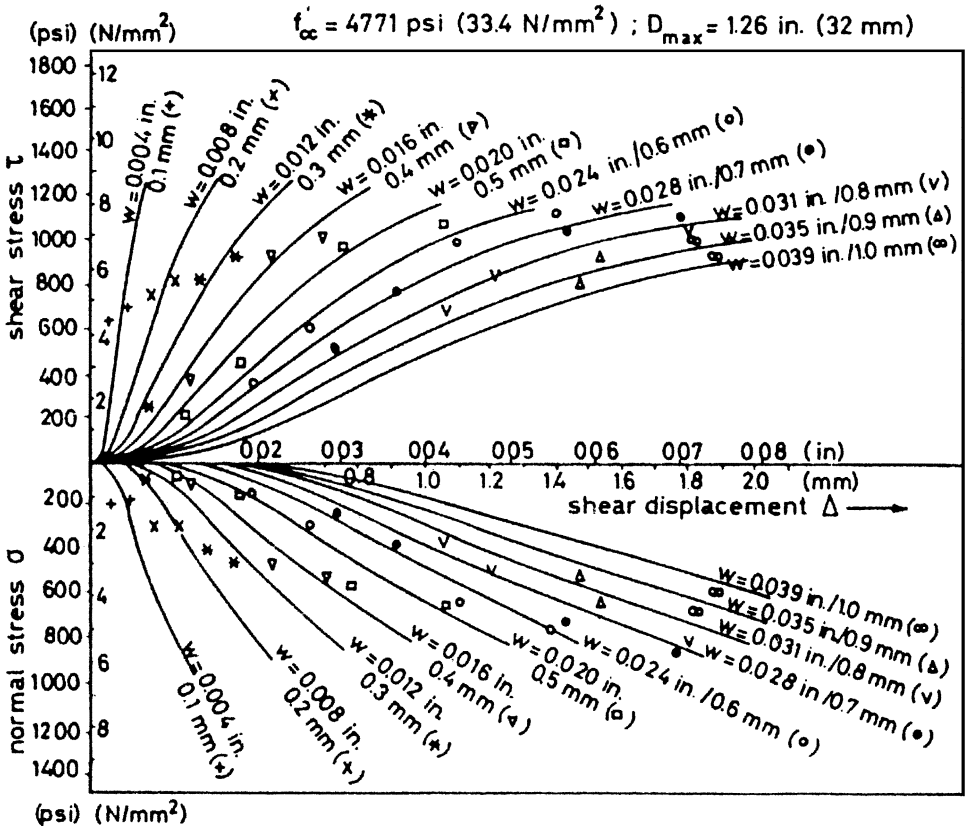

Fig. 4.3—Comparison of Walraven's experimental results and predictions for crack interface shear transfer (Walraven 1981).

uncracked compression zone. The integration of the shear stresses over the depth of the compression zone gives a shear force component, which is sometimes thought to be the explanation for the concrete contribution. Note that the shear force component referred to above is different from the vertical component of an inclined compression strut, which is discussed in Section 4.4.4.

In a slender member without axial compression, the shear force in the compression zone does not contribute significantly to the shear capacity because the depth of the compression zone is relatively small (Taylor 1974; Reineck 1991c). On the other hand, at locations of maximum movement, much of the shear is resisted in the compression zone, particularly after significant yielding of the longitudinal reinforcement.

4.3.3 *Interface shear transfer*—The interface shear transfer mechanism was clearly described in the 1973 ASCE-ACI Committee 426 report, based on work by Fenwick and Paulay (1968), Mattock and Hawkins (1972), and Taylor (1974). The physical explanation for normal-density concrete was aggregate interlock; that is, aggregates protruding from the crack surface provide resistance against slip. Because the cracks go through the aggregate in lightweight and high-strength concrete and still have the ability to transfer shear, however, the term "friction" or "interface shear" is more appropriate. These latter terms also indicate that this mechanism depends on the surface conditions and is not merely a material characteristic.

Significant progress (Gambarova 1981; Walraven 1981; Millard and Johnson 1984; Nissen 1987) has been made in the last two decades toward understanding this mechanism, which involves the relationships between four parameters: crack interface shear stress, normal stress, crack width, and crack slip. Walraven (1981) developed a model that considered the probability that aggregate particles (idealized as spheres) will project from the crack interface. Numerous test results are shown in Fig. 4.3. In Walraven's model, the relationship between stresses and displacements are a function of the concrete compressive strength; however, these relationships were developed for a range of normal (compressive) stresses beyond the range that is relevant for shear transfer in beams without stirrups. Other relationships have been proposed based on Walraven's experimental data (Kupfer et al. 1983; Vecchio and Collins 1986), which assume that the shear that can be transferred is a function of $\sqrt{f'_c}$. Although large differences may still occur between the constitutive laws of different researchers, it may be said that this mechanism is now well known and is widely accepted as an important shear-transfer mechanism.

The important role of interface shear transfer in the redistribution of diagonal compression fields in beams with stirrups is well known (Collins 1978; Kupfer et al. 1983; Dei Poli et al. 1990). In the compression field approaches for members with stirrups (Chapter 2), this effect is implicit within the diagonal crushing strength of concrete. In a number of the models discussed later in this chapter, the ability of diagonal cracks to transfer shear explicitly controls the capacity of members without stirrups.

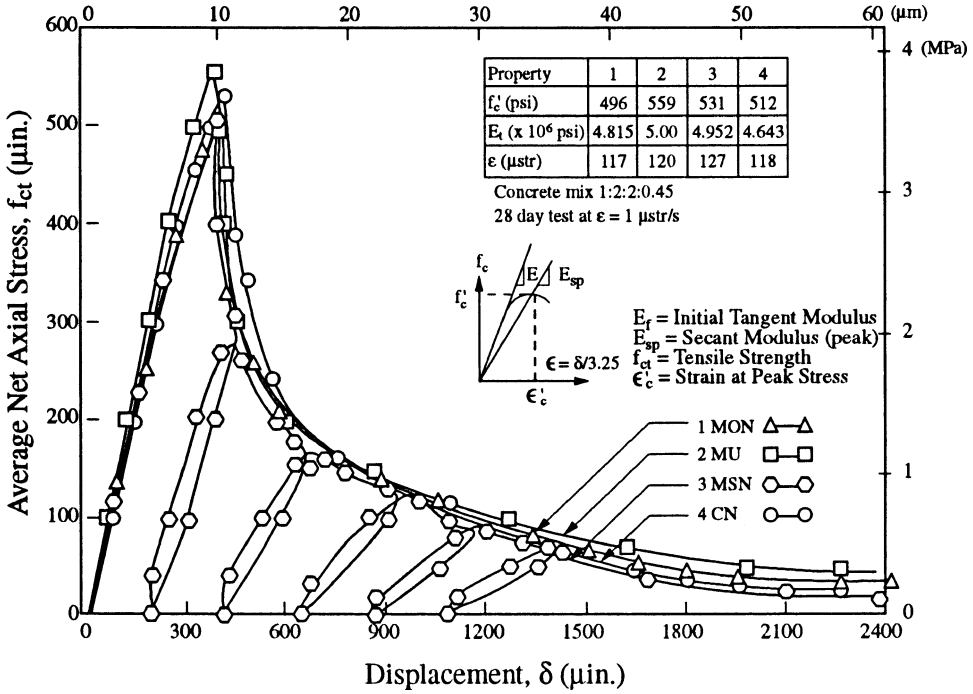

Fig. 4.4—Response of plain concrete loaded in uniaxial tension (Gopalaratnam and Shah 1985).

4.3.4 *Dowel action of longitudinal reinforcement*—Recent work by Vintzeleou and Tassios (1986) and Chana (1987) has reaffirmed the well-known work by Baumann and Rüsch (1970) on the resistance of dowels near a surface. Normally, dowel action is not very significant in members without transverse reinforcement, because the maximum shear in a dowel is limited by the tensile strength of the concrete cover supporting the dowel. Dowel action may be significant in members with large amounts of longitudinal reinforcement, particularly when the longitudinal reinforcement is distributed in more than one layer.

4.3.5 *Residual tensile stresses across cracks*—The basic explanation of residual tensile stresses is that when concrete first cracks, a clean break does not occur. Small pieces of concrete bridge the crack and continue to transmit tensile force up to crack widths in the range of 0.05 to 0.15 mm. The fact that there is a significant descending (softening) branch after the peak tensile stress is reached has been known for some time (Evans and Marathe 1968); however, methods for the reliable measurement of the softening branch have only recently been developed (Gopalaratnam and Shah 1985; Reinhardt et al. 1986). Figure 4.4 shows a typical response of concrete loaded in tension. The deformations are localized in a very small region (the fracture zone); therefore, the response should be expressed in terms of a stress-crack opening relationship and not strain (Evans and Marathe 1968; Gopalaratnam and Shah 1985; Reinhardt et al. 1986; ACI 446.1R).

The application of fracture mechanics (ACI 446.1R) to shear design is based on the premise that residual tensile stress is the primary shear-transfer mechanism. Other methods consider the contribution from residual tensile stresses such as Reineck's tooth model (1991c), which indicates that residual tensile stresses provide a significant portion of the shear resistance of very shallow members (that is, depths less than about 100 mm) where the width of flexural and diagonal cracks are small (Reineck 1991b).

4.4—Models for members without transverse reinforcement

4.4.1 *Introduction*—The different models that can be used to design members without transverse reinforcement may have to be classified into the following groups: 1) mechanical or physical models for structural behavior and failure; 2) fracture mechanics approaches; and 3) nonlinear finite element analysis. In recent decades, the importance of developing relatively simple physical models to explain empirical trends has become increasingly realized.

The shear resistance of a concrete member can be divided into two separate modes: beam action, where the tension force in the longitudinal reinforcement acting on a constant lever arm changes to balance the external moment; and arch action, where the internal lever arm (location of longitudinal compression stress resultant in concrete) changes to balance the moment. The method of choice for cases dominated by arch action is the strut-and-tie model, which is described in detail in Chapter 6. Some of the special considerations required when no transverse reinforcement is provided are discussed in this chapter. Regarding beam action, the physical/mechanical models can be classified further into tooth models, which begin with an assumed arrangement of cracks, and truss models with (smeared) concrete tension fields or concrete ties.

In the following, the empirical methods are presented first because they are the basis of the ACI 318M-95 approach. Fracture mechanics approaches for shear design, which are

only briefly discussed here, are presented first. The nonlinear finite-element method is not discussed in this report. Information on this approach can be found elsewhere (Isenberg 1993). The remaining physical/mechanical models are presented in order of historical development: tooth models, simple strut-and-tie models, and truss models with concrete ties.

4.4.2 *Fracture mechanics approaches*—Fracture mechanics approaches account for the fact that there is a peak tensile stress near the tip of a crack and a reduced tensile stress (softening) in the cracked zone. For the case of a beam that fails in shear due to the propagation of a single critical diagonal crack, fracture mechanics can be considered a more rational approach than empirical methods. This approach offers a possible explanation for the size effect in shear.

A number of different fracture mechanics models have been proposed over recent years. Among them, two well known ones are the fictitious crack model, by Hillerborg et al. (1976), and the crack band model, by Bažant and Oh (1983). A survey of fracture mechanics applications was recently given by Reinhardt (1986). Further information on fracture mechanics can be found in ACI 446.1R.

Fracture mechanics approaches are usually numerically demanding because of the complexity of the tensile stress-crack displacement relationships. As a result, empirical formulas are sometimes developed in terms of fracture mechanics parameters, like that by Bažant and Kim (1984) or Remmel (1994). These equations give little explanation of structural behavior, so the end result is often very similar to empirical formulas, as was pointed out by Walraven (1987).

4.4.3 *Simple strut-and-tie models*—The application of strut-and-tie models, which has its theoretical basis from the lower-bound theorem of plasticity (Drucker 1961, Nielsen et al. 1978, Marti 1985), requires a minimum amount of distributed reinforcement in all directions, including transverse reinforcement, to ensure sufficient ductility for redistribution of internal stresses after cracking. In the elastic stress distribution of deep members, significant shear is transmitted directly to the support by diagonal compression. This means that less redistribution is required after cracking, and it would seem reasonable to apply strut-and-tie models (cautiously) to deep members without transverse reinforcement. When members are very deep, all of the shear will be transferred directly to the support by compression stresses; however, premature failure of a compression strut without minimum distributed reinforcement may result from transverse splitting due to spreading of compression stress (Schlaich et al. 1987). Walraven and Lehwalter (1994) carried out tests to investigate the capacity increase beyond that due to spreading of the compression stress; in a bottle-like shape, they proposed a failure criterion for the compression strut that included a size effect.

The simple strut-and-tie approach has also been suggested for more slender members without transverse reinforcement; however, this may result in an unsafe solution, as discussed in Section 4.1 and shown in Fig. 4.1. Solutions have been suggested using a reduced compressive strength of the strut. One method (Collins and Mitchell 1986) for accomplishing this involves considering strain compatibility between the concrete strut and tension tie. As the strut becomes flatter, the transverse tensile strain in the strut increases, which reduces the diagonal crushing strength of concrete (Vecchio and Collins 1986). An alternate approach is that of Braestrup (1990), where the maximum diagonal compressive stress is not related to the strut inclination, but the shear capacity reduces with increasing shear span because of the geometry of the nodal zone, which depends on the support dimension, the cover-to-longitudinal reinforcement, and an assumed hydrostatic stress in the nodal zones.

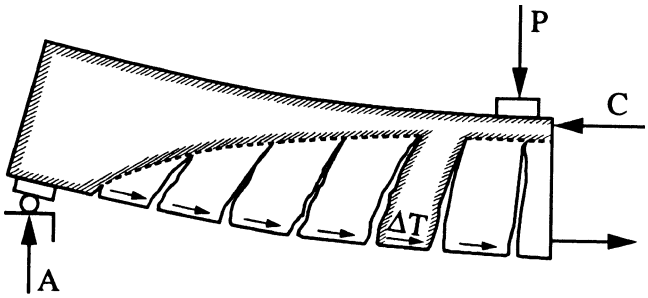

Fig. 4.5—Kani's tooth model (Kani 1964).

4.4.4 *Tooth model for slender members*—An early attempt to develop a rational model to explain flexure-shear cracking was Kani's tooth model (1964), in which the secondary diagonal cracks were believed to result from bending of concrete "teeth." The concrete between two adjacent flexural cracks was considered to be analogous to a tooth in a comb (Fig. 4.5). The concrete teeth were assumed to be free cantilevers fixed in the compression zone of the beams and loaded by the horizontal shear from bonded reinforcement.

Kani's model was evaluated by Fenwick and Paulay (1968) as well as Taylor (1974), who pointed out that the teeth are restricted from bending freely by the friction of the crack faces and the dowel action of the longitudinal reinforcement. Tooth models have been developed further to include these mechanisms (MacGregor and Walters 1967, Hamadi and Regan 1980, Reineck 1991c). With his tests, Chana (1987) confirmed the basic mechanisms of the tooth model by extensive measurements of the deformations before failure.

The main features of the tooth model are that discrete cracks are assumed and assumptions have to be made for the inclination and spacing of the cracks. Hamadi and Regan (1980) assume that the cracks are vertical and that their spacing is equal to half the effective depth ($s = d/2$) for a particular beam, whereas Reineck (1991c) assumes the cracks are inclined at 60 degrees with a spacing of 70% of the crack height determined from a flexural analysis; that is, $s = 0.7(d - c)$, where c = depth of compression. For a given crack spacing, the shear displacement and crack width can be calculated if the strains are known. This requires kinematic considerations, but as a result, gives the actual contributions of the different shear transfer mechanisms in the highly indeterminate system.

Based on extensive experimental work in interface shear, Hamadi and Regan (1980) developed a tooth model with simplified assumptions for the interface shear and the geometry of the tooth. Reineck (1991c) further developed the tooth model, considering all the shear-transfer mechanisms and

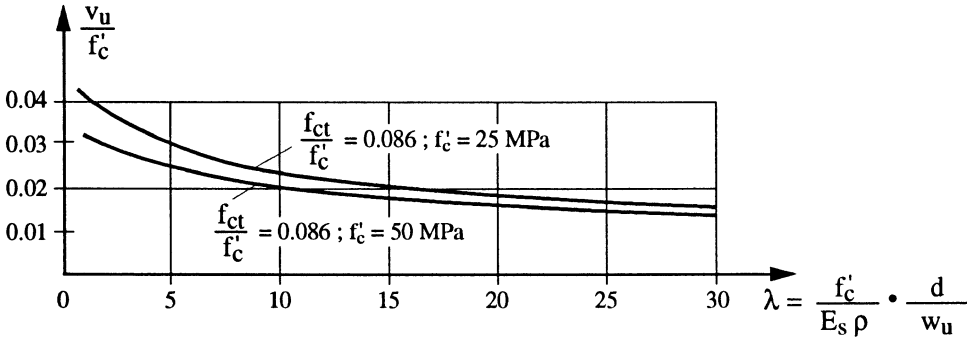

Fig. 4.6—Dimensionless diagram for ultimate shear force derived from mechanical model by Reineck (1991c).

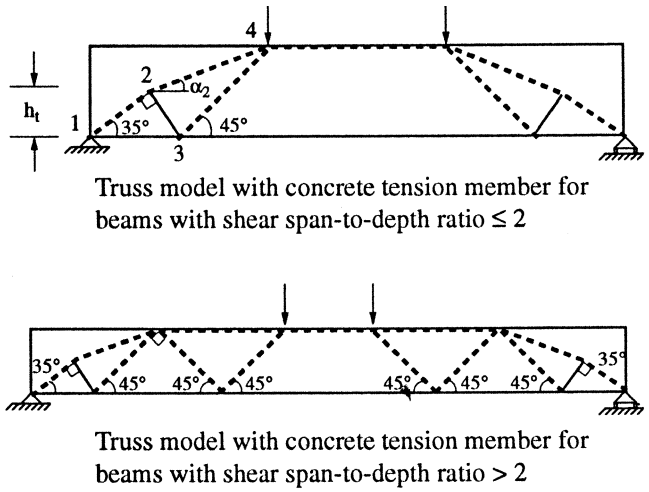

Fig. 4.7—Refined strut-and-tie models proposed by Al-Nahlawi and Wight (1992).

carried out a full nonlinear calculation including compatibility. The distribution of the shear force on the different shear mechanisms was similar to those found earlier by Taylor (1974); interface shear was the dominant shear mechanism, and dowel action was important for heavily reinforced members.

Based on his mechanical model, Reineck (1991c) derived an explicit formula for the ultimate shear force, which for members without axial force or prestress is

$$V_u = \frac{0.4 b_w d f_{ct} + V_{du}}{(1 + 0.054\lambda)} \quad (4\text{-}4)$$

where

f_{ct} = axial tensile strength = $0.246 f_c'^{2/3}$ (MPa); and
V_{du} = dowel force [$V_{du}/b_w d f_c' = 1.33\rho^{8/9}/(f_c')^{2/3}$, with f_c' in MPa units and d in m].

The parameter l is a dimension-free value for the crack width, which determines the friction capacity, and is defined by

$$\lambda = f_c' d / E_s \rho w_u \quad (4\text{-}5)$$

where

w_u = 0.09 mm = a limiting crack width;
d = effective depth (mm);
E_s = 2,000,000 (MPa); and
ρ = $A_s/b_w d$.

This parameter comprises the reinforcing ratio, ρ, and the depth, *d,* of the member; therefore, the formula can be presented in a simple diagram for the dimensionless shear force $v_u/f_c' = Vu/b_w d f_c'$ (Fig. 4.6), in which the concrete tensile strength is the only parameter. Similar diagrams could be developed using the more common parameters ρ and *d* (Reineck 1991c). Comparisons showed that this theoretically derived formula matches the tests as well as many empirical formulas.

4.4.5 *Truss models with concrete ties*—Although it may be possible to extend the simple strut-and-tie model approach to more slender members, clearly a different approach is needed to capture the shear failure of very slender members without transverse reinforcement where the concrete tensile stresses have the major role. Marti (1980) extended the plasticity approach by using a Coulomb-Mohr yield criterion for concrete that includes tensile stresses. Schlaich et al. (1987) suggested a refined strut-and-tie approach that includes concrete tension ties. Al-Nahlawi and Wight (1992) proposed a truss model with concrete compression struts inclined at either 45 or 35 degrees and concrete tension ties perpendicular to the struts (Fig. 4.7). An empirical rule was used for limiting the tension tie force based on the geometry of the truss. Muttoni (1990) proposed a truss model for less slender members (Fig. 4.8) in which, rather than going directly from the load point to the support, the inclined compression is bent around the initial flexural compression zone.

Reineck (1991c, 1982) has shown that such truss models with concrete ties fully comply with the tooth model discussed above. In the tooth model, the state of the stress in the B region is defined by the stresses at the crack, but from these stresses, the principal stresses in the tooth between the cracks may also be determined. The dominant action due to the friction along the crack surfaces then results in a biaxial tension-compression field, shown in Fig. 4.9(a) for constant friction stresses (Reineck 1982). The inclination of the principal compressive stress is equal to half the inclination of the cracks, which Reineck assumes to be at 60 degrees. The dowel action induces a concentrated tension force in the lower part of the tooth and results in bending of the tooth, which is resisted by friction stresses. Therefore, the strut-and-tie model of Fig. 4.9(b)

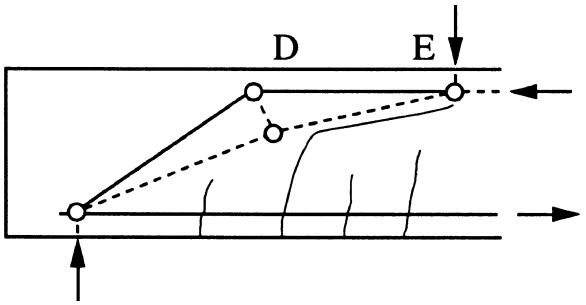

Fig. 4.8—Refined strut-and-tie model proposed by Muttoni (1990).

for the resulting state of stress shows, in the upper part of the tooth, an inclined stress field similar to Fig. 4.9(a).

4.4.6 *Modified compression field theory*—The MCFT (Vecchio and Collins 1986) can be implemented in different ways with varying levels of complexity, from a full, nonlinear finite-element analysis, to a multilayer sectional analysis that accounts for the variation of crack width over the section (Vecchio and Collins 1988), to the simplest case where only the crack width at the level of the flexural tension reinforcement is considered (Collins and Mitchell 1991). The latter case, which is most suitable for design, is analogous to a variable-angle truss model with diagonal concrete tension ties.

The MCFT is usually formulated in terms of average stresses; however, the method includes a check to ensure that the loads resisted by the average stresses can be transmitted across cracks. For members without transverse reinforcement, the stresses locally at a crack always control the capacity of the member, and the average stress calculation is used only in estimating the inclination of the critical diagonal crack. In calculating the stresses locally at a crack, it is assumed that the crack plane can resist only shear stress (no normal stress). As the horizontal plane should also be free of normal stress, the principal directions of the stresses locally at a crack should bisect the angles between the crack plane and the horizontal plane. In other words, the inclination of the principal compression stress (which is perpendicular to the direction of the principal tension stress) is half the inclination of the diagonal cracks, as summarized by the Mohr's circle in Fig. 4.10. One important consequence is that the shear stress on the crack plane is equal to the shear stress on the vertical and horizontal planes. Thus, the shear strength of a member is equal to the shear stress that can be resisted by the critical crack. Based on Walraven's experimental results (1981) for the maximum shear stress that can be resisted by a crack without the beneficial effects of compression, the shear resistance of a diagonally cracked member is given by

$$v_c \le \frac{0.18\sqrt{f'_c}}{0.3 + \frac{24w}{(a+16)}} \qquad (4\text{-}6)$$

where

w = crack width;

a = maximum aggregate size in mm; and

f'_c is in MPa (Vecchio and Collins 1986).

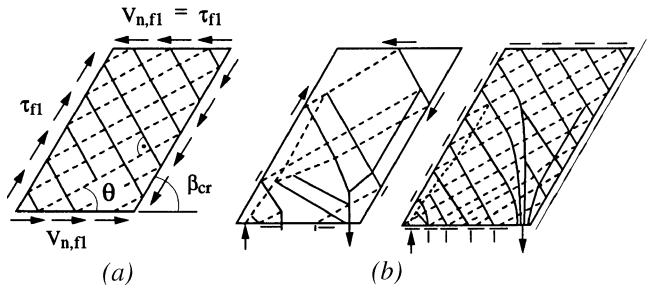

Fig. 4.9—Refined strut-and-tie model for crack friction and dowel action (Reineck 1991c): (a) constant friction stresses; and (b) simple and refined strut-and-tie model for dowel action combined with friction.

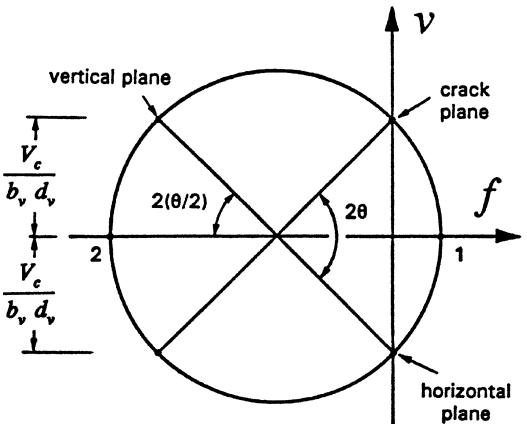

Fig. 4.10—Mohr's circle for biaxial stresses locally at crack in member without transverse reinforcement (Adebar and Collins 1996).

As in the tooth models, the width of a crack depends on the assumed crack spacing; however, unlike in the tooth models, the crack spacing and the inclination of the diagonal cracks are not assumed a priori in the MCFT. The crack spacing depends on the crack inclination. Cracks that are inclined at 90 degrees to the member axis are assumed to have a spacing $s_x = d_v$ (for members with one layer of reinforcement), whereas cracks at other inclinations β are assumed to have a spacing $s_\theta = s_x/\sin\beta$. This simple expression reflects the fact that longitudinal reinforcement has less ability to control cracks as they become flatter (smaller β).

In the MCFT, the inclination of diagonal cracks is calculated using a strain compatibility procedure involving average stresses and average strains. The diagonal cracks are assumed to be perpendicular to the principal tensile average stress direction. In that way, the influence of the loading (for example, the axial load and bending moment) on the inclination of the diagonal cracks (initial diagonal crack as well as the more important secondary diagonal cracks) are properly accounted for. For members without transverse reinforcement, the inclination of the diagonal cracks is given by

$$\theta = \tan^{-1}\left[\frac{\frac{0.33\sqrt{f'_c}}{1+\sqrt{500\varepsilon_1}}}{v_c}\right] \text{ (MPa)} \qquad (4\text{-}7)$$

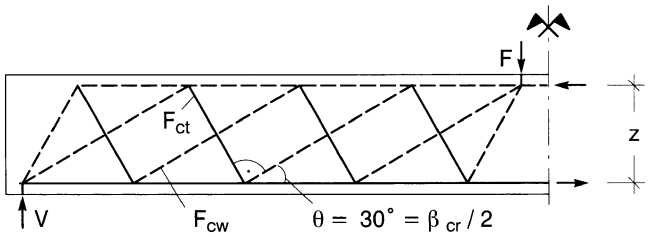

Fig. 4.11—Refined strut-and-tie model for diagonally cracked member without stirrups (Reineck 1991c).

where the numerator within the brackets is an empirical expression (Collins and Mitchell 1991) for the principal tensile average stress as a function of the principal tensile average strain ε_1.

A description of how the MCFT can be used to design members with or without transverse reinforcement is given in Chapter 2, and further information can be found in Collins and Mitchell (1991). Some additional discussion on the application of the modified compression field theory specifically to members without transverse reinforcement is given in Adebar and Collins (1996).

4.4.7 *Toward a consistent method*—Although the refined tooth models (Section 4.4.4) and the MCFT (Section 4.4.6) approach the problem from different directions, the end result of these two methods is very similar for members without transverse reinforcement. Although the two methods use different approaches to estimate the crack inclination and crack width, both methods consider that the ability of diagonal cracks to transfer interface shear stress is most important in determining the shear strength of members without transverse reinforcement.

The biaxial tension-compression field in the concrete (teeth) between the cracks for a constant shear stress along the cracks may be visualized by a truss model. This representation of the concrete stresses due to interface shear stresses was first developed by Reineck (1982) based on his tooth model (Reineck 1991c). As discussed earlier, the principal stresses locally at a crack (that is, the compression struts and tension ties of the truss model) bisect the angles between the diagonal crack and the horizontal plane. Reineck assumes that the inclination of the critical diagonal cracks will be 60 degrees; therefore, the inclination of his compression struts are at 30 degrees (Fig. 4.11). In the MCFT approach, the inclination of the critical diagonal cracks depends on the loading and the ability of the longitudinal reinforcement to control the secondary diagonal cracks. A generalization of Reineck's model involves a truss with compression struts inclined at half the inclination of the diagonal cracks, which may have any inclination (Adebar and Collins 1996). Thus, the modeling for members without transverse reinforcement is fully compatible with the strut-and-tie models explained in Chapter 6.

4.5—Important parameters influencing shear capacity

4.5.1 *Depth of member or size effect*—It was shown by Kani (1967) as early as 1967 that there is a very significant size effect on the shear strength of members without transverse reinforcement. Shioya et al. (1989) reaffirmed this fact and extended the available data to beam depths of 3000 mm. As shown in Fig. 4.12, the average shear stress to cause failure of the largest beam was about one-third the average shear stress to cause failure of the smallest beam.

There is general agreement that the main reason for this size effect is the larger width of diagonal cracks in larger beams; however, there is disagreement on how best to model this phenomenon. Some (Bažant and Kim 1984) believe that the most important consequence of wider cracks is reduced-residual tensile stresses and, as a result, propose using a size-reduction factor

$$\lambda = \frac{1}{\sqrt{1 + \frac{d}{d_o}}} \tag{4-8}$$

based on nonlinear fracture mechanics where d_o is an empirical parameter. Others believe that the most important consequence of wider cracks is a reduced ability to transmit crack interface shear stresses. As the crack spacing used to determine the limiting crack interface shear stress is a function of the specimen depth, no special factor is required to account for the size effect. Perhaps the strongest argument for this latter approach is that it leads to a consistent treatment of members with different arrangements of longitudinal reinforcement. Tests (Collins et al. 1993) have demonstrated that the size effect disappears when beams without stirrups contain well distributed longitudinal reinforcement. Figure 4.12 compares the results from the tests by Shioya et al. (1989) with the design method described in Chapter 2, whereas Fig. 4.13 compares the predictions of different formulas for the influence of size effect. The proposals by Okamura and Reineck consider the tests in Shioya et al. (1989) and, therefore, represent reasonable lower bounds, whereas the predictions using Zsutty's approach (1971) and ACI 318M-95 do not account for the size effect.

4.5.2 *Shear span-to-depth ratio (*a/d*) and support conditions*—It has long been recognized that, as members become deep (the shear span-to-depth ratio decreases below about 2.5), the average shear stress at failure becomes progressively larger than in slender beams. The reason for this is that, as members become deeper, it is easier for the shear to be transmitted directly to the support by a compression strut. The support conditions also strongly influence whether a direct compression strut can form. A compression strut is more likely to form if a member is loaded on the top face and supported on the bottom face (Adebar 1994).

Members in which a direct compression strut is likely to form should be designed using the strut-and-tie model approach described in Chapter 6, rather than a sectional design procedure. Collins and Mitchell (1991) demonstrated how the two methods can be combined to predict the strength of beams without stirrups over a wide range of shear span-to-depth ratios.

The simple strut-and-tie model assumes that all of the shear will be transmitted by compressive stresses, which

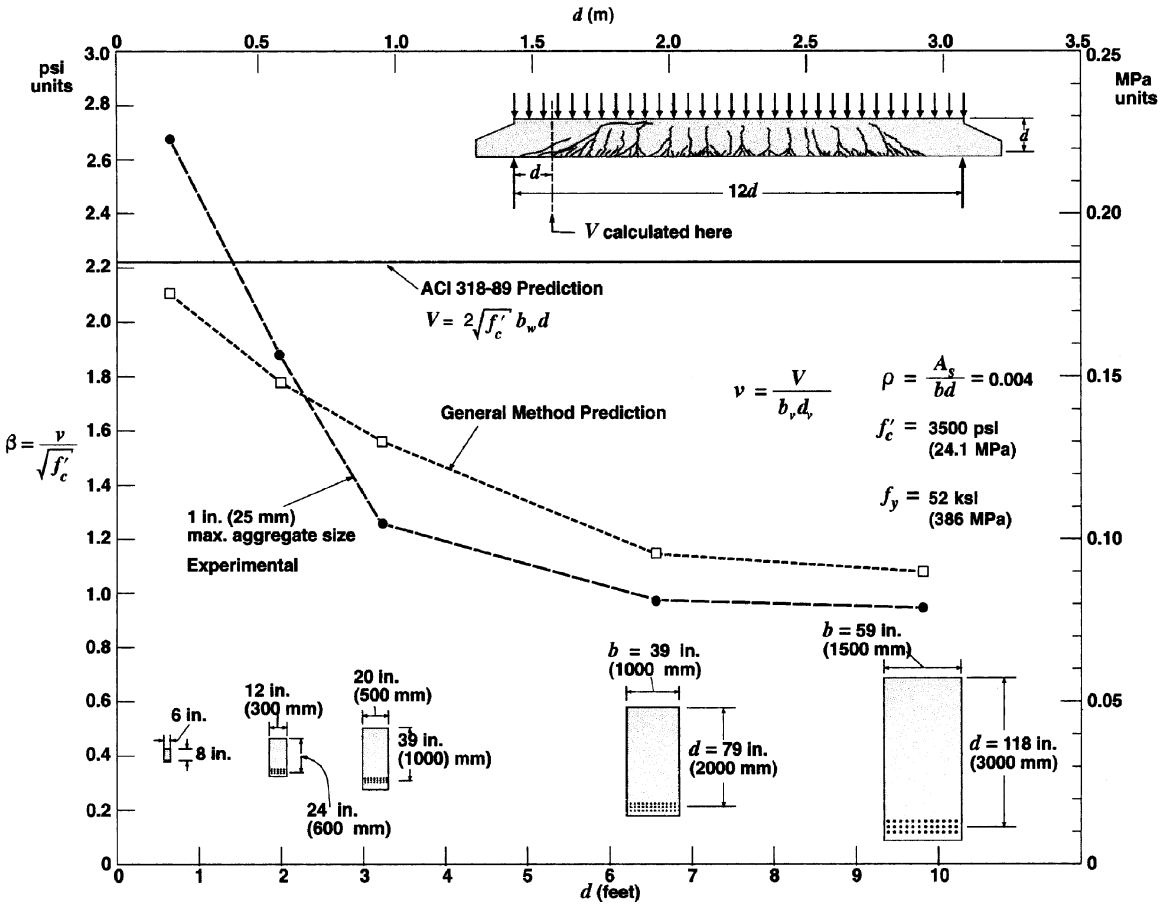

Fig. 4.12—Comparison of large-scale beam tested by Shioya et al. (1989) with predictions from ACI Code and MCFT (Collins and Mitchell 1991).

suggests that there will not be a size effect for such members. Experimental results (Walraven and Lehwalter 1990, 1994), however, indicate that deep members without transverse reinforcement do experience a very significant size effect. Thus, refined strut-and-tie models that consider concrete tensile stresses should be used to design deep members, unless minimum distributed longitudinal and transverse reinforcement is provided.

4.5.3 *Longitudinal reinforcement*—As can be seen in Fig. 4.14, members with low amounts of longitudinal reinforcement may fail at very low shear stresses. The 1973 ASCE-ACI Committee 426 report suggested that the following equation, incorporating the percentage of longitudinal tension reinforcement, be used to estimate the average shear stress at diagonal cracking

$$v_c = (0.8 + 100\rho)\frac{\sqrt{f'_c}}{12} \le 0.179\sqrt{f'_c} \quad \text{(MPa)} \qquad (4\text{-}9)$$

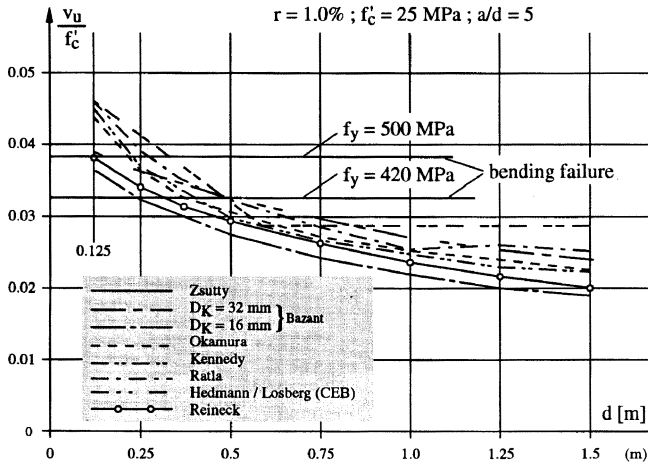

Fig. 4.13—Decrease of ultimate shear force (dimensionless value) with increasing depth of member size (size effect) according to different proposals (Reineck 1991c).

The report further suggested that the reduction in shear capacity can be explained by an increased crack width, resulting in lower interface shear transfer, correspondingly longer flexural cracks that reduce the size of the compression zone, and reduced dowel action.

In the design method presented in Chapter 2, the influence of the area of longitudinal reinforcement A_s is reflected in Eq. (2-9), which predicts larger tensile strains (and larger crack widths) in members with less longitudinal reinforcement and, as a result, lower shear strengths. The design method also requires that additional longitudinal reinforcement be provided to resist the large tensile force due to shear in diagonally cracked members without stirrups, as expressed by Eq. (2-12).

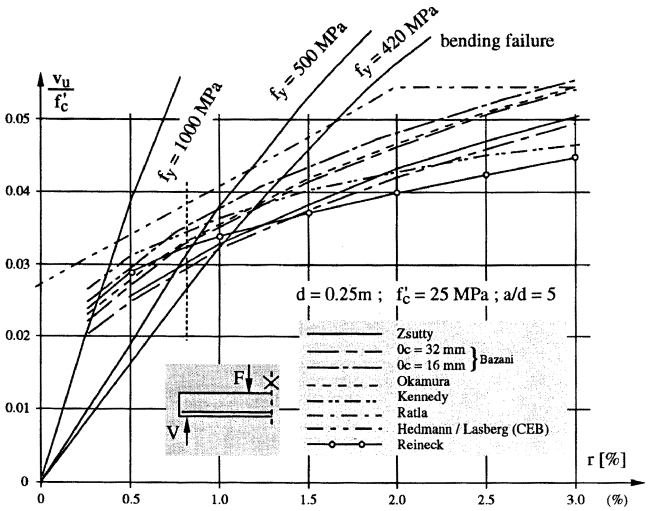

Fig. 4.14—Increase in ultimate shear capacity (dimensionless value) with increasing reinforcing ratio according to different proposals (Reineck 1991c).

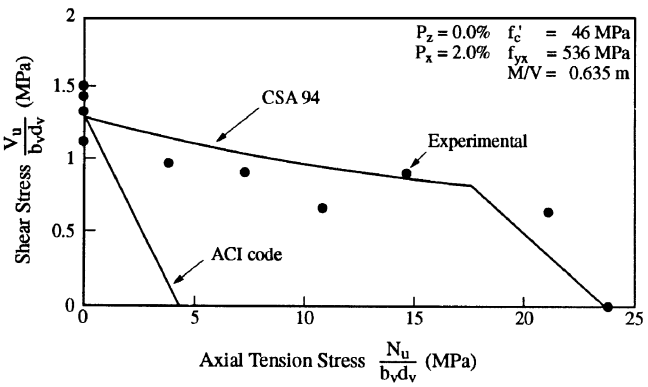

Fig. 4.15—Influence of axial load on shear strength of members without stirrups.

Figure 4.14 compares the predicted influence of the quantity of longitudinal reinforcement from a number of empirical formulas. The flexural capacity is also shown for different strengths of longitudinal reinforcement. From this figure follows the well-known fact that flexural failures rather than shear failures will govern the capacity of moderately long beams ($a/d \approx 5.0$) with low amounts of longitudinal reinforcement ($r < 1.0\%$) if the reinforcement is constant throughout the span.

4.5.4 *Axial force*—It is well known that axial tension decreases the shear strength of members without transverse reinforcement, and axial compression (due to an applied load or prestressing) in-creases the shear resistance. What is perhaps not very well understood is how much the shear capacity is influenced by axial load and what the influence is on the ductility of the member.

Members without shear reinforcement subjected to large axial compression and shear may fail in a very brittle manner at the instance of first diagonal cracking. As a result, a conservative approach should be used for such members. Recent tests by Gupta and Collins (1993) have demonstrated that the ACI 318 approach may be unconservative for members subjected to axial compression and shear.

On the other hand, for members without shear reinforcement but containing appropriate longitudinal reinforcement, the ACI 318M-95 procedure for members subjected to shear and tension can be very conservative. The code procedure, although intended for members subjected to significant axial tension, is based upon test results from members that did not contain appropriate longitudinal reinforcement to resist axial tension (Bhide and Collins 1993). Figure 4.15 compares the results from a series of beams without stirrups subjected to shear and tension (Adebar and Collins 1996) with predictions from ACI 318M-95 and the design method based on the modified compression field theory (Chapter 2). In Fig. 4.15, d_v represents the effective shear depth, b_v is the web width, and P_x and P_z are the reinforcement ratio in the orthogonal directions. A similar result is achieved with Reineck's tooth model (1982).

A typical crack pattern for a member subjected to large axial tension and shear is shown in Fig. 4.16. The initial cracks are very steep (close to 90 degrees) and extend over the full depth of the member. Thus, longitudinal reinforcement is required at the top as well as the bottom of the member, and the initial cracks, which are initially perpendicular to this reinforcement, are well controlled. As the loading is increased, new, flatter diagonal cracks form. Failure occurs only after the diagonal cracks become too flat to be controlled by the longitudinal reinforcement; therefore, members subjected to tension and shear are comparatively ductile.

4.6—Conclusions

More than 20 years after the 1973 ASCE-ACI Committee 426 state-of-the-art report expressed the hope that more rational methods could be developed for shear design, it can now be concluded that methods are available to explain the structural behavior and failure load of members without transverse reinforcement. Despite differences in the approaches, the main conclusion from most models is that concrete tensile stresses should be considered explicitly. Therefore, the empirical approaches in current codes can now be replaced by relationships based on truss models with concrete ties. The failure is not explained simply by the tensile stresses attaining the tensile strength, rather; it involves the breakdown of the shear transfer mechanisms at the crack. For smaller-sized members, the residual tensile stresses are very important, whereas for larger members (which have wide cracks prior to failure), the interface friction has the dominant role.

A number of parameters influencing the shear capacity of members without transverse reinforcement have been well explored during the last 20 years. It is certainly well known that there is a size effect on the shear strength of the member, and this fact should be addressed in ACI 318M-95. The strength of members with low reinforcing ratios was rarely investigated in the past and is often overestimated in present codes. The influence of both the size effect and the longitudinal reinforcement amount can be explained by the effect on the width of inclined cracks. The influence of the shear

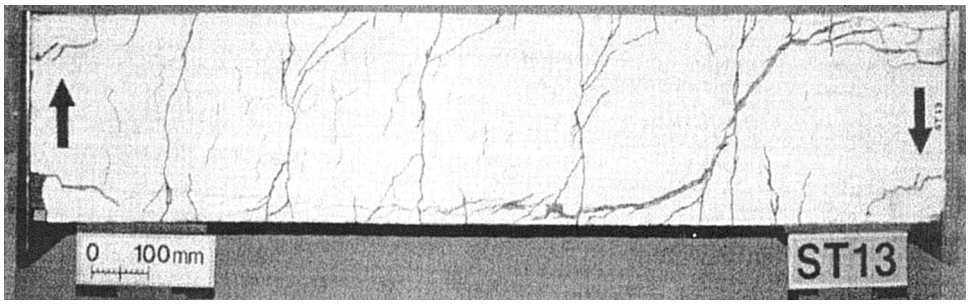

Fig. 4.16—Typical crack pattern without transverse reinforcement subjected to axial tension and shear (Adebar and Collins 1996).

span can be accounted for very simply by using a sectional approach for slender members and a strut-and-tie approach for short spans where a direct compression strut can form between the load and the support. Some caution is needed when applying strut-and-tie models to members without distributed transverse reinforcement.

Recent information on the behavior of members subjected to shear and axial tension illustrates a number of important issues to be considered in the choice of a consistent shear design model. First, as the initial diagonal cracks in a member subjected to tension and shear extend over the full depth of the member (Fig. 4.16), there is no compression zone to resist shear. Second, there is no fracture zone where a concentration of residual tensile stresses exists. Finally, the need to consider a changing critical diagonal crack inclination is apparent.

CHAPTER 5—SHEAR FRICTION

5.1—Introduction

Shear friction is treated as a separate chapter in this report because in ACI 318 it is treated separately from the concept of diagonal tension used for beam design. It is presented here to show a complete picture of models for shear design. The shear-friction concept permits one to treat problems where failure occurs by sliding along a plane of discontinuity. Construction joints and discrete cracks are common situations where sliding failures can be assessed readily by shear-friction theory. These discontinuities represent planes of weakness that may behave quite differently than the parent concrete. The shear-friction approach can account for the nature of the discontinuity (that is, roughness and interface with materials such as structural steel shapes). For this class of problem, shear friction is the preferred method of solution.

It should be emphasized that shear friction, as used in North America, is not another approach to shear design of slender beams. It may be regarded as a simplified version of the more refined and more recent methods described in Section 3.4.

5.2—Shear-friction hypothesis

The shear-friction approach, as it is known today, was first introduced by Birkeland and Birkeland (1966). It was originally developed to deal with force transfer across joints in precast-concrete construction. Figure 5.1 illustrates the shear-friction hypothesis. Assuming sliding along the failure plane *m-m*, and simple Coulomb friction, the shear force, V, required to produce sliding is equal to μP, where μ is the coefficient of friction between the two elements and P is the clamping force perpendicular to the sliding plane. The roughness of crack *m-m* will create a separation δ between the two halves (see Fig. 5.1(b)). If reinforcement is placed across the interface, the separation will develop tension T in the reinforcement. The tension provides an external clamping force on the concrete resulting in compression across the interface of equal magnitude. The roughness may be visualized as a series of frictionless fine sawtooth ramps having a slope of tan ϕ. Comparing Fig. 5.1(a) and (b), it is seen that $T \tan \phi$ is equivalent to the frictional force μP. Tests revealed that the separation δ is usually sufficient to yield the reinforcement crossing the crack. Thus

$$V_n = \mu A_s f_y \tag{5-1}$$

where μ = 1.7 for monolithic concrete, 1.4 for artificially roughened construction joints, and 0.8 to 1.0 for ordinary construction joints and for concrete to steel interfaces.

To prevent crushing of the concrete in the crack (caused by the clamping force from the steel), before yielding of the steel, the steel ratio across the crack was limited to 0.015 and the shearing stress was limited to not more than 5.5 MPa for concrete with f_c' = 27.6 MPa.

5.3—Empirical developments

The simple physical model put forward by Birkeland and Birkeland (1966) has proven remarkably useful and robust. It has formed a logical framework for further study and refinement. Hofbeck et al. (1969) conducted an extensive testing program and found that shear-friction theory provided conservative estimates for the interface shear transfer strength.

Mattock and Hawkins (1972) showed that the effects of direct stresses perpendicular to the crack agreed with predictions based on the models in Fig. 5.1. Mattock (1974) subsequently showed that the effects of reinforcement at an angle to the shear plane could also be predicted based on the models of Fig. 5.1.

Paulay et al. (1974) investigated various treatments for construction joints. With well-designed and well-constructed joints, one can produce an interface shear strength that is equal to or larger than the corresponding load capacity of the

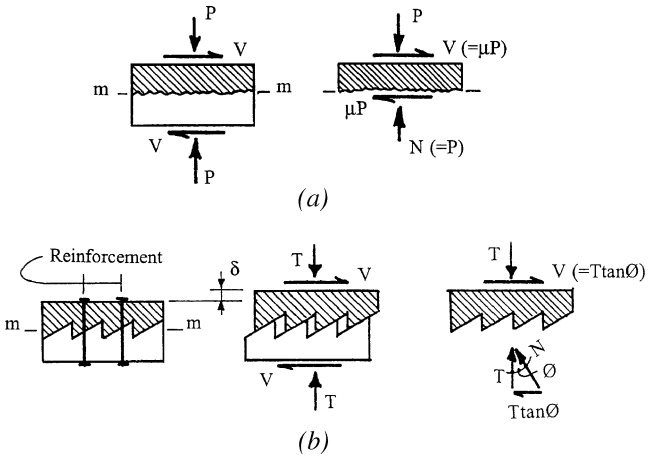

Fig. 5.1—Shear friction hypothesis (Birkeland and Birkeland 1966).

remainder of the member. For members cast in lifts, failure was found to occur in the zone immediately below the construction, that is, in the top-cast concrete in the lower lift. As such, one would expect to have weaker concrete in this region.

Mattock et al. (1976) investigated shear friction in lightweight concrete and found the friction values to be lower than in corresponding normalweight concrete. Mattock (1976) presented empirical equations that produce better predictions for monolithic uncracked concrete and low amounts of transverse reinforcement. For these situations, Eq. (5-1) is quite conservative. In effect, he introduced a constant cohesion term to supplement the friction term for Eq. (5-1). Mattock's equations have been found to be valid but somewhat conservative for concrete strengths up to 68 MPa (Walraven et al. 1987).

Walraven (1981), Walraven and Reinhardt (1981), and Walraven et al. (1987) have extended the range of variables studied and developed empirically based constitutive relationships for cracks that relate normal and shear displacements and stresses. Load history, such as previous sustained or repeated cyclic loading, was found to have little effect on the ultimate shear strength. It is believed that as ultimate load is approached, greater and virgin contact areas within the crack are mobilized. These virgin areas are not affected by the previous load history (Walraven et al. 1987). Loebert (1970), Tassios and Vintzeleou (1986), and others have also contributed to the empirical database. It is clear that for low normal stresses (less than about 1.5 MPa) the coefficient of friction is higher than previously thought. Thus, the apparent cohesion intercept introduced by Mattock is primarily due to an increase in μ rather than to the tension strength of uncracked monolithic concrete. Barton (1973), in effect, developed an empirical expression for μ as a function of clamping stress on the joint. As the clamping stress increases, the asperities that are in contact within the crack crush, producing a smoother crack and hence a lower μ.

Loov and Patnaik (1994) investigated the horizontal shear strength of composite concrete beams with a rough interface. Based on a review of the literature, and a series of tests, they proposed a single empirical equation that accounted for the concrete strength and the clamping stress.

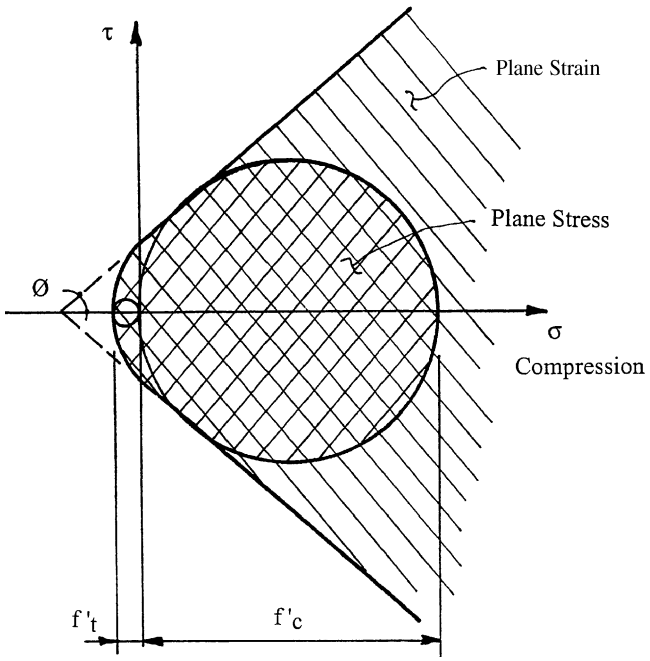

Fig. 5.2—Modified Mohr-Coulomb yield criterion for concrete with nonzero tension cutoff.

5.4—Analytical developments

In parallel with experimental developments, analytical developments by Nielsen (1971, 1984) and Nielsen et al. (1978) provide a theoretical basis for integrating the shear-friction approach in the theory of plasticity. They show that shear friction is an upper-bound solution within the general theory of plasticity. Shear friction is similar to limit equilibrium methods used in soil and rock mechanics. The failure planes used to determine active and passive earth pressures behind a retaining wall are examples of shear-friction planes. Using a modified Mohr-Coulomb yield criterion as shown in Fig. 5.2, one can readily predict shear-friction failures. It is worth noting that Nielsen had to introduce v, an efficiency factor into the plasticity analysis. The Mohr-Coulomb yield criterion is based on the tensile and compressive strengths of vf_t' and vf_c' respectively. Figure 5.3 illustrates typical results from plasticity theory. Even though the typical shear-friction test specimens are more representative of plane-stress conditions, one usually finds that the experimental results are bounded by predictions based on plane-strain and plane-stress conditions. Plasticity theory is particularly useful when the likely failure plane cannot otherwise be identified readily.

5.5—Code developments

Shear friction was adopted swiftly by ACI 318 and first appeared in the 1971 code. The values of μ specified in ACI 318M-95 have been reduced from those suggested by Birkeland and Birkeland (1966) to provide an appropriate margin of safety against shear failure. ACI 318M-95 recognizes the reduced friction values that exist with lightweight concrete through the introduction of the factor λ for lightweight concrete. Inclined reinforcement and the effects of external forces are accounted for. The maximum shear stress, v_n, is limited to the lesser of $0.2f_c'$ or 5.5 MPa to ensure that the section is not

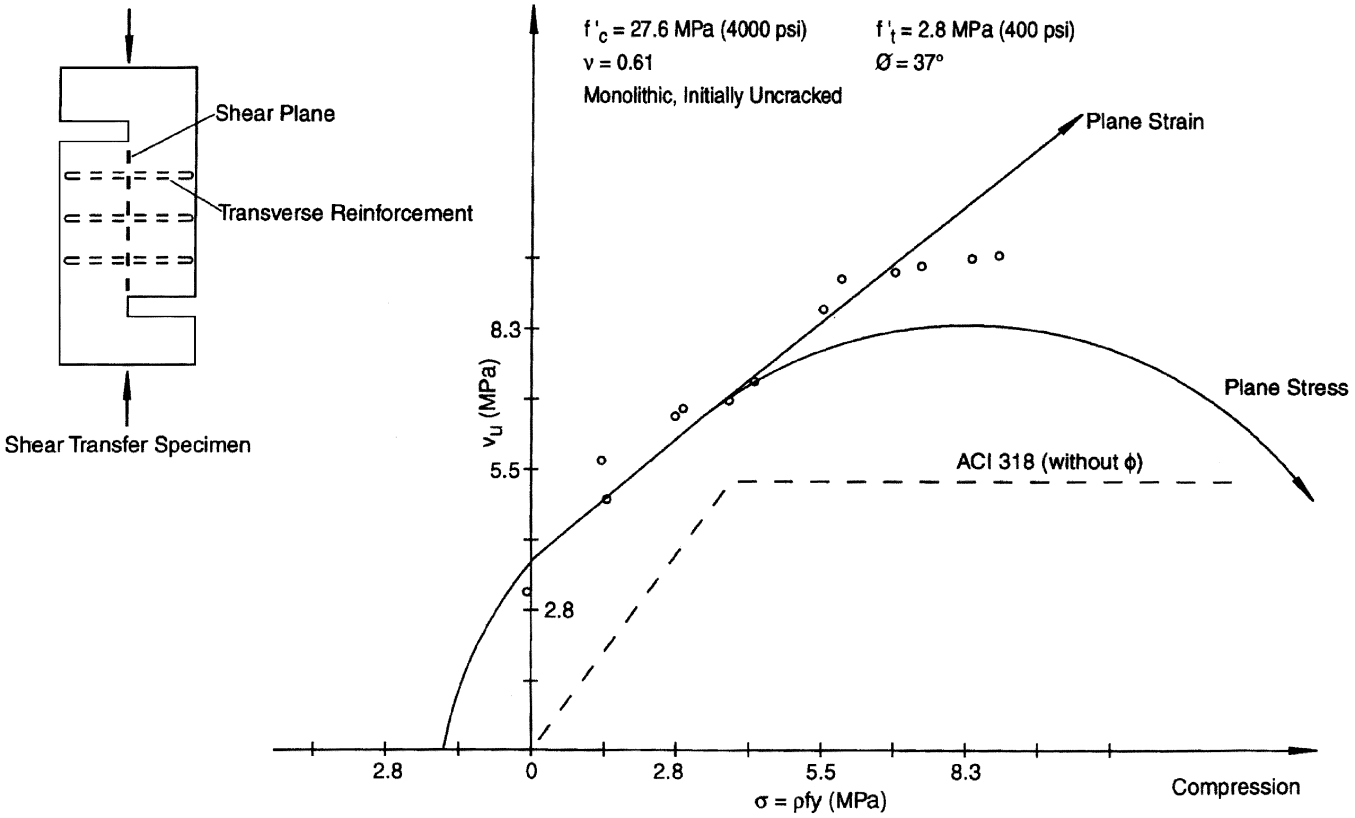

Fig. 5.3—Shear friction strength predictions (date from Hofbeck et al. 1969).

over-reinforced. It was recognized that the simple shear-friction provision of ACI 318M-95 was somewhat conservative, but relief was provided in Clause 11.7.3, which explicitly permits one to use "any other shear transfer design methods that result in prediction of strength in substantial agreement with results of comprehensive tests." As evident from Fig. 5.3, it would be particularly advantageous to do so when one has uncracked concrete and low amounts of reinforcement. In the case of composite concrete beams, Clause 17.5 may be used to advantage. In other situations, one should resort to the various approaches in the literature.

The Canadian code ("Design" 1994) has recently introduced two modified shear-friction formulations. Both approximate a Mohr-Coulomb yield envelope. One formulation, based on Loov and Patnaik (1994), produces a curve envelope that recognizes the benefits of increased concrete strength. The other formulation is similar to that proposed by Mattock (1976). It uses an initial cohesion term and a constant friction angle. Although it does not recognize the benefits of increased concrete strength, it can accommodate a wider range of surface roughness and cohesion. Adjusting the equations of CSA Standard A23.3-94 ("Design" 1994) to suit ACI 318M-95 load and resistance factors gives approximately

$$V_n = cA_c + A_{vf} f_y \mu \qquad (5\text{-}2)$$

where c, denoting cohesion, is equal to 0.3 MPa for concrete cast against clean hardened concrete, 0.55 MPa for concrete cast against clean hardened concrete intentionally roughened to a full amplitude of 6.25 mm, and 1.10 MPa for concrete cast monolithically. The quantity μ is the coefficient of friction per ACI 318M-95. The influence of inclined reinforcement is taken into account in the same manner as in ACI 318M-95.

CHAPTER 6—DESIGN WITH STRUT-AND-TIE MODELS

6.1—Introduction

As described in Chapter 1, truss models for the design of members have been used since the turn of the century (Ritter 1899; Mörsch 1920, 1922). One of the main advantages of using truss members to represent key resisting elements of a member is that the flow of forces can be easily visualized by the designer. The flow of compressive stresses is idealized with compression members called struts, and tension is taken by tension ties. Figure 6.1 shows how truss models using struts and ties can be used to idealize the flow of forces in members with a variety of span-to-depth ratios. This figure also shows the reinforcement required for a slender beam, a beam with a shear span-to-depth ratio a/d of 2.5, and a deep beam. Another advantage of using a truss model to idealize the flow of forces is that the influences of both shear and moment are accounted for simultaneously and directly in the design.

In the case of the slender beam, the concentrated load and reactions cause a disturbance in the internal flow of the stresses near the ends and the center of the beam (Fig. 6.1(a)). In current design procedures, these disturbed regions, or D regions, are treated separately in the design process. The regions of the slender beam where the flow of compressive stresses is uniform are referred to as beam regions, or B regions. The slender beam is modeled by a parallel chord

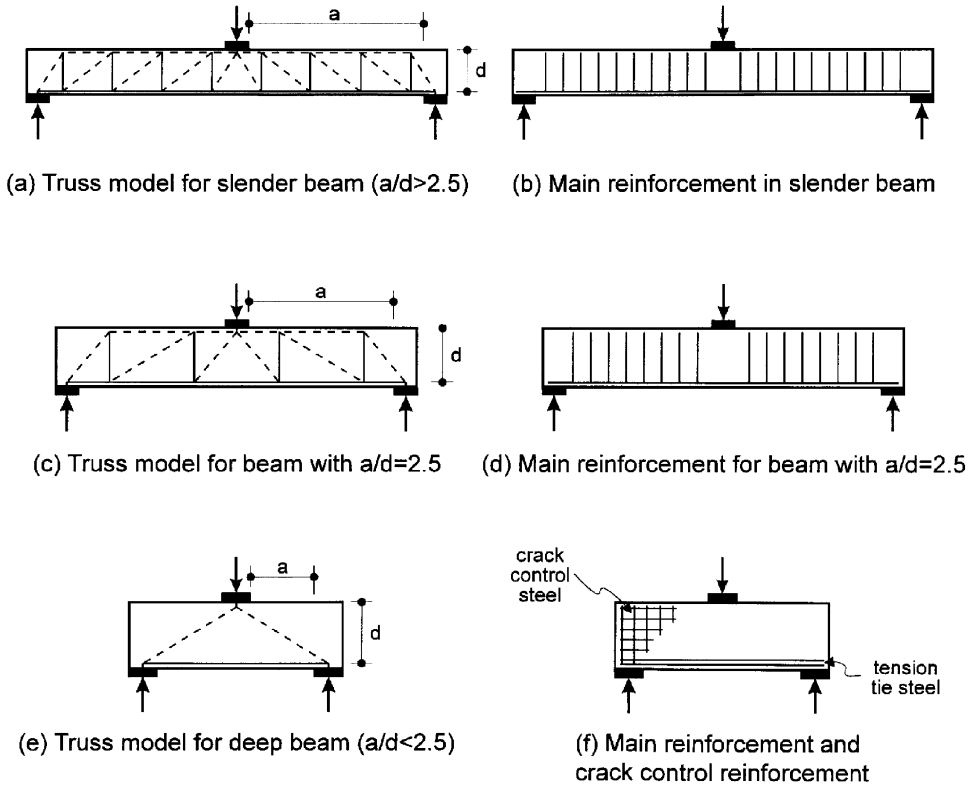

Fig. 6.1—Truss models showing transition from slender beams to deep beams.

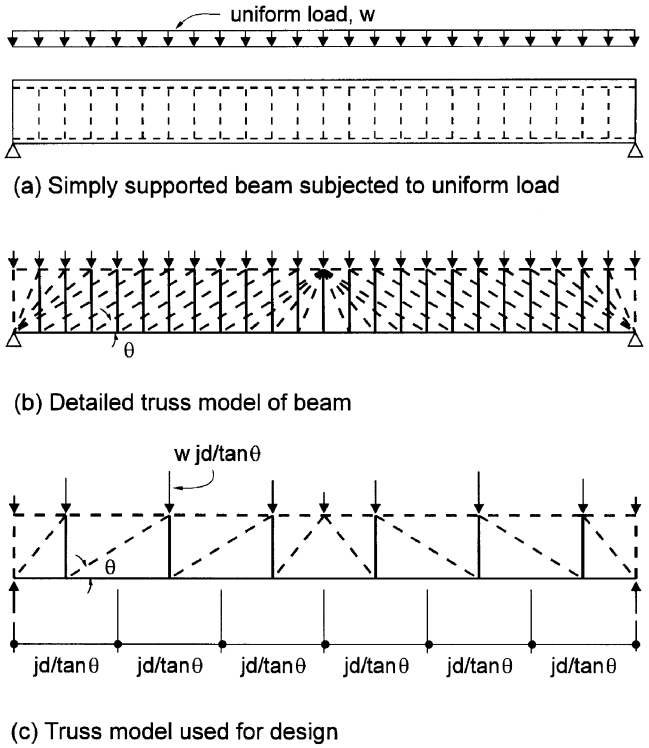

Fig. 6.2—Truss models for full member design.

truss with the flow of compressive stresses in the B regions idealized by a series of parallel compressive struts. The design can be carried out for the entire member using a full-member truss model. An example of this approach is given by Ramirez (1994) for the case of a prestressed concrete member. Alternatively, the design of the B regions can be carried out using a sectional design model, as described in Chapters 2 and 3.

Figure 6.1 shows the transition from a slender member to a deep beam. For low *a/d* ratios, the entire member becomes a disturbed region, where the normal assumptions of plane strain and uniform shear stress distribution are inappropriate. The strut-and-tie model is particularly useful in the design of D regions, which are characterized by a complex flow of internal stresses. The design of D regions using strut-and-tie models is discussed in Section 6.3.

6.2—Design of B regions

Figure 6.2 illustrates the manner in which a truss model is developed for the design of a member, according to the procedure recommended by Marti (1985). The design steps are as follows:

1. A reasonable angle of principal compression θ is chosen. Typical angles vary from about 18 to about 65 degrees.

2. The truss model used for design, having a depth equal to the flexural lever arm *jd* is sketched. Each vertical member represents a group of stirrups within a length *jd* cot θ. Each diagonal member of the simplified truss represents a zone of diagonal compression. Once the diagonal force *D* is found, then, using b_w as the effective web width resisting shear, the diagonal compressive stress in the concrete can be found from

$$f_2 = \frac{D}{b_w jd \cos\theta} = \frac{V}{b_w jd} \cdot \frac{1}{\sin\theta \sin\theta} \qquad (6\text{-}1)$$

3. Solve for the forces in the truss members and design the transverse and longitudinal reinforcement. Check the compressive stress in the concrete diagonals. Check that the reinforcement is sufficiently anchored at all critical points so that it can develop the necessary force in the steel.

Typically, the concrete contribution to the shear resistance, V_c, is conservatively ignored, $V_c = 0$, and the shear reinforcement is designed to resist all of the shear. There is no significant economic penalty arising from this conservatism for many situations where stirrups are typically provided. For members such as slabs and some joists that are constructed without transverse reinforcement, a truss model accounting for tensile stresses in the concrete can be used for design (see Chapters 3 and 4). Alternatively, a simplified approach with an empirical concrete contribution, such as in ACI 318M-95, could be used.

6.3—Design of D regions

6.3.1 *Definition of D region*—Strut-and-tie models are most appropriately used for the design of disturbed regions, or D regions, as shown in Fig. 6.3 (Schlaich et al. 1987). These D regions are characterized by a complex flow of internal stresses and include regions adjacent to discontinuities caused by abrupt changes of cross section or the presence of concentrated loads or reactions. In the design of these disturbed regions, it is inappropriate to assume that plane sections remain plane or that the shear stress is uniform over the depth of the member.

Figure 6.4 compares the experimentally determined shear strengths of a series of beams tested by Kani (1979) with the strength predictions using a sectional design model and a strut-and-tie model (Collins and Mitchell 1991). In these tests, the shear span-to-depth ratio *a/d* was varied from 1 to 7 and no web reinforcement was provided. At *a/d* values less than 2.5, the resistance is governed by strut-and-tie action, with the resistance dropping off rapidly as *a/d* increases. The failures in this region were governed by crushing the compressive struts that were sensitive to the size of the bearing plates. For *a/d* values greater than 2.5, the strength is governed by the conditions away from the supports and concentrated loads. In these regions, failure is governed by shear, owing to the large amount of longitudinal reinforcement in the beams. It is clear from this figure that for *a/d* values less than about 2.5, a strut-and-tie model more accurately predicts the strength, whereas for *a/d* values greater than about 2.5, a sectional design model that includes V_c caused by tensile stresses in the concrete is more appropriate.

Figure 6.5 gives examples of disturbed regions in which the flow of the compressive stresses is indicated by dashed lines and the tension ties are indicated by solid lines. Fig. 6.5(a) illustrates how the presence of the support reaction interrupts the uniform field of compressive stresses in the concrete, causing a disturbed region where the compressive stresses fan into the support. The corbel shown in Fig. 6.5(b) is a disturbed region characterized by compressive struts anchored by a tension tie through the column. The entire deep beam shown in Fig. 6.5(c) is a D region in which the concentrated load is transmitted directly to the supports by concentrated unidirectional compressive stresses or struts. The resisting mechanism resembles a tied arch with the reinforcement acting as a tension tie between the supports. Figure 6.5(d) illustrates the high compressive stresses from the concentrated loads fanning into a uniform field of compressive stresses in a wall.

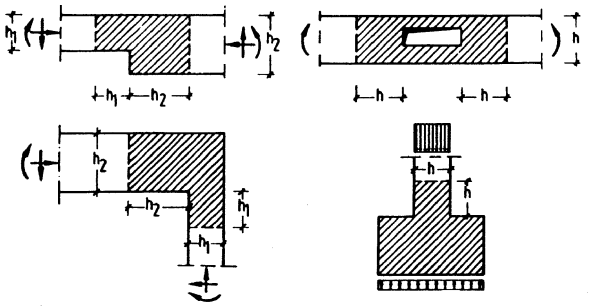

(a) D-regions caused by geometric discontinuities

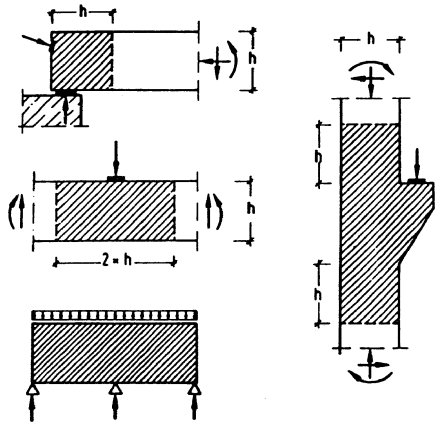

(b) D-regions caused by concentrated loads and/or geometric discontinuities

Fig. 6.3—D regions shown as shaded areas, adapted from Schlaich et al. (1987).

6.3.2 *Choosing strut-and-tie model*—The first step in design is to visualize the flow of the forces and identify B regions with parallel compressive fields and D regions with compressive struts representing the flow of concentrated compressive stresses in the concrete and tension ties representing the reinforcing steel. The visualization of the flow of compressive stresses in the concrete allows the development of a truss idealization consisting of compressive struts and the tension ties necessary for equilibrium. It takes experience to determine the most efficient strut-and-tie models for different situations. For any given situation, many strut-and-tie models are possible and no unique solution exists. Schlaich and Shäfer (1984) and Schlaich et al. (1987) have suggested that a strut-and-tie model be chosen after carrying out an elastic analysis. They suggested choosing the geometry of the truss model so that the angles of the compression diagonals are within ±15 degrees of the angle of the resultant of the compressive stresses obtained from an elastic analysis. Although this approach can give some guidance in choosing the geometry of the strut-and-tie model, it should be recognized that considerable redistribution of stresses takes place after cracking if the member is ductile. Figure 6.6(a) illustrates

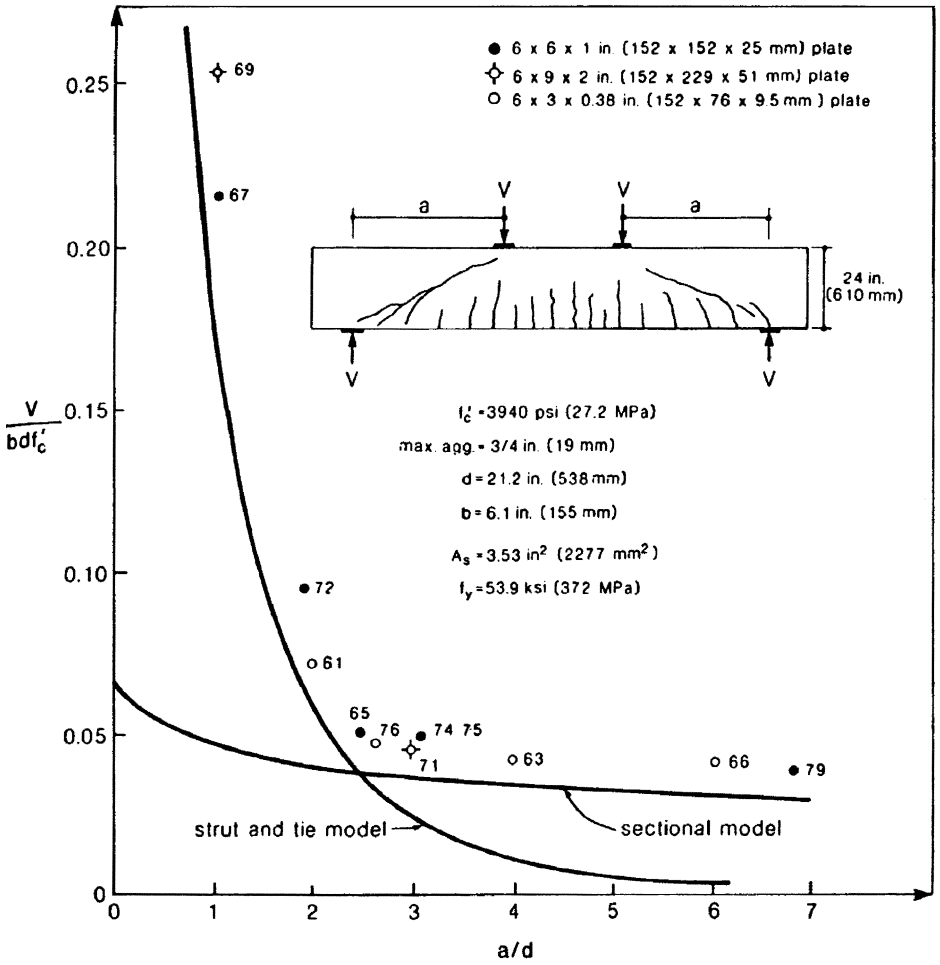

Fig. 6.4—Applicability of sectional design model and strut-and-tie model for series of beams tested by Kani (1979), adapted from Collins and Mitchell (1991).

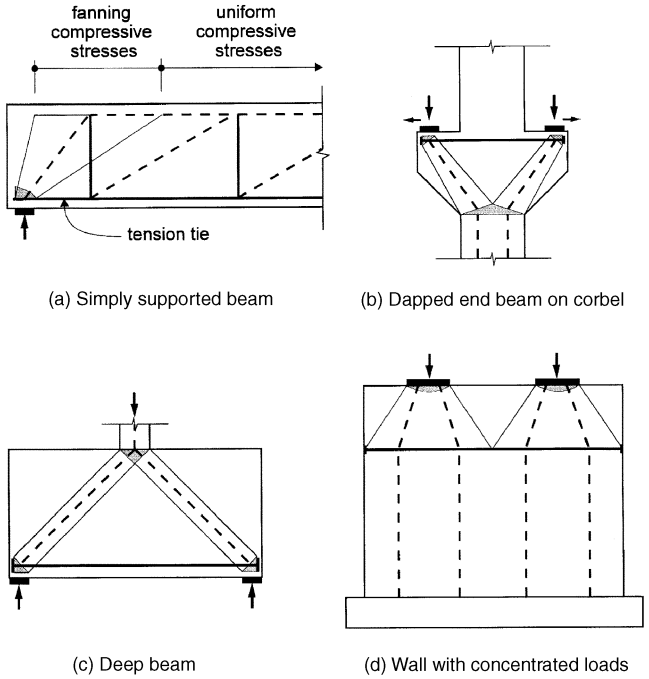

Fig. 6.5—Example of D regions modeled with compressive struts and tension ties.

the compressive stress fields for a deep beam. The compressive struts are actually bulging between the loading point and the supports, causing transverse tension idealized by the tension ties shown in Fig. 6.6(b). A simpler approach is to assume that the compressive struts can be idealized as straight line truss members following the centerline of the compressive struts, provided that additional reinforcement is provided to control cracking. To control cracking, most codes require that a minimum amount of reinforcement be provided in both the transverse and the longitudinal direction. For example, CSA Standard CAN3-A23.3-M84 (“Design” 1984) requires that a minimum reinforcement ratio equal to 0.002 be provided in both the transverse and the longitudinal direction. This small amount of uniformly distributed reinforcement is usually neglected in the strut-and-tie model and the truss idealization (Fig. 6.6(c)).

A simple truss idealization of the flow of the forces can be developed in which the zones of high unidirectional compressive stresses are modeled as compressive struts, and tension ties are used to model the principal tension reinforcement. Figure 6.7(a) illustrates the flow of the forces in a deep beam subjected to two point loads. The loads are assumed to be transferred to the supports by compressive struts, requiring a tension tie between the supports. The internal resisting mech-

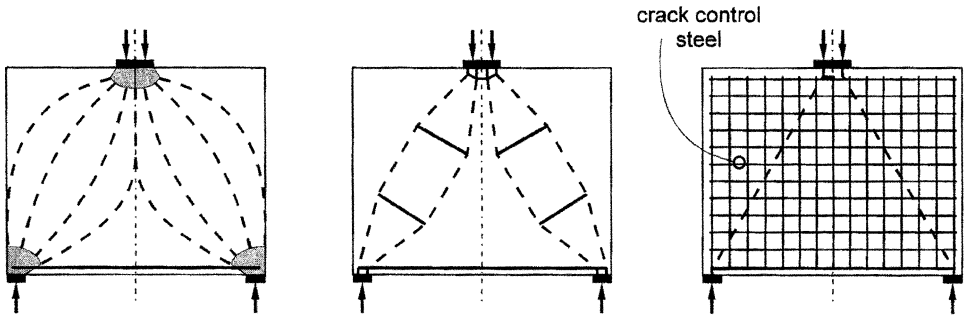

Fig. 6.6—Crack control reinforcement required with assumed straight-line compressive struts, adapted from Schlaich et al. (1987).

anism is shown as a truss model in Fig. 6.7. The strut-and-tie design method described below is based primarily on the design approach developed for the CSA Standard CAN3-A23.3-M84 ("Design" 1984; Collins and Mitchell 1985, 1984). The behavior of a variety of heavily instrumented D regions has been presented by Leonhardt and Walther (1966), Mattock et al. (1976), Rogowsky et al. (1986), Cook and Mitchell (1988), Adebar et al. (1990), and Jirsa et al. (1991).

6.3.3 *Checking compressive stresses in struts*—In the design using strut-and-tie models, it is necessary to check that crushing of the compressive struts does not occur. Marti (1985) pointed out that the cross-sectional area of the compressive struts is highly dependent on the details at their ends. Figure 6.8 gives examples of details that affect the geometry of the struts. Marti suggested that the compressive stress in the struts be limited to $0.6f_c'$ whereas Ramirez and Breen (1991) suggest a compressive stress limit of $2.5\sqrt{f_c'}$ in MPa units. Schlaich et al. (1987) and MacGregor (1997) have proposed compressive stress limits for the struts that depend on the stress conditions and angle of cracking surrounding the strut. Based on tests results, Bergmeister et al. (1991) proposed an equation for the stress limit of concrete struts as

$$f_c = \left(0.5 + \frac{1.25}{\sqrt{f_c'}}\right) f_c' \tag{6-2}$$

where f_c' is in MPa. This equation is proposed for concrete having a compressive strength ranging from 20 to 80 MPa.

Alshegeir and Ramirez (1990) proposed the stress limits listed in Table 6.1 to account for the level of concrete confinement by reinforcement, the disturbance resulting from cracking, and the existence of prestressing forces.

CSA Standard CAN3-A23.3-M84 ("Design" 1984) uses a compressive stress limit based on the work of Vecchio and Collins (1986), which considers the strain compatibility of the struts and the strain softening of diagonally cracked concrete. The compressive strength f_{2max} of the diagonally cracked concrete is given as

$$f_{2max} = \frac{f_c'}{0.8 + 170\varepsilon_1} \le 0.85f_c' \tag{6-3}$$

where

ε_1 = the principal tensile strain; and

f_c' = the cylinder compressive strength.

Compatibility of strains is used to determine the principal tensile strain from

$$\varepsilon_1 = \varepsilon_s + (\varepsilon_s + 0.002)\cos^2\alpha_s \tag{6-4}$$

where

ε_s = the required strain in the tension tie (usually taken as ε_y), the value 0.002 is the assumed strain in the compressive strut at crushing; and

α_s = the angle between the strut and the tie that crosses the strut.

It is necessary to determine ε_1 from Eq. (6-4) where α_s is the angle between the strut and the main tension tie reinforcement shown in Fig. 6.7(b). After determining f_{2max} from Eq. (6-3), the required capacity of the compressive strut N_u can be expressed as

$$\phi A_{cs} f_{2max} \ge N_u \tag{6-5}$$

where

A_{cs} = the effective cross-sectional area of the strut; and

ϕ = the capacity reduction factor for axial compression, equal to 0.70.

In some circumstances, it may be advantageous to provide reinforcing bars of area A_{ss} that are parallel to the strut and are restrained against buckling by the provision of ties. In this case, the design of the strut can be checked by

$$\phi(A_{cs} f_{2max} + A_{ss} f_y) \ge N_u \tag{6-6}$$

where f_y is the yield strength of the reinforcing bars.

6.3.4 *Design of nodal zones*—Figure 6.7 shows the strut-and-tie model and the idealized truss model for a deep beam. The locations of the intersection of the truss members, or nodes of the truss, represent regions of multidirectionally stressed concrete or nodal zones of the strut-and-tie model. The compressive strength of the nodal zone concrete depends on many factors, including the tensile straining

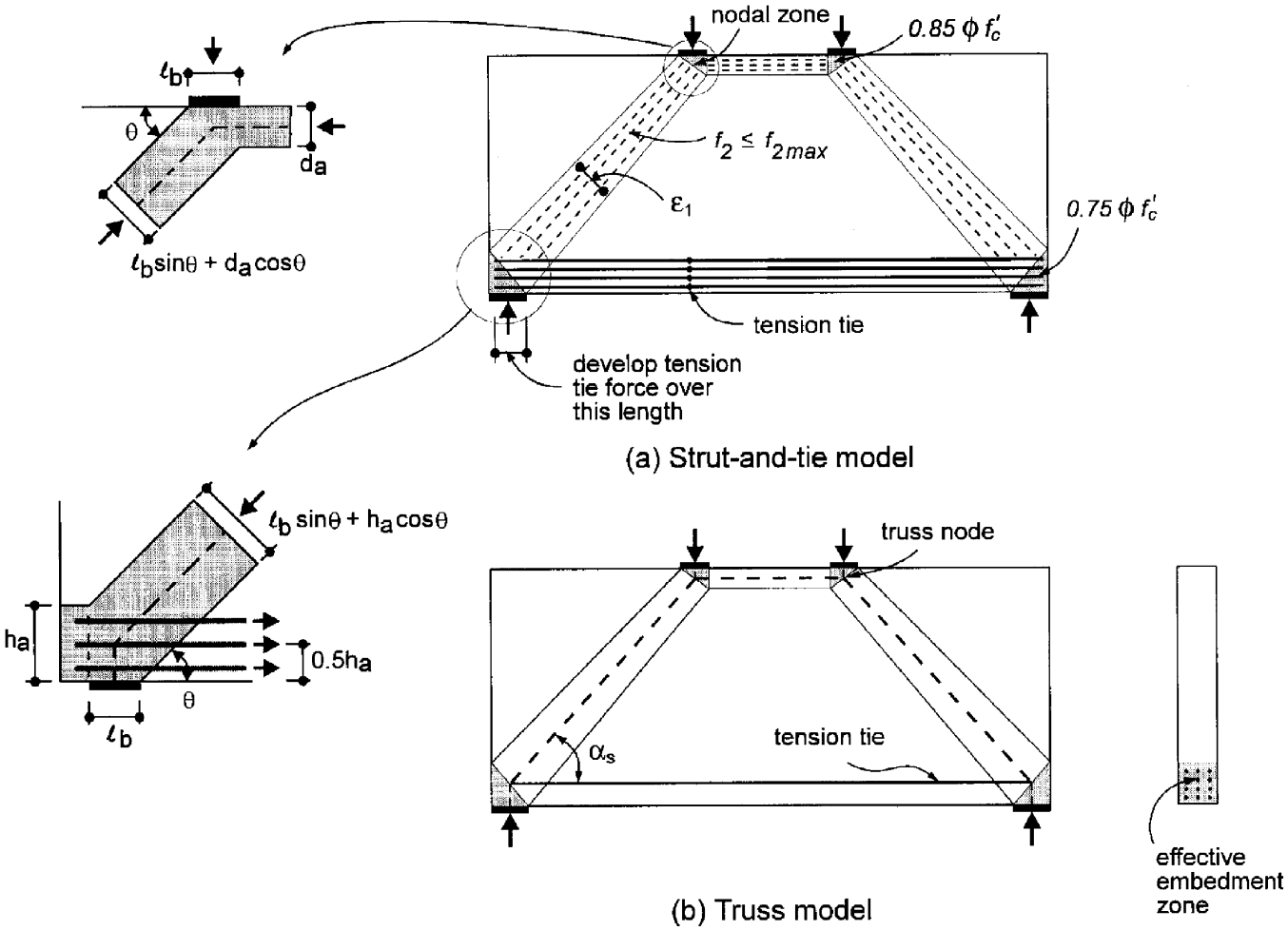

Fig. 6.7—Strut-and-tie model and idealized truss model for deep beam.

Table 6.1—Effective stress levels in concrete struts

Effective stress level (1)	Concrete struts (2)	Proposed by (3)
$0.8f'_c$	Undisturbed and uniaxial state of compressive stress that may exist for prismatic struts	Schlaich et al. (1987)
$0.68f'_c$	Tensile strains and/or reinforcement perpendicular to the axis of the strut may cause cracking parallel to the strut with normal crack width	Schlaich et al. (1987)
$0.51f'_c$	Tensile strains causing skew cracks and/or reinforcement at skew angles	Schlaich et al. (1987)
$0.34f'_c$	For skew cracks with extraordinary crack width. Skew cracks would be expected if modeling of the struts departed significantly from the theory of elasticity's flow of internal forces	Schlaich et al. (1987)
$0.85f'_c$	Moderately confined diagonal struts going directly from point load to support with shear span-to-depth ratio less than 2.0	Alshegeir and Ramirez (1990)
$0.75f'_c$	Struts forming arch mechanism	Alshegeir and Ramirez (1990)
$0.50f'_c$	Arch members in prestressed beams and fan compression members	Alshegeir and Ramirez (1990)
$0.95f'_c$	Undisturbed and highly stressed compression struts	Alshegeir and Ramirez (1990)
$v_2 f'_c$	Uncracked uniaxially stressed struts or fields	MacGregor (1997)
$v_2 (0.80)f'_c$	Struts cracked longitudinally in bulging compression fields with transverse reinforcement	MacGregor (1997)
$v_2 (0.65)f'_c$	Struts cracked longitudinally in bulging compression fields without transverse reinforcement	MacGregor (1997)
$v_2 (0.60)f'_c$	Struts in cracked zone with transverse tensions from transverse reinforcement	MacGregor (1997)
$v_2 (0.30)f'_c$	Severely cracked webs of slender beams with θ = 30 degrees	MacGregor (1997)
$v_2 (0.55)f'_c$	Severely cracked webs of slender beams with θ = 45 degrees	MacGregor (1997)

Note: $v_2 = 0.5 + 1.25/\sqrt{f'_c}$ in MPa after Bergmeister et al. (1991).

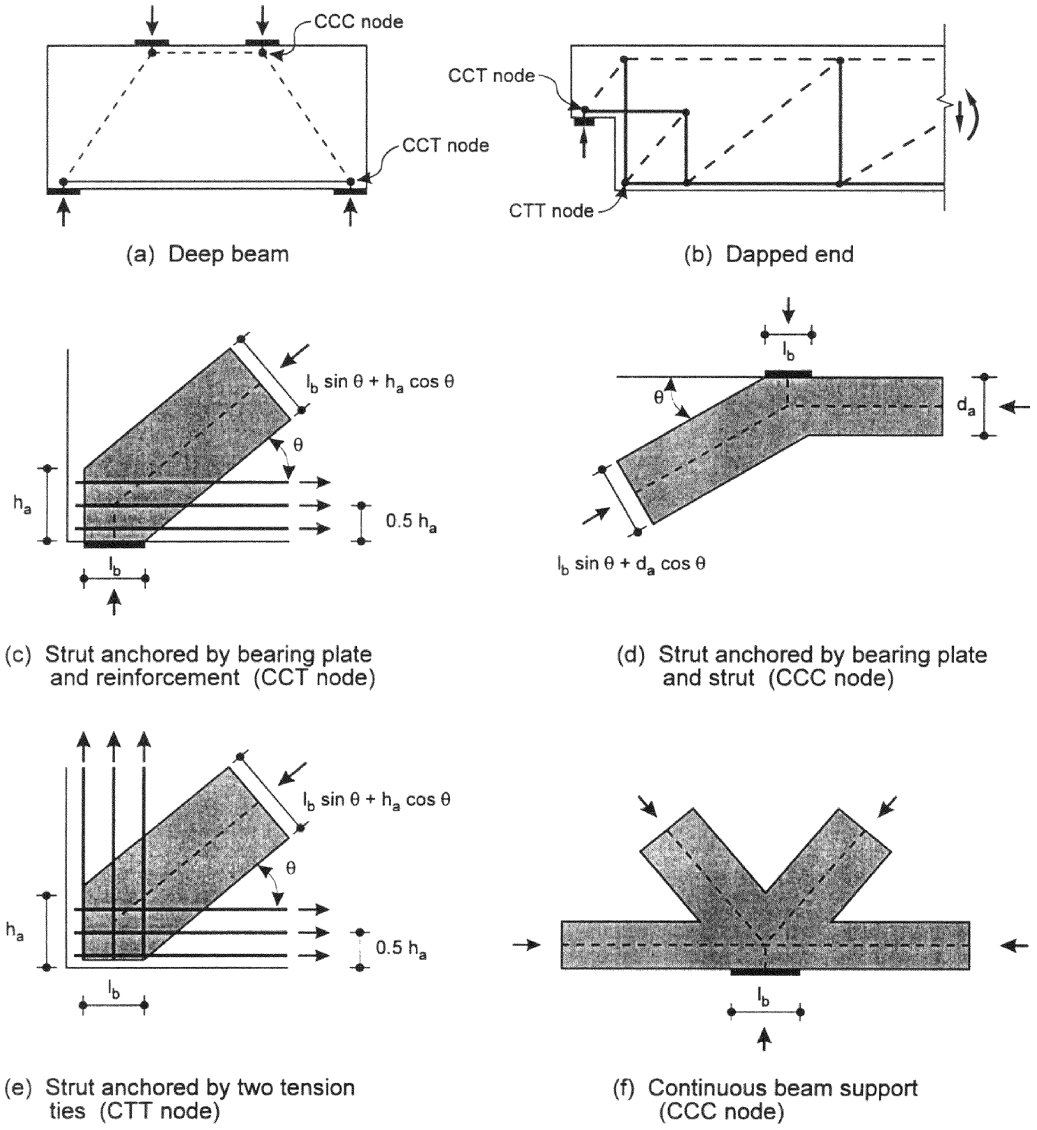

Fig. 6.8—Type of nodal zones (Jirsa et al. 1991) and dimensions of struts ("Design" 1984).

from intersecting tension ties, confinement provided by compressive reactions, and confinement provided by transverse reinforcement. To distinguish between the different straining and confinement conditions for nodal zones it is helpful to identify these zones as follows:

- CCT—nodal zone bounded by compression struts and one tension tie;
- CCC—nodal zone bounded by compression struts only; and
- CTT—nodal zone bounded by a compression strut and tension ties in two or more directions.

Figure 6.8 illustrates the different types of nodal zones for a deep beam and a beam with a dapped end together with examples of reinforcement details and dimensions required for determining the geometry of struts and nodal zones (Jirsa et al. 1991; "Design" 1984).

The Canadian standard ("Design" 1984) limits the concrete stress in the nodal zones to the following values:

- $0.85\phi f_c'$ in node regions bounded by compressive struts and bearing areas (CCC nodes);
- $0.75\phi f_c'$ in node regions anchoring a tension tie in only one direction (CCT nodes); and
- $0.60\phi f_c'$ in node regions anchoring tension ties in more than one direction (CTT nodes), where ϕ is the capacity-reduction factor for bearing (taken as 0.70 in ACI 318M-95).

In addition, the beneficial effects of confinement provided by transverse reinforcement can be accounted for by increasing these stress limits.

Marti (1985) described a procedure for evaluating stresses of nodal zones bounded by three or more intersecting struts. In this approach, the tie forces can be converted to compressive forces acting on the back face of the nodal zone. Also, the state of stress of nodal zones is assumed to be hydrostatic. If the strut widths are chosen so that the stresses in all struts are equal to $-\sigma$, then the stresses in the nodal zone are $\sigma_x = \sigma_y = \sigma_1 = \sigma_2 = -\sigma$, $\tau_{xy} = 0$, and $\sigma_z = \sigma_3 = 0$ and the sides of the nodal zone are perpendicular to the struts. He proposed that nodal zones and compressive struts could be stressed up to a limit of $0.6f_c'$.

Table 6.2—Effective stress levels in nodal zones

Effective stress level (1)	Nodes (2)	Proposed by (3)
$0.85f_c'$	CCC-nodes	Schlaich et al. (1987)
$0.68f_c'$	Nodes where reinforcement is anchored in or crossing the node	Schlaich et al. (1987)
$v_2 f_c'$	Nodes bounded by compressive struts and bearing areas	MacGregor (1997)
$v_2 (0.85) f_c'$	Nodes anchoring one tension tie	MacGregor (1997)
$v_2 (0.75) f_c'$	Nodes anchoring tension ties in more than one direction	MacGregor (1997)
$0.8f_c'$ for $f_c' \le 30$ MPa	Unconfined nodes without bearing plates	Bergmeister et al. (1991)
$(0.9 - 0.25f_c'/70)f_c'$ MPa for $30 < f_c' \le 70$ MPa	Unconfined nodes without bearing plates	Bergmeister et al. (1991)
$0.65f_c'$ for $f_c' \ge 70$ MPa	Unconfined nodes without bearing plates	Bergmeister et al. (1991)
$vf_c'(A/A_b)^{0.5} + \alpha(A_{core}/A_b)f_{lat}(1 - s/d)^2 \le 2.5f_c'$	Confined nodes	Bergmeister et al. (1991)
$vf_c'(A/A_b)^{0.5}$	Unconfined nodes with bearing plates	Bergmeister et al. (1991)
$2.5f_c'$	Triaxially confined nodes	Bergmeister et al. (1991)

Note: A, A_b, and A_{core} are, respectively, area of confined concrete, bearing plate, and the confined strut; f_{lat} = lateral pressure ($2f_y A_s/(ds)$); A_s = area of one leg of confining reinforcement; μ = efficiency factor; s = pitch or spacing of confining reinforcement; d = diameter of core; α = parameter (4.0 for spiral confinement, 2.0 for square closed hoop confinement anchored with longitudinal reinforcement, and 1.0 for square closed hoop confinement without longitudinal reinforcement anchorage); and $v_2 = 0.5 + 1.25/\sqrt{f_c'}$ in MPa after Bergmeister et al. (1991).

Schlaich et al. (1985) and MacGregor (1997) also proposed values of effective stress levels of nodal zones. Based on the test results of 10 isolated CCT nodes and nine CTT nodes, Jirsa et al. (1991) recommended an effective concrete strut stress level of $0.8f_c'$.

Bergmeister et al. (1991) proposed several equations of effective concrete strength for various kinds of nodes, including reinforcement, unconfined nodes with bearing plates, and triaxially confined nodes. The proposed equations are listed in Table 6.2. An upper limit of $2.5f_c'$ was recommended for situations with a large amount of confinement.

Adebar and Zhou (1993) suggested stress limits for the concrete compressive struts confined by plain concrete based on the results of analytical and experimental studies. The limiting stress for deep members without reinforcement distributed over the depth (for example, pile caps) is limited to

$$f_c = \phi 0.6 f_c' (1 + 2\alpha\beta) \tag{6-7}$$

where

$$\alpha = 0.33(\sqrt{A_2/A_1} - 1) \le 1.0 \tag{6-8}$$

$$\beta = 0.33\left(\left(\frac{l_s}{b_s}\right) - 1\right) \le 1.0 \tag{6-9}$$

The ratio l_s/b_s, which represents the slenderness ratio (length/width) of the compression strut, should not be taken less than 1. The parameter α accounts for the degree of confinement, whereas the parameter β accounts for the geometry of the compressive stress field and ϕ is a capacity-reduction factor for axial compression. In the expression for α, A_1, and A_2 resent the loaded area and the supporting surface area, respectively. The lower bearing-stress limit of $\phi 0.6f_c'$ was suggested if there is no confinement, regardless of the length of the compressive strut. For relatively short compressive struts with a large degree of confinement, the upper limit suggested was $\phi 1.8f_c'$.

6.3.5 *Design of tension ties*—Once the required force N_u in the tension tie has been determined from the statics of the truss model, the area of reinforcement can be determined from

$$\phi(A_{st}f_y + A_{ps}(f_{ps} - f_{se})) \ge N_u \tag{6-10}$$

where

A_{st} = area of reinforcing bars;
A_{ps} = area of prestressed reinforcement;
f_y = yield strength of reinforcing bars;
f_{ps} = stress in prestressed reinforcement at ultimate;
ϕ = capacity-reduction factor for axial tension (0.9); and
f_{se} = stress in prestressing steel after all losses.

Note that Eq. (6-10) assumes that a portion of the prestress has been accounted for using an external compression on the member of $A_{ps}f_{se}$. If the prestressing is treated as a tension tie having an initial tensile force of $A_{ps}f_{se}$, then the full force $A_{ps}f_{ps}$ can be used in Eq. (6-10).

6.3.6 *Anchorage of tension ties*—An important aspect of the design of D regions is the anchorage of tension ties to develop the required stress in the reinforcement. The tension tie reinforcement shown in Fig. 6.7 should develop the required stress in the steel at the inner face of the bearing to avoid failure by loss of anchorage. Anchorage may be achieved by an appropriate embedment length over the bearing areas or by mechanical anchorage. Another important aspect of the design of the anchorage regions is to spread the anchorage of the tie reinforcement over a large enough area to avoid nodal zone crushing. Therefore the distance h_a, shown in Fig. 6.7, should be such that the tension tie force divided by the effective embedment area does not exceed the appropriate nodal zone stress limit.

6.3.7 *Design procedure*—The steps in the design of a D region, such as the deep beam shown in Fig. 6.7, are as follows:

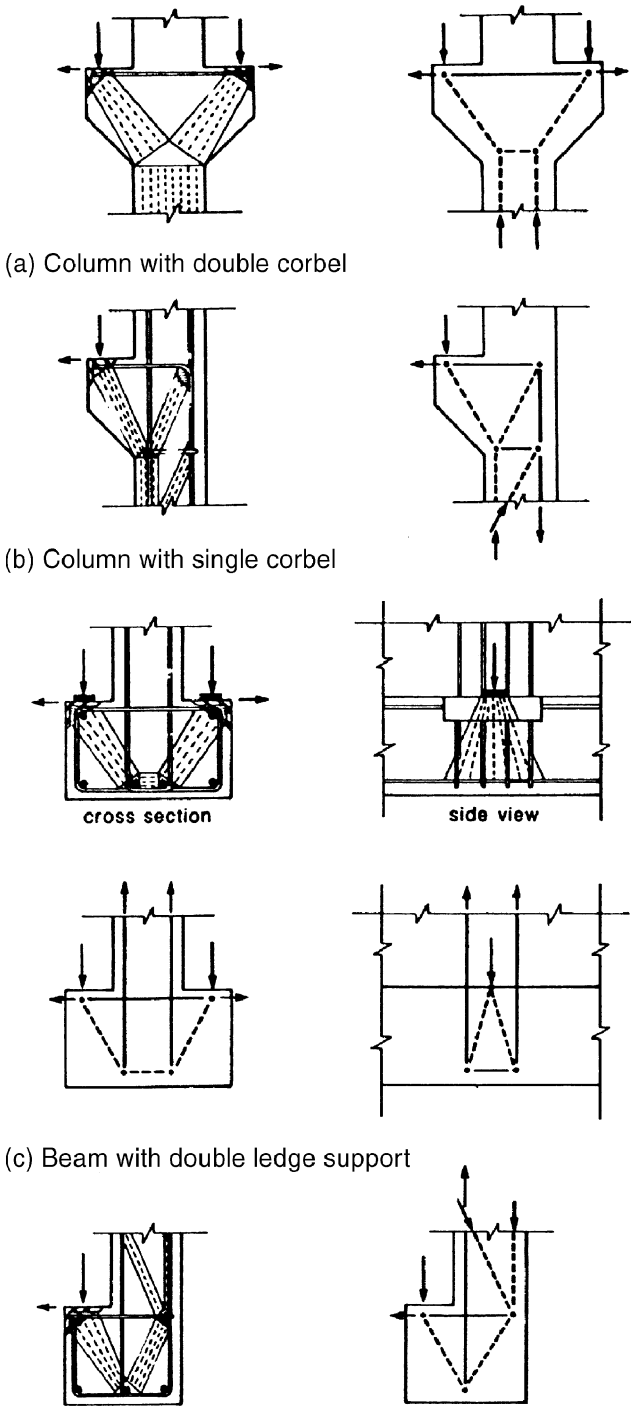

Fig. 6.9—Strut-and-tie model idealizations for brackets, ledges, and corbels (Cook and Mitchell 1988).

1. Sketch the flow of the forces in the D region and locate nodal zones that are the regions bounded by struts, tension ties, or bearing areas;

2. Determine the dimensions of the loading and reaction areas such that the nodal zone stresses are less than the permissible limits;

3. Determine the geometry of the truss model. The compressive struts are represented by truss members located at their centerlines, and the tension ties are represented by truss members at the centroid of the reinforcement. The nodes of the truss are located at the intersections of struts, tension ties, and applied loads or reactions. In determining the geometry, it is important to account for the actual dimensions of the nodal zones. The dimensions of the nodal zones are dependent on the sizes of the bearing plates, where used, and the anchorage details of the tension ties. (Note: Because the force in the tension tie is not known at this stage, it will be necessary to make an estimate of the required anchorage area so that the size of the nodal zone and hence the geometry of the truss model can be determined.);

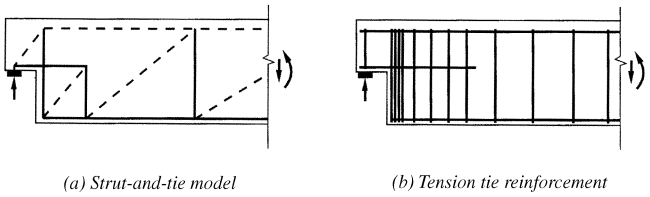

Fig. 6.10—Beam with dapped end, adapted from Schlaich et al. (1987): (a) strut-and-tie model; and (b) tension tie reinforcement.

4. Determine the forces in the truss members. If the truss is statically indeterminate (for example, a continuous deep beam) it will be necessary to estimate the relative stiffnesses of the truss members to solve for the forces in the struts and ties;

5. Determine the required areas of the tension tie reinforcement (see Eq. (6-10));

6. Ensure that the anchorages of the tension ties are sufficient and that the tension ties are spread over a sufficient anchorage area to satisfy the nodal zone stress limits; and

7. Calculate the compressive stresses in the struts at critical locations using the effective strut areas. Check that the calculated compressive stresses in the struts are less than f_{2max} (see Eq. (6-3) and (6-4) or Table 6.1).

The design of D regions using the above steps may involve an iterative procedure.

6.3.8 *Examples of strut-and tie models*—Figures 6.9 to 6.11 show strut-and-tie models suggested by Cook and Mitchell (1988) and Schlaich et al. (1987) with the corresponding truss idealizations for different examples of D regions including brackets, corbels, ledges, a dapped end, and deep beams. The truss models for the continuous deep beams shown in Fig. 6.11(b) and (c) are statically indeterminate; therefore, it is necessary to assume the relative stiffness of the truss members to find the forces in the truss member. Guidance on more sophisticated truss models for deep beams is given by Rogowsky and MacGregor (1986).

Strut-and-tie models are well suited to designing the reinforcement required in anchorage regions of post-tensioned tendons (Schlaich et al. 1987; Collins and Mitchell 1991; Burdet et al. 1991). Figure 6.12 illustrates strut-and-tie models used to model the flow of forces for the case of the anchorage of two post-tensioned tendons (Burdet et al. 1991). For the case where the tendon anchorages are within the quarter points of the section, the flow of forces in the anchorage zone will be similar to that induced by a single

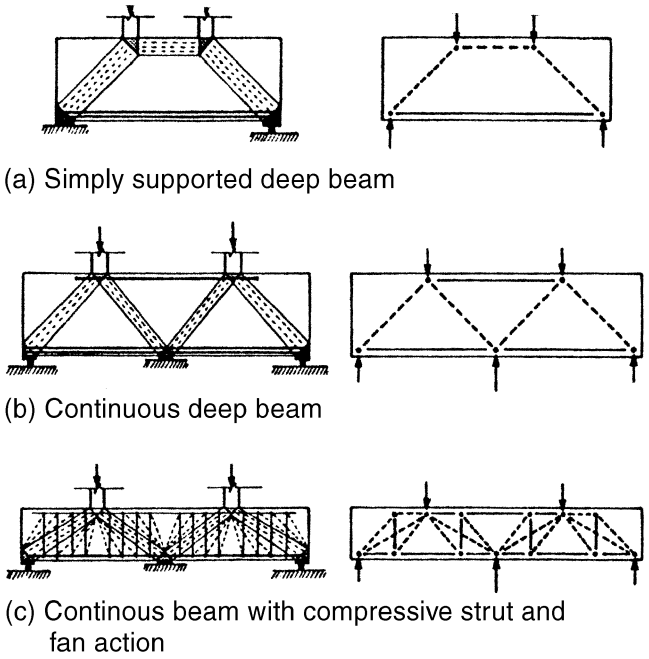

Fig. 6.11—Strut-and-tie models and truss idealizations for deep beams (Cook and Mitchell 1988).

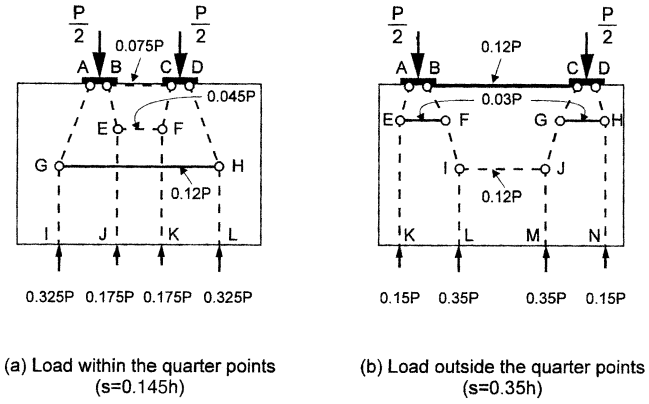

*Fig. 6.12—Strut-and-tie models for design of anchorage zones with two post-tensioned tendons (Burdet et al. 1991): (a) load within quarter points (*s = *0.145*h*) and (b) load outside quarter points (*s = *0.35*h*).*

anchorage device (Fig. 6.12(a)). For the case with the tendons anchored outside of the kern, there is a different flow of forces with a tension tie required near the end face of the member (Fig. 6.12(b)).

Figure 6.13 illustrates the strut-and-tie model and the three-dimensional truss idealization suggested by Adebar et al. (1990) for a column supported by a pile cap. Schlaich et al. (1987) and Muttoni et al. (1997) have presented examples of the strut-and-tie modeling of deep beams and walls with openings, post-tensioned buttress anchorage regions, bridge piers, and bridge diaphragms. Detailed design examples of D regions using the design approach described in this report are given by Collins and Mitchell (1991) and MacGregor (1992).

More research is required to be able to predict service load behavior of D regions.

CHAPTER 7—SUMMARY

7.1—Introduction

This report focused on the presentation of new shear design approaches. The work presented is limited to monotonic loads on one-way flexural members covering both B and D regions. The interaction of shear and torsional effects is not covered in this report. Although the methods presented can be applied to shear and torsion, in several instances this fact remains to be shown and verified with sufficient tests.

The approaches reviewed cover the entire range of structural concrete from reinforced to fully prestressed concrete members. The so-called concrete contribution to the shear strength has been discussed. Thus, this report addresses members with and without shear reinforcement.

This report does not attempt to endorse any of the individual approaches presented. Instead, the goal is to illustrate the common base of these new approaches and how they supplement each other. By doing so, the report attempts to answer the challenge put forth by ASCE-ACI Committee 426 in 1973.

7.2—Truss models

Since the early 1900s, engineers have used truss models to follow the flow of internal forces in structural-concrete members and provide structural systems made out of concrete and reinforcement that ensure equilibrium. The original 45 degree truss model of Ritter (1899) and Mörsch (1920, 1922) has been adopted either explicitly or implicitly by most major codes as the basis for their shear and torsion design specifications. Throughout this report, the reader has been exposed to this concept in forms ranging from sectional truss models and compression field approaches for beams to generalized strut-and-tie models. Their application extended to the full range of structural concrete in members with and without shear reinforcement.

As explained in Chapter 1, beginning with the earlier concept of a sectional design approach based on a constant con-crete contribution supplementing a constant 45 degree angle truss, the truss model approach was first introduced by M. O. Withey into the American literature in 1907. At this time Withey noted that the 45 degree truss model alone yielded conservative results when compared with test evidence. This observation was confirmed by Talbot in 1909. As a result, since its origins, shear design in the United States has included a concrete contribution, V_c, to supplement the 45 degree truss model. More modern versions of design specifications, such as the 1978 Comité Euro-International du Béton-Fédération International de la Précontrainte (CEB-FIP) Model Code for Concrete Structures, have extended this concept by recognizing the capability for redistribution of internal forces of reinforced and prestressed concrete beams containing stirrup reinforcement. This approach has been set up as a variable-angle truss with some established semiempirical limits for the angle of inclination supplemented with a concrete contribution. The concrete contribution included the presence of prestressing as well as the possibility of a diminished contribution after significant redistribution of internal forces. This reduction was deemed to be the result of crack

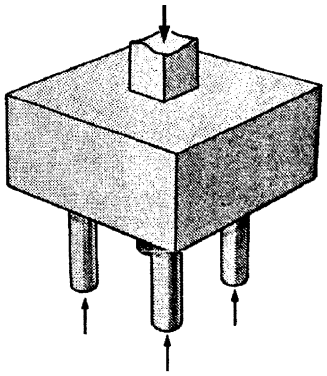

Pile cap supported on four piles

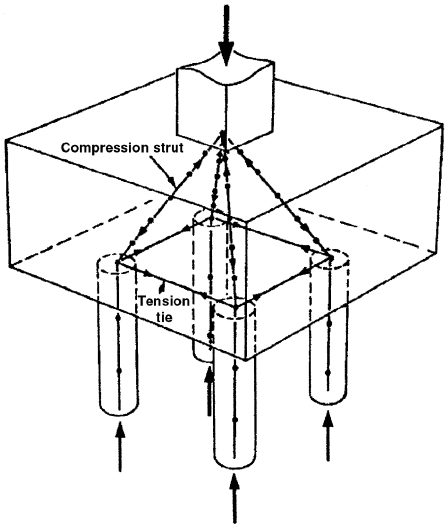

Simple three-dimensional truss model for a four-pile cap

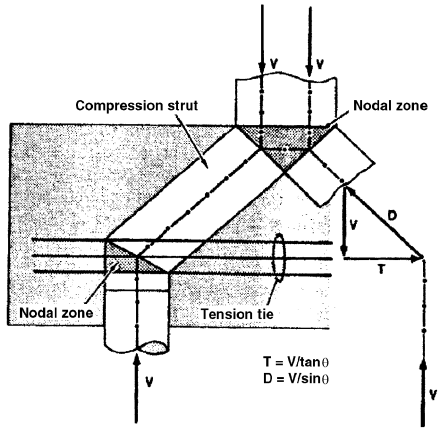

Components of the idealized load-resisting strut-and-tie model

Fig. 6.13—Strut-and-tie models and three-dimensional truss model for column supported on four-pile cap (adapted from Adebar et al. [1993]).

inclinations deviating significantly from 45 degrees and the resulting wider crack widths from this redistribution.

Kupfer (1964) provided a solution for the angle of inclination of the diagonal cracks from the analysis of a truss model consisting of linearly elastic members and neglecting the tensile strength of the concrete. Baumann (1972) derived a similar solution for wall elements. Mitchell and Collins (1974) abandoned the notion of cracked linear behavior and developed the CFT for torsion in 1974 to allow for evaluation of the angle of inclination of the diagonally cracked concrete through the entire range of loading (see Chapter 2). This approach, extended by Collins (1978) to the case of shear, neglected the presence of tensile stresses in the concrete between the cracks. The compression field approach views the cracked concrete as a material where the principal stress and strain axes coincide. Under a given loading condition, the direction of the uniaxial compression field will rotate as needed to satisfy equilibrium. Marti (1992) has shown that for a wall element with orthogonal reinforcement in the x and y directions, and assuming linear elastic behavior for both steel and concrete, the compression field approach leads to Baumann's and originally Kupfer's solutions for the angle of inclination of the diagonally cracked concrete. These approaches essentially neglected the so-called concrete contribution term.

The truss-model-related theories discussed in the preceding paragraph are based on the assumption that the compression struts are parallel to the principal compressive stress orientation and that no stresses are transferred across the cracks. Vecchio and Collins (1986) (see Chapter 2) introduced the MCFT based on the assumption that tensile stresses in the concrete between the cracks contribute significantly to the shear resistance. The basic assumption was that these tensile stresses transverse to the axis of the strut exist at points between the inclined cracks, but are zero at the cracks. In their derivation, the tensile strength of the concrete strut diminishes as the principal strain ε_1 increases. The explanation is that the tensile strength of the concrete may be limited by the ability of the crack surfaces to transmit shear stresses that will depend on the crack width and the maximum size of the aggregate.

Refined methods have attempted to supplement the truss model strength with a concrete contribution term. Such methods are discussed in Chapter 3. An example of such approaches has been called the truss analogy with crack friction. In this approach, shear stresses are transferred across the cracks by friction. It can be regarded as a development based on the shear-friction theory discussed briefly in Chapter 5. As a failure mechanism approach, it starts with basic assumptions for the spacing and the shape of the cracks in the B region of a structural-concrete member subjected to shear forces. In this sense, it is a discrete approach with respect to cracking. Two results from the assumption that shear stresses are transferred across the cracks are that the angle of the principal compression stress in the web does not coincide with the angle of the cracks, θ, and there is a vertical component of the frictional forces, V_f, along the crack face contributing to the shear strength. Several researchers postulate that V_f could represent the concrete contribution appearing in ACI 318M-95.

Truss models approaches have been generalized to all parts of the structure in the form of strut-and-tie models. Structural-concrete members with an adequate distribution of minimum transverse and longitudinal reinforcement can be designed using the simple strut-and-tie models described in Chapter 6. Three key advantages of this approach are that 1) the flow of internal forces is clearly visualized by the designer; 2) the effects of both shear and moment are accounted for simultaneously and directly in the design; and 3) the design of B-and D-type regions and the transitions between them can be conducted in a unified and consistent manner. Thus, the design can be carried out for the entire member using a full-member truss model as a generalized strut-and-tie model. Alternatively, the design of B regions can be carried out using a sectional model, such as the ones described in Chapters 1, 2, and 3.

The use of strut-and-tie models is especially advantageous in the design of D regions characterized by a complex flow of internal forces resulting in significant nonlinear distribution of strains. Although this report is directed at the design of one-way flexural members under monotonic loads, the design of D regions appearing in this type of member is discussed thoroughly in Chapter 6. The same basic principles presented in this report could be extended to other types of D regions such as beam-column joints. The effects of dynamic load and torsion in this and other relevant cases, however, are not within the scope of this report.

7.3—Members without transverse reinforcement

Many structural elements such as slabs, footings, and joists are built without transverse reinforcement (that is, stirrups or bent bars). The design of these members cannot be covered by a truss approach that ignores the tensile strength of the concrete. In this report, an extensive review of design models and analytical methods for structural members with no transverse reinforcement has been given (see Chapter 4). Although the case of two-way shear is not covered, much of the work presented and presently under way in members without transverse reinforcement is geared toward the development of more rational methods for punching shear.

Since the 1973 ASCE-ACI Committee 426 report was issued, an additional mechanism of shear transfer in the form of residual tensile stresses transmitted directly across cracks has been identified. The 1973 ACI 426 report identified four mechanisms of shear transfer: 1) shear stresses in the uncracked concrete; 2) aggregate interlock or shear friction; 3) dowel action of the longitudinal reinforcement; and 4) arch action. The question of which mechanisms will contribute most to the shear resistance of diagonally cracked concrete beam does not have a unique answer. As discussed in Chapter 4, the importance of the contribution of the individual mechanisms will depend on the specific member and loading conditions. For example, the amount of the shear stress carried across the uncracked concrete that can be significant in columns under compressive axial load, bending and shear, is relatively small in slender members without axial compression because the depth of the compression zone is smaller. Dowel action, which is not very significant when the dowels are near the surface, cannot be neglected when the member has high reinforcement ratios. It may be very significant, even in members with lower reinforcement ratios, when the longitudinal reinforcement is distributed in layers. Researchers have recognized this complexity and the importance of developing physical models to explain this behavior. The existing mechanical or physical models are presented in Chapter 4.

Despite differences in the approaches, the main conclusion from the models discussed in Chapter 4 is that concrete tensile stresses should be considered explicitly. Failure is not explained simply by the tensile stress reaching the tensile strength of the concrete, however, but involves the mechanism of shear transfer at the cracks. In other words, for smaller-sized members, the residual stresses are very important, whereas for larger members, with several cracks before failure, the friction across the cracks has a more important role. Another important conclusion is that relationships based on smeared or discrete truss models considering the tensile strength of the concrete are now available to replace the largely empirical approaches in current codes of practice. This is particularly true for ACI 318M-95, where the observation that the shear stress at failure decreases as the depth of the member increases is not properly recognized.

7.4—Additional work

During the past 20 years, considerable improvements have been made in understanding the behavior and improving the design of structural-concrete members subject to shear to the extent that there is now a solid foundation for advancing, unifying, and simplifying our design specifications. Such solid foundation is provided by truss model approaches and related theories. The challenge presented by the 1973 ASCE-ACI Committee 426 report has been answered. Realistic models exist now for deep beams, corbels, shear walls, and other unusual design problems. Much work remains to be done, however. The effects of dynamic loading on the truss model approach still need to be accounted for. Rational models for the complex problem of punching shear are still needed in

codes of practice. The enhanced shear strength of prestressed concrete members calls for additional study. Additional experimental verification is needed for the nodal zones of strut-and-tie models. Finally, a survey on the state-of-the-art for combined shear and torsion remains to be conducted. The next challenge is to integrate, simplify, and give a physical significance to the design regulations for torsional strength.

APPENDIX A—ACI 318M-95 SHEAR DESIGN APPROACH FOR BEAMS

$$V_n = V_c + V_s$$

$$V_s = A_v f_y d/s \le (2/3)\sqrt{f'_c}\, b_w d$$

V_c = concrete contribution

For nonprestressed beams

$$(\sqrt{f'_c}/6) b_w d$$

For prestressed beams

$$[(\sqrt{f'_c}/20) + 5(V_u d/M_u)] b_w d$$

$$\text{but } (1/6)\sqrt{f'_c}\, b_w d \le V_c \le 0.4\sqrt{f'_c}\, b_w d$$

or the lesser of V_{ci} or V_{cw}

$$V_{ci} = (\sqrt{f'_c}/20) b_w d + V_d + (V_i M_{cr}/M_{max})$$

$$\text{but } V_{ci} \ge (1/7)\sqrt{f'_c}\, b_w d$$

$$V_{cw} = 0.3(\sqrt{f'_c} + f_{pc}) b_w d + V_p$$

For axial compression and shear

$$V_c = [1 + (N_u/14A_g)](\sqrt{f'_c}/6) b_w d$$

For axial tension and shear

$$V_c = [1 + (0.3N_u/A_g)](\sqrt{f'_c}/6) b_w d$$

Detailing rules are as follows:

- Reinforcement shall extend beyond the point at which it is no longer required to resist flexure for a distance equal to the effective depth of the member or $12d_b$, whichever is greater.
- Flexural reinforcement shall not be terminated in a tension zone unless shear at cutoff ≤ 2/3 shear permitted; stirrup area A_v in excess of that required for shear and torsion, is provided [$A_v \ge 0.4 b_w s/f_y$; $s \le d/8\beta_b$]; or for No. 36 bars or smaller, shear at the cutoff ≤3/4 of the permitted, and continuing reinforcement provides double the area required for flexure at the cutoff.
- At simple supports and points of inflection, the diameter of the positive moment tension reinforcement shall be limited so that $l_d \le (M_n/V_u) + l_a$.

A-1—Notation

A_g = gross area of section (mm^2)
A_v = area of shear reinforcement within a distance s (mm^2)
b_w = web width or diameter of circular section (mm)
d = distance from extreme compression fiber to centroid of longitudinal tension reinforcement, which need not be less than $0.80h$ for prestressed members (mm) (for circular sections, d need not be less than the distance from extreme compression fiber to centroid of tension reinforcement in opposite half of member)
f'_c = specified compressive strength of concrete (MPa)
$\sqrt{f'_c}$ = square root of specified compressive strength of concrete (MPa)
f_{pc} = compressive stress in concrete (after allowance for all prestress losses) at centroid of cross section resisting externally applied loads or at junction of web and flange when the centroid lies within the flange (MPa) (in a composite member, f_{pc} is resultant compressive stress at centroid of composite section, or at junction of web and flange when the centroid lies within the flange, due to both prestress and moments resisted by precast member acting alone)
f_y = specified yield strength of nonprestressed reinforcement (MPa)
h = overall thickness of member (mm)
l_a = additional embedment length at support or at point of inflection (mm)
l_d = development length (mm)
M_{cr} = moment causing flexural cracking at section due to externally applied loads
M_{max} = maximum factored moment at section due to externally applied loads
M_u = factored moment at section
N_u = factored axial load normal to cross section occurring simultaneously with V_u (to be taken as positive for compression, negative for tension, and to include effects of tension due to creep and shrinkage)
s = spacing of shear or torsion reinforcement in direction parallel to longitudinal reinforcement (mm)
V_c = nominal shear strength provided by concrete
V_{ci} = nominal shear strength provided by concrete when diagonal cracking results from combined shear and moment
V_{cw} = nominal shear strength provided by concrete when diagonal cracking results from excessive principal tensile stress in web

V_d = shear force at section due to unfactored dead load
V_i = factored shear force at section due to externally applied loads occurring simultaneously with M_{max}
V_s = nominal shear strength provided by shear reinforcement
V_p = vertical component of the effective prestress force at the section
V_u = factored shear force at section
β = ratio of area of tension reinforcement cut off to total area of tension reinforcement at the section

A-2—Acknowledgments

This report is dedicated to the memory of Professor Peter Gergely, who chaired Committee 445 when this work was started. This report was written by members of a subcommittee of ASCE-ACI Committee 445 on Shear and Torsion. It was reviewed and balloted by the voting members of Committee 445. The subcommittee (445-1) acknowledges the guidance of Peter Marti, who as a former chairman of Committee 445 was instrumental in supporting the work on this report.

APPENDIX B—REFERENCES

B-1—Referenced standards and reports

The standards and reports listed below were the latest editions at the time this document was prepared. Because these documents are revised frequently, the reader is advised to contact the proper sponsoring group if it is desired to refer to the latest version.

American Concrete Institute

318M Building Code Requirements for Structural Concrete and Commentary
446.1R Fracture Mechanics of Concrete: Concepts, Models, and Determination of Material Properties

These publications may be obtained from this organization:

American Concrete Institute
P.O. Box 9094
Farmington Hills, MI 48333-9094

B-2—Cited references

ACI Committee 318, 1951, "Building Code Requirements for Reinforced Concrete (ACI 318-51)," ACI JOURNAL, *Proceedings* V. 48, Apr. 1951, pp. 589-652.

ACI Committee 318, 1971, "Building Code Requirements for Reinforced Concrete (ACI 318-71)," American Concrete Institute, Farmington Hills, Mich., 78 pp.

Adebar, P., 1994, "Testing Structural Concrete Beam Elements," *RILEM: Materials and Structures*, V. 27, No. 172, pp. 445-451.

Adebar, P., and Collins, M. P., 1996, "Shear Strength of Members without Transverse Reinforcement," *Canadian Journal of Civil Engineering*, V. 23, No. 1, pp. 30-41.

Adebar, P.; Kuchma, D.; and Collins, M. P., 1990, "Strut-and-Tie Models for the Design of Pile Caps," *ACI Structural Journal*, V. 87, No. 1, Jan.-Feb., pp. 81-92.

Adebar, P., and Zhou, Z., 1993, "Bearing Strength of Compressive Struts Confined by Plain Concrete," *ACI Structural Journal*, V. 90, No. 5, Sept.-Oct., pp. 534-541.

Al-Nahlawi, K. A., and Wight, J. K., 1992, "Beam Analysis using Concrete Tensile Strength in Truss Models," *ACI Structural Journal*, V. 89, No. 3, May-June, pp. 284-289.

Alshegeir, A., and Ramirez, J. A., 1990, "Analysis of Disturbed Regions with Strut-and-Tie Models," *Structural Engineering Report* No. CE-STR-90-1, Purdue University, West Lafayette, Ind.

Aoyagi, Y., and Yamada, K., 1983, "Strength and Deformation Characteristics of Reinforced Concrete Shell Elements Subjected to In-Plane Forces," *Proceedings,* Japanese Society of Civil Engineers, Tokyo, 331, pp. 167-190.

ASCE-ACI Committee 326, 1962a, "Shear and Diagonal Tension," ACI JOURNAL, *Proceedings* V. 59, No. 1, Jan., pp. 1-30.

ASCE-ACI Committee 326, 1962b, "Shear and Diagonal Tension," ACI JOURNAL, *Proceedings* V. 59, No. 1, Jan., pp. 277-344.

ASCE-ACI Committee 326, 1962c, "Shear and Diagonal Tension," ACI JOURNAL, *Proceedings* V. 59, No. 1, Jan., pp. 352-396.

ASCE-ACI Committee 426, 1973, "The Shear Strength of Reinforced Concrete Members," *Journal of Structural Division*, ASCE, V. 99, No. 6, pp. 1091-1187.

ASCE-ACI Committee 426, 1978, "Suggested Revisions to Shear Provisions for Building Codes," American Concrete Institute, Farmington Hills, Mich.

Barton, N., 1973, "Review of New Shear-Strength Criterion for Rock Joints," *Engrg. Geol.*, V. 7, pp. 287–332.

Baumann, T., 1972, "Zur Frage der Netzbewehrung von Flachen trag-werken (On the Problem of Net Reinforcement of Surface Structures)," *Bauingenieur*, V. 47, No. 10, pp. 367-377.

Baumann, T., and Rüsch, H., 1970, "Versuche zum Studium der Ver-dübelungswirkung der Biegezugbewehrung eines Stahlbetonbalkens," *DAfStb H.210*, Wilhelm Ernst und Sohn, Berlin, pp. 43-83.

Bažant, Z. P., and Kim, J.-K., 1984, "Size Effect in Shear Failure of Longitudinally Reinforced Beams," ACI JOURNAL, *Proceedings* V. 81, No. 5, Sept.-Oct., pp. 456-468.

Bažant, Z. P., and Oh, B. H., 1983, "Crack Band Theory for Fracture of Concrete," *RILEM*, V. 16, No. 93, pp. 155-177.

Belarbi, A., and Hsu, T. T. C., 1991, "Constitutive Laws of Reinforced Concrete in Biaxial Tension-Compression," *Research Report UHCEE 91-2*, University of Houston, Tex.

Belarbi, A., and Hsu, T. T. C., 1994, "Constitutive Laws of Concrete in Tension and Reinforcing Bars Stiffened by Concrete." *ACI Structural Journal*, V. 91, No. 4, July-Aug., pp. 465-474.

Belarbi, A., and Hsu, T. T. C., 1995, "Constitutive Laws of Softened Concrete in Biaxial Tension-Compression," *ACI Structural Journal*, V. 92, No. 5, Sept.-Oct., pp. 562-573.

Bergmeister, K.; Breen, J. E.; and Jirsa, J. O., 1991, "Dimensioning of the Nodes and Development of Reinforcement," *Report IABSE Colloquium on Structural Concrete*, IABSE, Zurich, pp. 551-564.

Bhide, S. B., and Collins, M. P., 1989, "Influence of Axial Tension on the Shear Capacity of Reinforced Concrete Members," *ACI Structural Journal*, V. 86, No. 5, Sept.-Oct., pp. 570-581.

Birkeland, P. W., and Birkeland, H. W., 1966, "Connections in Precast Concrete Construction." ACI JOURNAL, *Proceedings* V. 63, No. 3, Mar., pp. 345-368.

Braestrup, M. W., 1990, "Shear Strength Prediction—Plastic Method," *Reinforced Concrete Deep*, F. K. Kong, ed., Blackie and Son, London/Van Nostrand Reinhold, New York, pp. 182-203.

Bridge Design Specifications and Commentary, 1994, 1st Edition, American Association of State Highway and Transportation Officials, Washington, D.C.

Brock, G. et al., 1964, discussions of "The Riddle of Shear Failure and its Solution" by G. N. J. Kani, ACI JOURNAL, *Proceedings* V. 61, No. 12, Dec., pp. 1587-1636.

Burdet, O. L.; Sanders, D. H.; Roberts, C. L.; Breen, J. E.; and Fenves, G. L., 1991, "Models and Tests of Anchorage Zones of Post-Tensioning Tendons," *IABSE Colloquium on Structural Concrete*, Zurich, pp. 545–550.

Caflisch, R.; Krauss, R.; and Thurlimann, B., 1971, "Biege-und Schub-versuche and teilweise Vorgespannten Betonbalken," *Serie C., Bericht 6504-3*, Institut fur Baustatik, ETH, Zurich.

"CEB-FIP Model Code for Concrete Structures," 1978, *International System of Unified Standard Codes of Practice for Structures*, Comité Euro-International du Béton, Paris, V. II.

Chana, P. S., 1987, "Investigation of the Mechanism of Shear Failure of Reinforced Concrete Beams," *Magazine of Concrete Research*, V. 39, No. 12, pp. 196-204.

Collins, M. P., 1978, "Toward a Rational Theory for RC Members in Shear," *Journal of Structural Division*, ASCE, V. 104, No. 4, pp. 649-666.

Collins, M. P., and Mitchell, D., 1980, "Shear and Torsion Design of Prestressed and Nonprestressed Concrete Beams," *PCI Journal*, V. 25, No. 5, pp. 32-100.

Collins, M. P., and Mitchell, D., 1981a, Discussion of "Shear and Torsion Design of Non-prestressed Concrete Beams," *PCI Journal*, V. 26, No. 6, pp. 96-118.

Collins, M. P., and Mitchell, D., 1985, "Chapter 4—Shear and Torsion," *CPCA Concrete Design Handbook*, Canadian Portland Cement Association, Ottawa, Canada, pp. 4-1 to 4-51.

Collins, M. P., and Mitchell, D., 1986, "A Rational Approach to Shear Design—The 1984 Canadian Code Provisions," ACI JOURNAL, *Proceedings* V. 83, No. 6, June, pp. 925-933.

Collins, M. P., and Mitchell, D., 1991, *Prestressed Concrete Structures*, Prentice-Hall, Englewood Cliffs, N.J.

Collins, M. P.; Mitchell, D.; Adebar, P. E.; and Vecchio, F. J., 1996, "A General Shear Design Method," *ACI Structural Journal*, V. 93, No. 1, Jan.-Feb., pp. 36-45.

Collins, M. P.; Mitchell, D.; and MacGregor, J. G., 1993, "Structural Design Considerations for High-Strength Concrete," *Concrete International*, V. 15, No. 5, May, pp. 27-34.

Collins, M. P., and Porasz, A., 1989, "Shear Design for High-Strength Concrete," *Proceedings, Workshop on Design Aspects of High-Strength Concrete, Comité Euro-International du Béton Bulletin d'Information*, CEB, Paris, 193, pp. 77-83.

Comité Euro-International du Beton (CEB), 1978, "Shear and Torsion, June: Explanatory and Viewpoint Papers on Model Code Chapters 11 and 12, prepared by CEB Committee V," CEB, Paris, *CEB* Bulletin 12.

Comité Euro-International du Beton (CEB), 1982, "Shear, Torsion, and Punching: Progress Report by CEB Committee IV," *Member Design*, CEB, Paris, CEB Bulletin 146.

Comité Euro-International du Beton (CEB)-Fédération International de la Precontrainte (FIP), 1993, *Model Code 1990, 1993, (MC90)*, Thomas Telford, London.

Cook, W. D., and Mitchell, D., 1988, "Studies of Disturbed Regions near Discontinuities in Reinforced Concrete Members," *ACI Structural Journal*, V. 85, No. 2, Mar.-Apr., pp. 206-216.

Daschner F., and Kupfer, H., 1982, "Versuche zur Schubkraftubertra-gung an Rissen von Nornal- und Leichtbeton," *Bauingenieur*, 59, pp. 57-60.

Dei Poli, S.; Gambarova, P. G.; and Karakoc, C., 1987, "Aggregate Interlock Role in RC Thin-Webbed Beams in Shear," *Journal of Structural Engineering*, ASCE, V. 113, No. 1, pp. 1-19.

Dei Poli, S.; Prisco, M. D.; and Gambarova, P. G., 1990, "Stress Field in Web of RC Thin-Webbed Beams Failing in Shear," *Journal of Structural Engineering*, ASCE, V. 116, No. 9, pp. 2496-2515.

"Design of Concrete Structures for Buildings," 1984, *CAN3-A23.3-M84*, Canadian Standards Association, Rexdale, ON, Canada.

"Design of Concrete Structures," 1994, Canadian Standards Association, Rexdale, Ontario, Canada.

Drucker, D. C., 1991, "On Structural Concrete and the Theorems of Limit Analysis: IABSE Report 2, Zürich, EC2, 1991, Eurocode No. 2," *Design of Concrete Structures, Part 1: General Rules and Rules for Buildings*, Thomas Telford, London.

Eibl, J., and Neuroth, 1988, "Untersuchungen zur Druckfestigkeit von bewehrtem Beton bei gleichzeitig wirkendem Querzug," Institut fur Massivbau und Baustofftechnologie, University of Karlsruhe, Germany.

Eurocode No. 2, 1991, "Design of Concrete Structures, Part 1: General Rules and Rules for Buildings," Thomas Telford, London.

Evans, R. H., and Marathe, M. S., 1968, "Microcracking and Stress-Strain Curves for Concrete in Tension," *Materials and Structures, Research and Testing*, RILEM, Paris, V. 1, No. 1, pp. 61-64.

Fenwick, R. C., and Paulay, T., 1968, "Mechanisms of Shear Resistance of Concrete Beams," *Journal of Structural Division*, ASCE, V. 94, No. 10, pp. 2325-2350.

Gambarova, P. G., 1979, "Aggregate Interlock Role in RC Thin-Webbed Beams in Shear," *Journal of Structural Division*, ASCE, V. 113, No. 1, pp. 1-19.

Gambarova, P. G., 1981, "On Aggregate Interlock Mechanism in Reinforced Concrete Plate with Extensive Cracking," *IABSE Colloquium*, Zurich, pp. 105-134.

Gambarova, P. G., and di Prisco, M., 1991, "Interface Behaviour," *Behavior and Analysis of Reinforced Concrete Structures under Alternate Actions including Inelastic Response*, V. 1, General Models, CEB Bulletin 210, Lausanne, Switzerland.

Gopalaratnam, V. S., and Shah, S. P., 1985, "Softening Response of Plain Concrete in Direct Tension," ACI JOURNAL, *Proceedings* V. 82, No. 2, Mar.-Apr., pp. 310-323.

Gupta, P., and Collins, M. P., 1993, "Behaviour of Reinforced Concrete Members Subjected to Shear and Compression," *Report*, Department of Civil Engineering, University of Toronto, Ontario, Canada.

Hamadi, Y. D., 1976, "Force Transfer across Cracks in Concrete Structures," PhD thesis, Polytechnic of Central London.

Hamadi, Y. D., and Regan, P. E., 1980, "Behaviour in Shear of Beams with Flexural Cracks," *Magazine of Concrete Research*, V. 32, No. 1, pp. 67-77.

Hillerborg, A.; Modéer M.; and Petersson, P. E.; 1976, "Analysis of Crack Formation and Crack Growth in Concrete by Means of Fracture Mechanics and Finite Elements," *Cement and Concrete Research,* V. 6, pp. 773-782.

Hofbeck, J. A.; Ibrahim, I. A.; and Mattock, A. H., 1969, "Shear Transfer in Reinforced Concrete," ACI JOURNAL, *Proceedings* V. 66, No. 2, Feb., pp. 119-128.

Hsu, T. T. C., 1993, *Unified Theory of Reinforced Concrete*, CRC Press, Boca Raton, Fla., 336 pp.

Hsu, T. T. C.; Mau, S. T.; and Chen, B, 1987, "A Theory of Shear Transfer Strength of Reinforced Concrete," *ACI Structural Journal*, V. 84, No. 2, Mar.-Apr., pp. 149-160.

IABSE, 1991a, "IABSE—Colloquium Stuttgart 1991: Structural Concrete IABSE Report," IABSE, Zurich, 62, pp. 1-872.

IABSE, 1991b, "IABSE—Colloquium Stuttgart 1991: Structural Concrete—Summarizing Statement," *Structural Engineering Int.*, V. 1, No. 3, pp. 52-54.

Isenberg, J., 1993, "Finite Element Analysis of Reinforced Concrete Structures II," *Proceedings, International Workshop*, New York.

Jirsa, J. O.; Breen, J. E.; Bergmeister, K.; Barton, D.; Anderson, R.; and Bouadi, H., 1991, "Experimental Studies of Nodes in Strut-and-Tie Models," *IABSE Colloquium, Structural Concrete*, Zurich, pp. 525-532.

Kani, G. N. J., 1964, "The Riddle of Shear Failure and its Solution," ACI JOURNAL, *Proceedings* V. 61, No. 4, Apr., pp. 441-467.

Kani, G. N. J., 1967, "How Safe Are Our Large Reinforced Concrete Beams?" ACI JOURNAL, *Proceedings* V. 64, No. 3, Mar., pp. 128-141.

Kani, M. W.; Huggins, M. W.; and Wiltkopp, P. F., 1979, *Kani on Shear in Reinforced Concrete*, Department of Civil Engineering, University of Toronto, Ontario, Canada.

Kirmair, M., 1987, "Das Schubtragverhalten Schlanker Stahlbeton-balken—Theoretische und Experimentele Untersuchungen fur Leicht-und Normalbeton," Dissertation, University of Munich, Germany.

Kirschner, U., and Collins, M. P., 1986, "Investigating the Behaviour of Reinforced Concrete Shell Elements," *Publication* No. 86-09, Department of Civil Engineering, University of Toronto, Canada.

Kollegger, J., and Mehlhorn, G., 1988, "Biaxial Tension-Compression Tests on Reinforced Concrete Panels," *Forschungsberichte aus dem Fachgebeit Massivbau,* No. 6, Gesamthochschule Kassel, Kassel, West Germany.

Kollegger, J., and Mehlhorn, G., 1990, "Experimentelle Untersuchungen zur Bestimmung der Druckfestigkeit des gerissenen Stahlbetons bei einer Querzugbeanspruchung," *DAtStb H.413*, Beuth, Berlin.

Kupfer, H., 1964, "Erweiterung der Mörsch schen Fachwerkanalogie mit Hilfe des Prinzips vom Minimum der Formanderungsarbeit (Generalization of Mörsch's Truss Analogy Using the Principle of Minimum Strain Energy)," *Comite Euro-International du Beton, Bulletin d'Information,* No. 40, CEB, Paris, pp. 44-57.

Kupfer, H., and Bulicek, H., 1991, "Comparison of Fixed and Rotating Crack Models in Shear Design of Slender Concrete Beams," *Progress in Structural Engineering*, D. E. Grierson, et al., eds., Kluwer, Dordrecht, The Netherlands, pp. 129-138.

Kupfer, H. B., and Gerstle, K., 1973, "Behaviour of Concrete under Biaxial Stresses," *Journal of the Engineering Mechanics Division*, ASCE, V. 99, No. 4, pp. 853-866.

Kupfer, H., Mang, R., and Karavesyrouglou, M., 1983, "Failure of the Shear-Zone of R.C. and P.C. Girders—An Analysis with Consideration of Interlocking of Cracks," *Bauingenieur*, 58, pp. 143-149. (in German)

Kupfer, H., and Moosecker, W., 1979, "Beanspruchung und Verformung der Schubzone des schlanken profilierten Stahlbeton balkens," *For-schungsbeitrage fur die Baubraxis*, Wilhelm Ernst und Sohn, Berlin, pp. 225-236.

Lampert, P., and Thurlimann, B., 1971, "Ultimate Strength and Design of Reinforced Concrete Beams in Torsion and Bending," *IABSE*, No. 31-I, pp. 107-131.

Leonhardt, F., 1965, "Reducing the Shear Reinforcement in Reinforced Concrete Beams and Slabs," *Magazine of Concrete Research*, V. 17, No. 53, pp. 187-198.

Leonhardt, F., 1977, "Schub bei Stahlbeton und Spannbeton: Grundlagen der neueren Schubbemessung," BuStb 72 H.11, 270–277 und H.12, pp. 295-302.

Leonhardt, F., and Walther, R., 1966, "Wardetiger Trager," *Deutscher Ausschuss fur Stahlbeton, Bulletin* No. 178, Wilhelm Ernst und Sohn, Berlin.

Lipski, A., 1971/1972, "Poutres a ame mince en beton arme ou precon-traint," *Ann. d. Travaux Publ. d. Belgique* No. 1-2.

Loeber, P. J., 1970, "Shear Transfer by Aggregate Interlock," MS thesis, University of Canterbury, Christchurch, New Zealand.

Loov, R. E., and Patniak, A. K., 1994, "Horizontal Shear Strength of Composite Concrete Beams with a Rough Interface," *PCI J.*, V. 39, No. 1, pp. 48-109.

MacGregor, J. G., 1992, *Reinforced Concrete Mechanics and Design*, 2nd Edition, Prentice-Hall, Englewood Cliffs, N.J., 848 pp.

MacGregor, J. G., and Walters, J. R. V., 1967, "Analysis of Inclined Cracking Shear in Slender RC Beams," ACI JOURNAL, *Proceedings* V. 64, pp. 644-653.

Mallee, R., 1981, "Zum Schubtragverhalten stabformiger Stahlbeton-elemente," *DAfStbH.323*, Berlin.

Marti, P., 1980, "Zur Plastischen Berechnung von Stahlbeton (On Plastic Analysis of Reinforced Concrete)," *Report* No. 104, Institute of Structural Engineering, ETH, Zurich.

Marti, P., 1985, "Basic Tools of Reinforced Concrete Beam Design," ACI JOURNAL, *Proceedings* V. 82, No. 1, Jan.-Feb., pp. 46-56.

P. Marti, 1985, discussion of "Basic Tools of Reinforced Concrete Design," ACI JOURNAL, *Proceedings* V. 82, No. 6, Nov.-Dec., pp. 933-935.

Marti, P., 1991, "Dimensioning and Detailing," *IABSE Colloquium on Structural Concrete, IABSE Report*, Zurich, 62, pp. 411-443.

Marti, P., and Meyboom, J., 1992, "Response of Prestressed Elements to In-Plane Shear," *ACI Structural Journal*, V. 89, No. 5, Sept.-Oct., pp. 503-514.

Mattock, A. H., 1974, "Shear Tansfer in Concrete Having Reinforcement at an Angle to the Shear Plane," *Shear in Reinforced Concrete*, V. 1, SP-42, American Concrete Institute, Farmington Hills, Mich., pp. 17-42.

Mattock, A. H., 1976, "Design Proposal for Reinforced Concrete Corbels," *PCI Journal*, V. 21, No. 3, pp. 18-42.

Mattock, A. H.; Chen, K. C.; and Soongswang, K., 1976, "The Behavior of Reinforced Concrete Corbels," *PCI Journal*, V. 21, No. 2, pp. 52-77.

Mattock, A. H., and Hawkins, N. M., 1972, "Research on Shear Transfer in Reinforced Concrete.," *PCI Journal*, V. 17, No. 2, pp. 55-75.

Mattock, A. H.; Li, W. K.; and Wang, T. C., 1976, "Shear Transfer in Lightweight Reinforced Concrete," *PCI Journal*, V. 21, No. 1, pp. 20-39.

Millard, S. G., and Johnson, R. P., 1984, "Shear Transfer in Cracked Reinforced Concrete," *Magazine of Concrete Research*, V. 37, No. 130, pp. 3-15.

Millard, S. G., and Johnson, R. P., 1986, Discussion of "Shear Transfer in Cracked Reinforced Concrete," *Magazine of Concrete Research*, V. 38, No. 134, pp. 47-51.

Mitchell, D., and Collins, M. P., 1974, "Diagonal Compression Field Theory—A Rational Model for Structural Concrete in Pure Torsion," ACI JOURNAL, *Proceedings* V. 71, pp. 396-408.

Mörsch, E., 1909, *Concrete-Steel Construction*, McGraw-Hill, New York. (English translation by E. P. Goodrich).

Mörsch, E., 1920, "Der Eisenbetonbau-Seine Theorie und Anwendung (Reinforced Concrete Construction—Theory and Application)," 5th Edition, Wittwer, Stuttgart, V. 1, Part 1.

Mörsch, E., 1922, "Der Eisenbetonbau-Seine Theorie und Anwendung," 5th Edition, Wittwer, Stuttgart, V. 1, Part 2.

Muller, P., 1978, "Plastische Berechnung von Stahlbetonscheiben und-balken (Plasticity Analysis of Reinforced Concrete Wall and Beams), *Report* No. 83, Institute of Structural Engineering, ETH, Zurich.

Muttoni, A., 1990, "Applicability of the Theory of Plasticity for Dimensioning Reinforcing Concrete," PhD thesis, ETH Zurich Birkhäuser, Basel. (in German)

Nielsen, M. P., 1971, "Om jernbetonskivers styrke," *Polyteknisl Forlag*, Copenhagen (On the Strength of Reinforced Concrete Discs), *Acta Polytech. Scand.*, Ci-70, Copenhagen.

Nielsen, M. P., 1984, *Limit Analysis and Concrete Plasticity*, Prentice-Hall, Englewood Cliffs, N.J.

Nielsen, M. P., and Braestrup, N. W., 1975, "Plastic Shear Strength of Reinforced Concrete Beams," *Technical Report* 3, Bygningsstatiske Meddelelser, V. 46.

Nielsen, M. P.; Braestrup, M. W.; Jensen, B. C.; and Bach, F., 1978, "Concrete Plasticity, Beam Shear–Shear in Joints–Punching Shear," *Special Publication*, Danish Society for Structural Science and Engineering, Lyngby, Denmark.

Nissen, I., 1987, "Riβverzahnung des Betons-gegenseitige Rißuferverschie-bungen und ubertragbare Krafte," Dissertation, University of Munich.

Niwa, J., Yamada, K., Yokozawa, K., and Okamura, M., 1986, "Reevaluation of the Equation for Shear Strength of RC-Beams without Web Reinforcement," Translated from *Proceedings, Japan Society of Civil Engineering*, V. 5, No. 372, pp. 1986-1988.

Norges Byggstandardiseringsrad (NBR), 1989, "Prosjektering av betongkonstruksjoner Beregnings-og konstruksjonsregler (Concrete Structures Design Rules)," *NS 3743*, Norges Standardiseringsforbund, Oslo.

Okamura, H., and Higai, T., 1980, "Proposed Design Equation for Shear Strength of R.C. Beams without Web Reinforcement," *Proceedings, Japan Society of Civil Engineering*, 300, pp. 131-141.

Pang, X.-B. D., and Hsu, T. T. C., 1992, "Constitutive Laws of Reinforced Concrete in Shear," *Res. Rep. UHCEE 92-1*, Department of Civil and Environmental Engineering, University of Houston, Tex.

Pang, X.-B. D., and Hsu, T. T. C., 1995, "Behavior of Reinforced Concrete Membrane Elements in Shear," *ACI Structural Journal*, V. 92, No. 6, Nov.-Dec., pp. 665-679.

Pang, X.-B. D., and Hsu, T. T. C., 1996, "Fixed-Angle Softened-Truss Model for Reinforced Concrete," *ACI Structural Journal*, V. 93, No. 2, Mar.-Apr., pp. 197-207.

Park, R., and Paulay, T., 1975, *Reinforced Concrete Structures*, Wiley, New York.

Paulay, T.; Park, R.; and Phillips, M. H., 1974, "Horizontal Construction Joints in Cast-in-Place Reinforced Concrete," *Shear in Reinforced Concrete*, SP-42, American Concrete Institute, Farmington Hills, Mich., pp. 599-616.

Ramirez, J. A., 1994, "Strut-and-Tie Design of Pretensioned Members," *ACI Structural Journal*, V. 91, No. 5, Sept.-Oct., pp. 572-578.

Ramirez, J. A., and Breen, J. E., 1991, "Evaluation of a Modified Truss-Model Approach for Beams in Shear," *ACI Structural Journal,* V. 88, No. 5, Sept.-Oct., pp. 562-571.

Regan, P., 1993, "Research on Shear: A Benefit to Humanity or a Waste of Time?" *Structural Engineering*, 71(19/5), pp. 337-347.

Regan, P. E., and Braestrup, M. W., 1985, "Punching Shear in Reinforced Concrete—A State of the Art Report," *CEB* Bulletin 168, Lausanne, Switzerland.

Reineck, K.-H., 1982, "Models for the Design of Reinforced and Prestressed Concrete Members," *CEB Bulletin* 146, Paris, pp. 43-96.

Reineck, K.-H., 1989, "Theoretical Considerations and Experimental evidence on Web Compression Failures of High-Strength Concrete Beams," *CEB Bulletin* 193, Lausanne, Switzerland, pp. 61-73.

Reineck, K.-H., 1990, "Mechanical Model for the Behaviour of Reinforced Concrete Members in Shear," PhD thesis, University of Stuttgart.

Reineck, K.-H., 1991a, "Modelling of Members with Transverse Reinforcement," *IABSE Colloquium on Structural Concrete, IABSE Report,* IABSE, Zurich, 62, pp. 481-488.

Reineck, K.-H., 1991b, "Model for Structural Concrete Members without Transverse Reinforcement," *IABSE Colloquium Structural Concrete, IABSE Report*, IABSE, Zurich, 62, pp. 643-648.

Reineck, K.-H., 1991c, "Ultimate Shear Force of Structural Concrete Members without Transverse Reinforcement Derived from a Mechanical Model," *ACI Structural Journal*, V. 88, No. 5, Sept.-Oct., pp. 592-602.

Reinhardt, H. W., 1986, "The Role of Fracture Mechanics in Rational Rules for Concrete Design," *IABSE Survey S-34/86 in IABSE Per. 1/1986*, IABSE, Zurich.

Reinhardt, H. W.; Cornelissen, H. A. W.; and Hordijk, D. A., 1986, "Tensile Tests and Failure Analysis of Concrete," *Journal of Structural Enginering*, ASCE, V. 112, No. 11, pp. 2462-2477.

Remmel, G., 1994, '"Zum Zug- und Schubtragverhalten von Bauteilen aus hochfestem Beton," *DAfStb, H.444*, Beuth, Berlin.

Ritter, W., 1899, "Die bauweise hennebique," *Schweizerische Bauzei-tung*, V. 33, No. 7, pp. 59-61.

Rogowsky, D. M., and MacGregor, J. G., 1986, "Design of Reinforced Concrete Deep Beams," *Concrete International: Design and Construction*, V. 8, No. 8, Aug., pp. 49-58.

Rogowsky, D. M.; MacGregor, J. G.; and Ong, S. Y., 1986, "Tests of Reinforced Concrete Deep Beams," ACI JOURNAL, *Proceedings* V. 83, No. 4, July-Aug., pp. 614-623.

Schäfer, K.; Schelling, G.; and Kuchler, T., 1990, "Druck- und Querzug in bewehrten Betonelementen," *DAfStb H.408*, Beuth, Berlin.

Schlaich, J., and Schäfer, K., 1983, "Zur Druck-Querzug-Festigkeit des Stahlbetons," *BuStb 78*, H.3, pp. 73-78.

Schlaich, J., and Schäfer, K., 1984, "Konstrulerenim Stahlbeton-bau," *Beton-Kalender 1984*, Wilhelm Ernst und Sohn, Berlin, pp. 787-1004.

Schlaich, J.; Schäfer, I.; and Jennewein, M., 1987, "Towards a Consistent Design of Structural Concrete," *Journal of the Prestressed Concrete Institute*, V. 32, No. 3, pp. 74-150.

Shioya, T.; Iguro, M.; Nojiri, Y.; Akiayma, H.; and Okada, T., 1989, "Shear Strength of Large Reinforced Concrete Beams, Fracture Mechanics: Application to Concrete," *Fracture Mechanics: Application to Concrete*, SP-118, V. C. Li and A. P. Bažant, eds., American Concrete Institute, Farmington Hills, Mich., pp. 259-279.

Shirai, S., and Noguchi, H., 1989, "Compressive Deterioration of Cracked Concrete," *Proceedings, ASCE Structural Congress 1989: Design, Analysis, and Testing*, ASCE, New York, pp. 1-10.

Stevens, N. J.; Uzumeri, S. M.; and Collins, M. P., 1991, "Reinforced Concrete Subjected to Reversed Cyclic Shear—Experiments and Constitutive Model," *ACI Structural Journal*, V. 88, No. 2, Mar.-Apr., pp. 135-146.

"Standard Building Regulations for the Use of Reinforced Concrete," 1920, *American Standard Specification* No. 23, American Concrete Institute, Farmington Hills, Mich., pp. 283-322.

Talbot, A. N., 1909, "Tests of Reinforced Concrete Beams: Resistance to Web Stresses Series of 1907 and 1908," *Bulletin* 29, University of Illinois Engineering Experiment Station, Urbana, Ill.

Tassios, T. P., and Vintzeleou, E. N., 1986, "Concrete-to-Concrete Friction," *Journal of Structural Engineering*, ASCE, V. 113, No. 4, pp. 832-849.

Tassios, T. P., and Vintzeleou, E. N., 1987, "Concrete-to-Concrete Friction," *Journal of Structural Engineering*, ASCE, V. 113, No. 4, pp. 832-849.

Taylor, H. P. J., 1974, "The Fundamental Behaviour of Reinforced Concrete Beams in Bending and Shear," *Shear in Reinforced Concrete*, SP-42, American Concrete Institute, Farmington Hills, Mich., pp. 43-77.

Thurlimann, B.; Marti, P.; Pralong, J.; Ritz, P.; and Zimmerli, B., 1983, "Vorlesung Zum Bortbildungs kurs fur Bauingenieure," Institute fur Bautecknik und Konstruktion, ETH, Zurich.

Vecchio, F. J., and Collins, M. P., 1982, "The Response of Reinforced Concrete to In-Plane Shear and Normal Stresses," *Publication* No. 82-03, Department of Civil Engineering, University of Toronto, Canada.

Vecchio, F. J., and Collins, M. P., 1986, "The Modified Compression Field Theory for Reinforced Concrete Elements Subjected to Shear," ACI JOURNAL, *Proceedings* V. 83, No. 2, Mar.-Apr., pp. 219-231.

Vecchio, F. J., and Collins, M. P., 1988, "Predicting the Response of Reinforced Concrete Beams Subjected to Shear Using the Modified Compression Field Theory," *ACI Structural Journal*, V. 85, No. 4, July-Aug., pp. 258-268.

Vecchio, F. J., and Collins, M. P., 1993, "Compression Response of Cracked Reinforced Concrete," *Journal of Structural Engineering*, ASCE, V. 119, No. 12, pp. 3590- 3610.

Vecchio, F. J.; Collins, M. P.; and Aspiotis, J., 1994, "High-Strength Concrete Elements Subjected to Shear," *ACI Structural Journal*, V. 91, No. 4, July-Aug., pp. 423-433.

Vintzeleou, E. N., and Tassios, T. P., 1986, "Mathematical Models for Dowel Action under Monotonic Conditions," *Magazine of Concrete Research*, 38, pp. 13-22.

Wagner, H., 1929, "Ebene Blechwandträger mit sehr dünnem Stegblech (Metal Beams with Very Thin Webs)," *Zeitschrift für Flugtechnik und Motorloftschiffahr*, 20 (8-12), Berlin.

Walraven, J. C., 1980, "Aggregate Interlock: A Theoretical and Experimental Analysis," PhD thesis, Delft University, The Netherlands.

Walraven, J. C., 1981, "Fundamental Analysis of Aggregate Interlock," *Journal of Structural Division*, ASCE, V. 108, pp. 2245-2270.

Walraven, J. C., 1987, "Shear in Prestressed Concrete Members," *A State-of-the-Art Report; CEB Bulletin* 180, Paris.

Walraven, J. C.; Frenay, J.; and Pruijssers, A., 1987, "Influence of Concrete Strength and Load History on the Shear Friction Capacity of Concrete Members," *PCI Journal*, V. 21, No. 1, pp. 66-84.

Walraven, J., and Lehwalter, N., 1990, "Einfluß des Maßstabs in schub-beanspruchten Bauteilen ohne Schubbewehrung," *BuStb 85*, H.9, pp. 228–232.

Walraven, J., and Lehwalter, N., 1994, "Size Effects in Short Beams Loaded in Shear," *ACI Structural Journal*, V. 91, No. 5, Sept.-Oct., pp. 585-593.

Walraven, J. C., and Reinhardt, H. W., 1981, "Concrete Mechanics Port A—Theory and Experiment on the Mechanical Behaviour of Cracks in Plain and Reinforced Concrete Subjected to Shear Loading," University of Delft, The Netherlands, 26(1A).

Withey, M. O., 1907, "Tests of Plain and Reinforced Concrete Series of 1906," *Bulletin of the University of Wisconsin, Engineering Series*, V. 4, No. 1, pp. 1-66.

Withey, M. O., 1908, "Tests of Plain and Reinforced Concrete Series of 1907," *Bulletin of the University of Wisconsin, Engineering Series*, V. 4, No. 2, pp. 1-66.

Woo, K., and White, R. N., 1991 "Initiation of Shear Cracking in Reinforced Concrete Beams with No Web Reinforcement," *ACI Structural Journal*, V. 88, No. 3, May-June, pp. 301-308.

Yoon, Y. S.; Cook, W. D.; and Mitchell, D., 1996, "Minimum Shear Reinforcement in Normal, Medium and High-Strength Concrete Beams," *ACI Structural Journal*, V. 93, No. 5, Sept.-Oct., pp. 576-584.

Zhang, L. X., 1995, "Constitutive Laws of Reinforced Membrane Elements with High-Strength Concrete," PhD dissertation, Department of Civil and Environmental Engineering, University of Houston, Tex.

Zsutty, T. C., 1971, "Shear Strength Prediction for Separate Categories of Simple Beams Tests," ACI JOURNAL, *Proceedings* V. 68, No. 2, Feb., pp. 138-143.